Design of Innovative Dynamic Systems for Seismic Response Mitigation

by

Douglas Seymour

B.A., University of Cambridge, 2011

B.Sc., Canterbury Christ Church University, 2007

MASSACHUSETTS INSTITUTE OF TECHNOLOGY
JUN 22 2012
LIBRARIES

Submitted to the Department of Civil and Environmental Engineering
in Partial Fulfillment of the Requirements for the Degree of
Master of Science in Civil and Environmental Engineering
at the
MASSACHUSETTS INSTITUTE OF TECHNOLOGY
June 2012

ARCHIVES

© 2012 Massachusetts Institute of Technology. All rights reserved.

Signature of Author _____
Department of Civil and Environmental Engineering
May 10, 2012

Certified by _____
Jerome J. Connor
Professor of Civil and Environmental Engineering
Thesis Supervisor

Accepted by _____
Heidi M. Nepf
Chair, Departmental Committee for Graduate Students

Design of Innovative Dynamic Systems for Seismic Response Mitigation

by

Douglas Seymour

Submitted to the Department of Civil and Environmental Engineering
on May 10, 2012 in Partial Fulfillment of the Requirements for
the Degree of Master of Science in Civil and Environmental Engineering

ABSTRACT

Rocking wall systems consist of shear walls, laterally connected to a building, that are moment-released in their strong plane. Their purpose is to mitigate seismic structural response by constraining a building primarily to a linear fundamental mode. This constraint prevents mid-story failure, and maximizes energy dissipation by activating the maximum number of plastic hinges throughout the structure. This is a useful response mitigation system, but suffers from some difficulties, stemming primarily from the considerable mass of the wall. Those difficulties are notably expensive foundations, and very high inertial forces imparted to the building, with subsequent need for expensive lateral connectors.

The purposes of this work are to analyze current implementations of rocking wall systems, present an early reference on their application, present the first systematic methodology for their design, clarify their analysis, and introduce an alternative structural system that avoids their difficulties. A quasi-static analysis model is used for predicting the seismic mitigation performance of rocking walls and rocking columns. The stiffness matrix is generalized for an N-story building equipped with these structural systems. The model presented enables optimization of the design parameters, and consequently improved system effectiveness, analytical tractability, and material usage. The case study is a rocking wall system installed in a building located in Tokyo, Japan. A software package is developed, providing an illustrative implementation of the methods derived.

Thesis Supervisor: Jerome J. Connor
Title: Professor of Civil and Environmental Engineering

Acknowledgments

I wish to give recognition to some of the many people who aided me in the completion of this paper. First, to my advisor and friend Professor Jerry Connor, who taught me what it is to be a civil engineer. Professor Connor suggested the topic, which is just one of a great many ideas that he has helped me with. I would also like to thank my mechanical vibrations teacher and friend Professor Eduardo Kausel for greatly advancing my understanding of vibrations.

I would also like to thank Professor Simon Laflamme, once Ph.D. candidate at MIT and now professor at Iowa State University, for his help with the presentation of an earlier paper on this topic, which aided my ability to produce a comprehensible academic paper tremendously. I would also like to thank Professor Wada and Dr. Qu of the Tokyo Institute of Technology for their assistance in providing data regarding the case study building. Professor Wada first sparked my interest in rocking walls with a presentation he gave to Professor Connor's class in 2010, and is presently the preeminent author in this field.

Douglas Seymour, April 2012

Contents

		Page
1.	Introduction	11
1.1.	Rocking Walls within the Taxonomy of Dynamic Structures	
1.2.	Outline and Purpose of Rocking Walls	
1.3.	Application of Rocking Walls	15
1.4.	Outline History of Rocking Walls	16
2.	Literature Review	18
2.1.	Rocking Wall Design	
2.1.1	Design for Resistance to Lateral Loads	
2.1.2	Damping Design	19
2.1.3	Design for Serviceability	
2.2.	Lateral Load Bearing Capacity	20
2.3.	Damping of Rocking Wall Systems	21
2.4.	Ensuring Maximum Energy Dissipation with Linear Deformations	22
2.5.	Case Study: Retrofit of the G3 Building	23
2.5.1.	Response of the Case Study Building to Seismic Loading in the Transverse Direction	26
3.	Rocking Wall Design	28
3.1.	Problem Statement	
3.2.	Method	
3.3.	Introduction to Analytical Model	29

3.4.	Solving an Analytical Model without Rocking Wall	31
3.5.	Solving an Analytical Model with Rigid Rocking Wall	
3.6.	Solving an Analytical Model with Flexible Wall, Assumed Modes	33
3.7.	Solving an Analytical Model with Flexible Wall, Assumed Modes, Full Analysis	34
3.8.	Applying Seismic Action to the Analytical Model	38
3.9.	Applying Static Equivalent Seismic Action	39
3.10.	Solving an Analytical Model with Flexible Wall, with Full Stiffness Matrix	42
3.11	Benchmark Buildings	50
3.12.	Software Implementation	52
3.13.	Software to Implement ASCE 7-05 Equivalent Seismic Loads	55
4.	Analysis of Rocking Wall Design	57
4.1.	Natural Frequencies of the Simulations	
4.2.	Natural Frequencies of the System With and Without Rocking Wall	58
4.3.	Modes of the System With Varying Stiffness of Rocking Wall	
4.4.	Maximum Story Drift Angle With Varying Rocking Wall Width	60
4.5.	Forces Applied to the Building by the Rocking Wall Inertia	62
4.6.	Comparison with Given Case Study Building Data	64
5.	Study to Determine Whether the Case Study Rocking Wall Caused Damage During the Tōhoku Earthquake	70
5.1.	The Mathematical Model of the Building	71
5.2.	Finite Element Modeling	72
5.3.	Dynamics	75

5.4.	Units and Consistency	77
5.5.	Mass for Dynamic Analysis	78
5.6.	Finding and Processing the Link Axial Forces in ADINA	
5.7.	The Addition of Damping to the Model	79
5.8.	Calculation of the Static Shear Wall Cracking Moment	80
5.9.	Conclusions of the Finite Element Study	81
6.	Rocking Column Design	83
6.1.	Rationale for Design	
6.2.	Introduction to Rocking Column Design	84
6.3.	Further Rocking Column Design	86
6.4.	Conclusions of the Finite Element Study	88
6.5.	Conclusions of the Finite Element Study	89
6.6.	Analysis of the Benefits of Rocking Columns	91
6.6.1	Lateral Force Reduction	
6.6.2	Foundations Reduction	92
6.6.3	Cost Effective Connections	
6.6.4	Greater Story Drift Reduction, with Potential for Further Reductions	
6.6.5	Overall Comparative Effectiveness	93
7.	Suggested Extensions	94
8.	Conclusions	95
9.	References	97

10. Appendices 101

Appendix A. The 20 Significant United States Earthquakes 1933-2006 103

Appendix B. A Set of Benchmark Building Models for Use in Simulations 125

Appendix C. MATLAB Code for Solving the Rocking Wall as a Flexible Continuous System, using Lagrange 167

Appendix D. MATLAB Code to Find the Stiffness Matrix of Building-Rocking Wall System 171

1. Introduction

1.1. Rocking Walls within the Taxonomy of Dynamic Structures

Dynamic structures avoid structural damage by shifting the burden of energy dissipation to chosen structural elements, preferably non-critical and replaceable elements. Damage that would result in severe injury, and damage that would prevent future serviceability of the structure, can be avoided by choosing the manner in which input energy is dissipated.

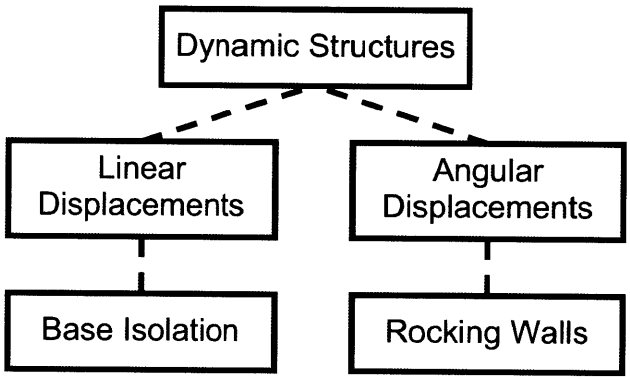

Figure 1.1.1. A partial taxonomy of dynamic structures

In addition to preventing loss of life, dynamic structures enable structures to be serviceable after a seismic event, and as such can be a highly sustainable approach to structural design in earthquake-prone regions.

1.2. Outline and Purpose of Rocking Walls

A rocking wall is a dynamic structural system that employs one or more stiff structural elements, moment-released at the base, to force a building that is subjected to dynamic loads to fail in a near-linear mode. This approach is intended to prevent mid-story failure, which is illustrated in *figure 1.4.1*, by maximizing energy dissipation, as discussed in *section 2.4*. As illustrated in

figure 1.2.1, rocking walls are designed to rock only in the strong plane of the wall. This is in strong contrast to a shear wall that is simply unrestrained at its base.

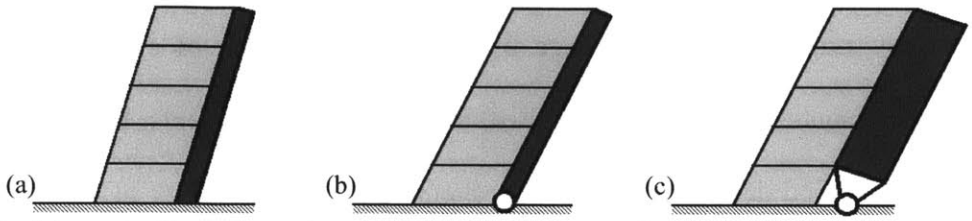

Figure 1.2.1. Schematic illustration of a simple unfixed shear wall contrasted with a rocking wall system. (a) Building with fixed shear wall, (b) Building with unfixed shear wall, (c) Building with rocking wall

All rocking walls have been constructed from reinforced concrete, as far as known at the time of writing. As a result, the pin and foundations at the base of the wall must be highly substantial, as illustrated in *figure 2.1.2*. Additionally, the lateral loads that the rocking wall imposes on the surrounding structure during an earthquake are found, by an analytical method presented in this work, to be very high partially due to the large mass of rocking wall, as discussed in *section 4.5*. As a result, very substantial lateral supports are required to connect the rocking wall to the building. All of these issues increase the cost of installation of a rocking wall system substantially.

The Tokyo case study building, first introduced in *section 2.5*, was damaged in the Tōhoku earthquake of March 2011. Few buildings in Tokyo were significantly damaged in that event, since as observed in Tokyo, the accelerations observed were one or two orders of magnitude lower intensity than those observed nearer the epicenter. In *section 5*, a finite element study is presented that supports the theory that the inertial loads from the rocking walls were very high during the earthquake, and thus a rocking wall was in fact the cause of that damage.

In response to these findings, it is suggested that new, higher lateral forces, as discussed in *section 4.5*, be considered when designing systems to be installed adjacent to rocking walls. Additionally, a much lighter steel system, resembling a deep column more than a wall, is proposed in *sections 6-7*. To differentiate the two systems, the new structural system will be referred to as a *rocking column*. Rocking columns achieve the goals of rocking walls at considerably less cost, by reducing the strength of additional foundations required, and the strength of lateral supporting connections that are required, in addition to material costs that are predicted to be significantly lower, making rocking columns more commercially viable than rocking walls have been.

Buildings that could be considered for rocking wall retrofit are in the approximate range 3 to 20 stories. The fundamental mode of such buildings is approximately linear.[1] As a result of this, the addition of a rocking wall adds a large mass but little stiffness to the fundamental mode. Thus it is clearly seen that the addition of a rocking wall will tend to decrease the frequency of the fundamental mode of the building, since frequency is inversely proportional to the root of mass. However, subsequent modes of such buildings are highly non-linear, as illustrated in *figure 1.2.2*, and thus a rocking wall adds a high stiffness to all other modes of the building, tending to increase those frequencies significantly, since frequency is proportional to the square root of the stiffness, and this effect is generally stronger than that of the mass in this situation. Thus for buildings that could be considered for rocking wall retrofit, the addition of a rocking wall tends to move all natural frequencies further away from the highest energy frequencies of earthquakes. This is clearly illustrated in *figure 1.2.3*.

[1] *Chopra (2006)*

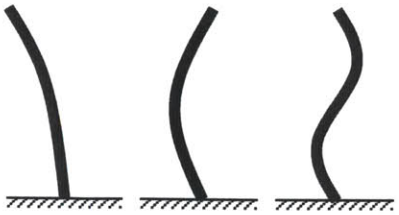

Figure 1.2.2. A schematic of the first three dynamic modes of a typical medium-height building. In general, subsequent modes follow the same trend.

As *figure 1.2.2* illustrates, while the first mode of a building is often near linear, it is not, in general, exactly linear.

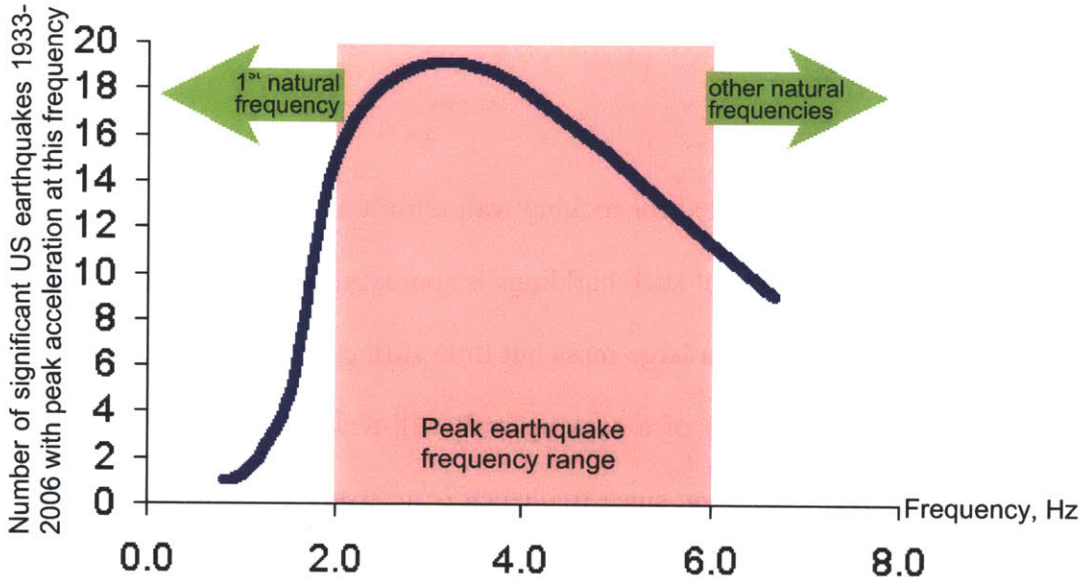

Figure 1.2.3. Illustration showing how the application of a rocking wall system shifts the natural frequencies of a building away from the peak frequency range of earthquakes. The seismic data used to produce this figure may be found in Appendix A.

1.3. Application of Rocking Walls

For newly constructed buildings, there are many ways to prevent seismic damage, and a number of ways to apply the benefits of dynamic structures. For example, the entire structural frame could be allowed to rock, with energy dissipation being performed by replaceable fuses, as illustrated in *figure 1.3.1*. However, clearly for existing structures such a solution is not feasible, and other ways must be found to apply the benefits of dynamic structures.

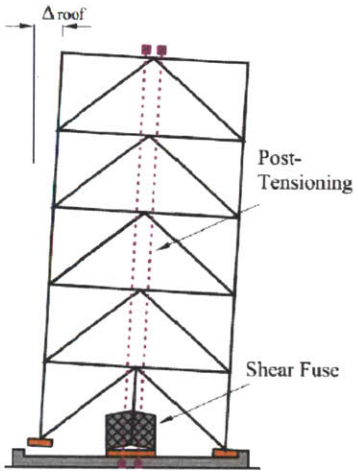

Figure 1.3.1. A rocking frame structure[2].

Rocking wall retrofit projects are limited by the availability of appropriate locations to attach rocking walls. Most often, such locations will be limited to the exterior of a building. In addition, for buildings that are large in plan, rocking walls must be spaced at some reasonable distance throughout the building. Clearly, it is not sufficient to use rocking walls to linearize the response of a building in one location alone. Rocking walls must be spaced throughout the building to ensure the whole response of the building is linearized under dynamic loading. This approach can be seen in the case study introduced in *section 2.5*, a building which is large in plan, and uses *6* equally spaced rocking walls.

As will also be seen from that case study, the building to be retrofitted was long and thin, and the rocking walls were to be installed to the exterior, as would be most common, as illustrated in *figure 2.5.2*. This meant that it was only appropriate to install rocking walls in the longitudinal direction of the building, since if rocking walls were installed to the transverse direction of the building, the center of the building in plan would be largely unsupported, since the distance between rocking walls would be very large. This would result in the desired linearized transverse mode for the thin edges of the building in plan, but the transverse mode for the center of the building in plan would remain unlinearized.

In general, there is no particular problem with installing rocking walls in both orientations of a building. But in the case study, although rocking walls were added to the longitudinal direction, it was decided to stiffen the transverse response by adding conventional transverse shear walls, rather than add transverse rocking walls.

1.4. Outline History of Rocking Walls

The concept of rocking shear walls, though not in a form that matches current implementations, was introduced by Ajrab *et al.*[3] The work they presented was built on studies by Housner, who investigated the free vibration of rigid rocking blocks.[4]

Mander and Cheng defined an approach to rocking, structural flexibility, and prestressing, as *damage avoidance design.*[5] The performance objective of the *DAD* philosophy for a maximum assumed earthquake (MAE) is simply that the structure remains elastic at all times during ground

[2] *Deirlein (2010), p3*
[3] *Ajrab et al. (2004)*

shaking. For example, elastic rotations might be defined as rotations of less than 1%, 0.6°. Usually much less is preferred, for example the design criteria for the case study retrofit project was a peak story drift angle of 1/250 radian (0.4% or 0.23°)[6]. For a maximum considered earthquake (MCE)[7], the structure may yield with limited damage (for example defined as plastic rotations of less than 0.5%) to the conventional reinforced concrete framing elements[8]. Rocking can achieve these objectives, and are particularly relevant to retrofit applications.

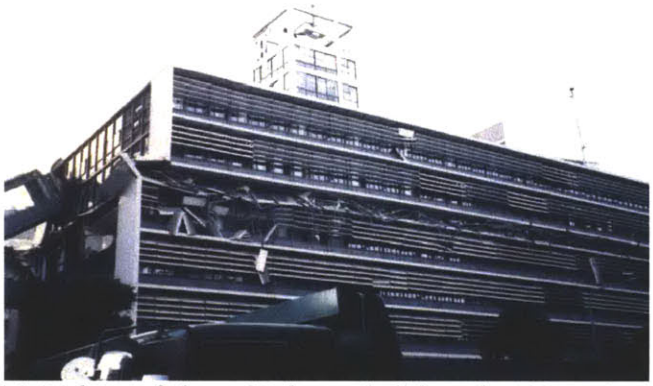

Figure 1.4.1. Mid-story failure of Kobe city hall from the 1995 Kobe earthquake.

[4] *Housner (1963)*
[5] *Mander and Cheng (1997)*
[6] *Wada (2010)(2), p6*
[7] *FEMA (1997), p32*
[8] *Ajrab et al. (2004), p4*

2. Literature Review

2.1. Rocking Wall Design

The present work proposes that rocking walls are most appropriate for retrofit applications, due to their relatively high cost and less than ideal architectural characteristics. However, earlier papers on this subject considered that rocking walls would be applied to new buildings, and play a significant role in the primary lateral load bearing capacity of the structure.

2.1.1. Design for Resistance to Lateral Loads

There are three central issues that have been considered in rocking wall design. The first is that adequate resistance to lateral loads must be maintained. Since it was originally proposed that the moment capacity at the base of walls be removed, this load bearing capacity must be transferred to three other classes of mechanism, being the moment capacity of shear wall-to-frame connections, the resistance to overturning of the weight of the wall itself, and to additional mechanisms, such as bracing, or post-tensioned tendons running through the wall, which are illustrated in *figure 2.1.1*. Pekcan *et al.* suggested that such tendons be draped to match the shape of the moment diagram induced under the assumed inertial loading.[9] Note that the original rocking wall concept presented is that of a flat base. If the rocking wall is pinned at the base, as for example in the retrofit at the Tokyo Institute of Technology[10], then clearly the weight of the wall itself offers no moment resistance.

[9] *Pekcan et al. (2000)*

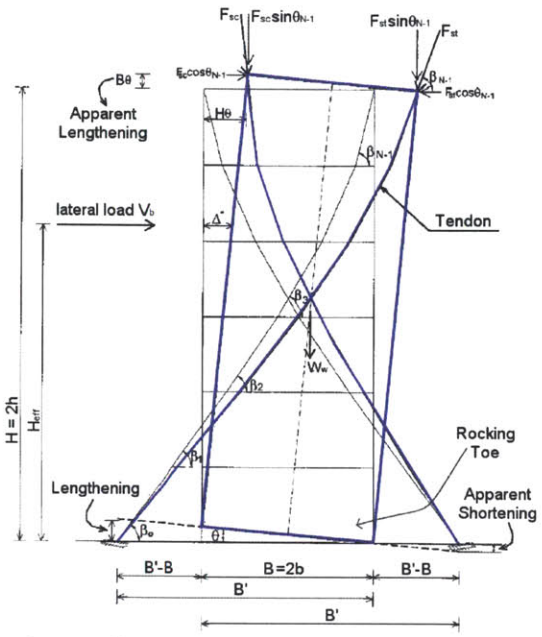

Figure 2.1.1. A non-hinged rocking wall on rigid foundation, with supplemental supportive tendons[11] *(adapted)*

2.1.2. Damping Design

Secondly, the rocking wall-supported structure must fulfil the primary intent of dynamic structures by dissipating energy in a chosen, predictable way. Mander *et al.* conclude that a tendon-supported rocking structure provides only limited damping, for example *1-2%* of critical.[12] Percassi showed that the addition of damping devices to the tendons themselves would enhance the damping offered by the system.[13]

2.1.3. Design for Serviceability

The third central issue in rocking wall design, is the degree to which the structure is serviceable following a seismic event. Kishiki & Wada discuss how following the Northridge and Kobe earthquakes, many buildings became structurally unviable, leading to a termination of social and

[10] *Wada et al. (2009)*
[11] *Ajrab et al. (2004), p2*
[12] *Mander et al. (1998)*

industrial activities, and consequently severe economic loss[14]. A flat-based rocking wall as illustrated in *figure 2.1.1* may suffer from toe crushing, and if rigid wall-frame connections are used, these may also be significantly damaged. Such severe damage invariably requires that the building be reconstructed, since further seismic performance cannot be predicted.[15] An open pin design, fabricated from cast iron, at the base of the rocking wall would prevent severe damage to the wall toes during rocking, as shown in *figure 2.1.2.*[16]

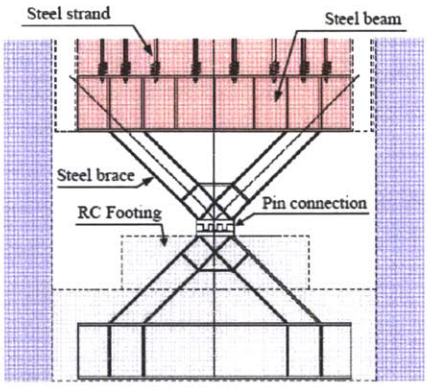

Figure 2.1.2. A rocking wall may be hinged at the base to prevent toe damage (foundations not shown)

2.2. Lateral Load Bearing Capacity

For a flat-based rocking wall on a rigid surface, and which is otherwise unsupported, it is readily seen from statics that the lateral load that can be supported is:

$$V_{max} = \frac{W_w}{H_{eff}}(b - h\theta) \qquad (2.1)$$

where W_w is the weight of the wall, H_{eff} is the point of application of the lateral load, b is half the width of the wall, h is half the height of the wall, and θ is the small angle through which the wall has moved, as in *figure 2.1.1.*

[13] *Percassi (2000)*
[14] *Kishiki and Wada (2009), p1*
[15] *Wada et al. (2009), p1*
[16] *Wada et al. (2009), p7*

Further load-bearing capacity that may be derived is provided by the moment capacity of floor-wall connections, and frame bracing. Example formulae providing the loading-bearing capacity offered by floor-wall connections and supportive tendons are derived by Ajrab *et al.*[17]

Of course in the case of a retrofit application of rocking walls, it will usually be reasonable to assume that the existing structure has sufficient lateral load bearing capacity, except for seismic loading, which is addressed as a special case by dynamic structures. All known applications of rocking walls to date have been retrofit applications.

2.3. Damping of Rocking Wall Systems

The four sources of damping in a rocking wall-supported structure are inherent damping, which is typically taken to be *5%* for concrete structures, radiation damping due to the impact of a flat-based rocking wall with the ground, hysteretic damping due to plastic behavior within the frame, and supplemental damping such as dampers attached to the system. Formulae to illustrate radiation damping and hysteretic damping are given by Ajrab *et al.*[18]

Various types of additional damping devices have been proposed, such as the fuse elements in series with tendons proposed by Ajrab *et al.*, and externally-mounted mild steel material dampers proposed by Marriott *et al.*[19] and implemented by Wada *et al.*[20] Such devices may be installed with the intent that they be replaced after a seismic event.[21]

[17] *Ajrab et al. (2006), p2*
[18] *Ajrab et al. (2006), p3*
[19] *Mariott et al. (2008), p2*
[20] *Wada et al. (2009)*
[21] *Wada et al. (2009), p2*

2.4. Ensuring Maximum Energy Dissipation with Linear Deformations

The introduction of rocking wall system to a frame building may be motivated by showing the benefit of a global failure mode with low rotations as opposed to a local failure mode with high rotations. Consider for example the simple frame with the three failure modes shown in *figure 2.4.1*.

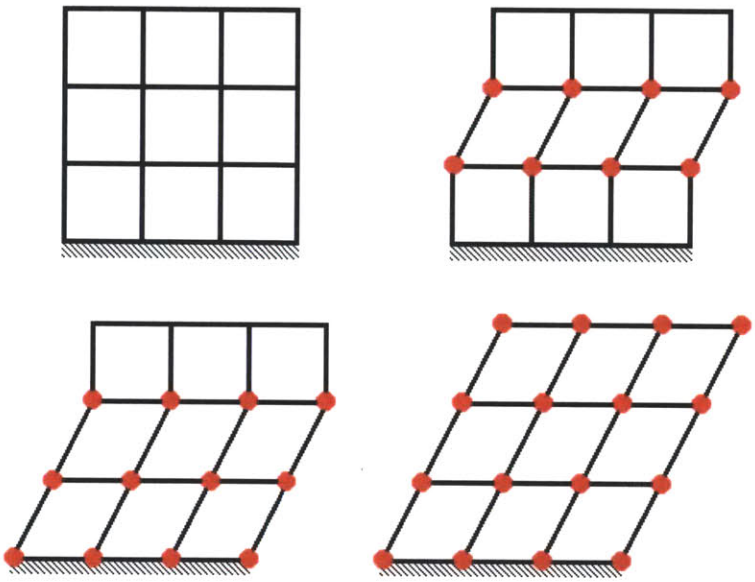

Figure 2.4.1. (a) A schematic 3 story frame, (b), (c) its two non-ideal pushover failure modes, (d) its ideal pushover failure mode

It is readily seen that as the number of plastic hinges increases in the failure mode, so does the ability of the structure to dissipate energy. The first two failure modes shown have low energy dissipation, and so the rotations induced will be large, with high potential for loss of life and severe structural damage. However the final failure mode uses all possible plastic hinges, and thus has the maximum energy dissipation per unit rotation. Thus in this mode the rotations will be smaller, and the probability of saving life and further structural serviceability is maximized.[22]

[22] *Wada et al. (2009), p2*

Hence the focus for seismic retrofit need not be strengthening the individual members which would deform excessively under seismic loading, but rather the control of the global behaviour of the structure to prevent damage from weak modes.[23]

Additionally, it may be noted that the non-ideal failure modes are more likely to occur under higher-mode excitation, since those forms are more congruent with the higher mode shapes, as illustrated in *figure 1.2.2.*

Hence, if a rocking wall is designed to be rigid enough to resist the partial failure modes, the frame will tend to fail in the preferable global failure mode. A rocking wall thus suppresses higher mode vibrations,[24] by moving the natural frequencies away from the peak energy range of earthquakes, as seen in *figure 1.2.3.*

2.5. Case Study: Retrofit of the G3 Building

To further understand the principles involved in the retrofit of a rocking wall, the retrofit of the G3 Building at the Tokyo Institute of Technology, as discussed by Wada *et al.*,[25] will be considered. The case study building was found to be inadequate for modern seismic codes, and appropriate for retrofit. The design criteria for the retrofit project was a peak story drift angle of 1/250 radian (0.4%, 0.23°), to prevent the shear failure of the reinforced concrete frame.[26]

[23] *Wada et al. (2009), p6*
[24] *Wada et al. (2009), p10*
[25] *Wada et al. (2009)*
[26] *Wada (2010)(2), p6*

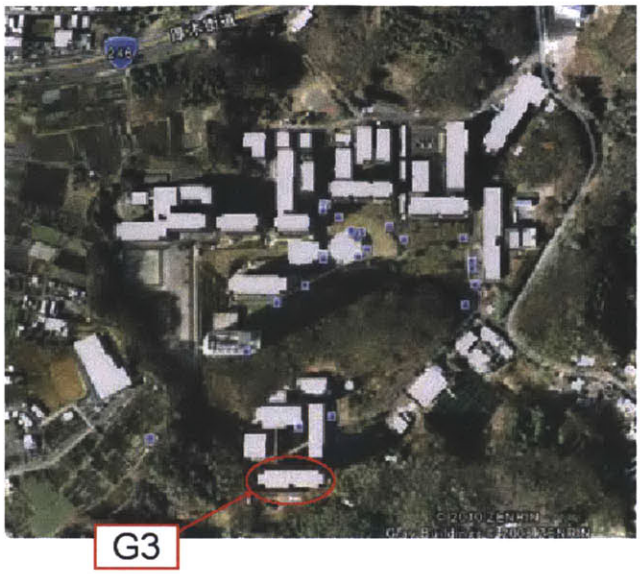

Figure 2.5.1. (a) The case study building in the Suzukakedai Campus of the Tokyo Institute of Technology[27(adapted)], *(b) A 3D model of the retrofitted case study building, where yellow represents new structure to be retrofitted*[28].

As is seen from *figures 2.5.1(b)* and *2.5.2*, the design proposed by Wada *et al.* consists of wide and shallow rocking walls (*14.4ft* by *2ft* in plan) which rock in the longitudinal direction of the building. The rocking walls represent an additional 56% of the existing steel reinforced concrete frame area, in plan. The wall is prestressed to allow for the large vertical tensile forces which will result from inertial motion, and is designed to remain elastic during severe seismic motion.[29] As is seen from *figure 2.5.2*, this retrofit only stiffens the response at six approximately evenly-distributed locations. The existing floor diaphragm stiffness between the rocking walls is

[27] *Wada (2010)(2)*

intended to ensure that the response throughout the structure is close to the response at the rocking walls themselves. The cross section of a rocking wall is seen in *figure 2.5.3*.

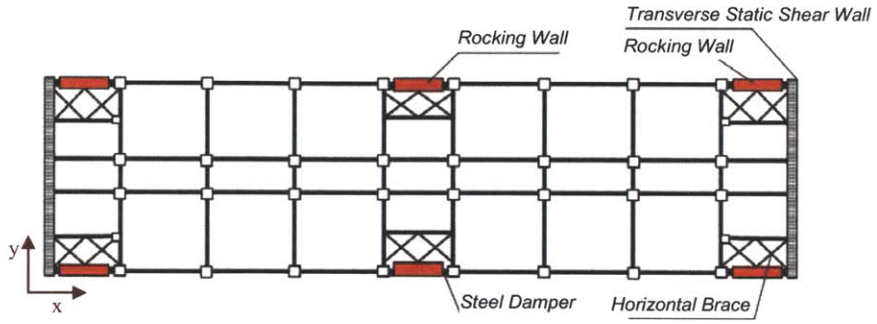

Figure 2.5.2. A plan view of the retrofitted case study building. Red represents rocking walls.[30(adapted)]

As shown in *figure 2.5.3*, the motion of the rocking walls in the case study building is damped by the use of steel dampers (type *LY226*[31]), such as those shown in *figure 2.5.4*. These dampers reduce the story drift further than with the rocking walls alone. As discussed previously, the peak story drift is already reduced by the rocking wall without any damping by equalizing the drift burden throughout the structure.

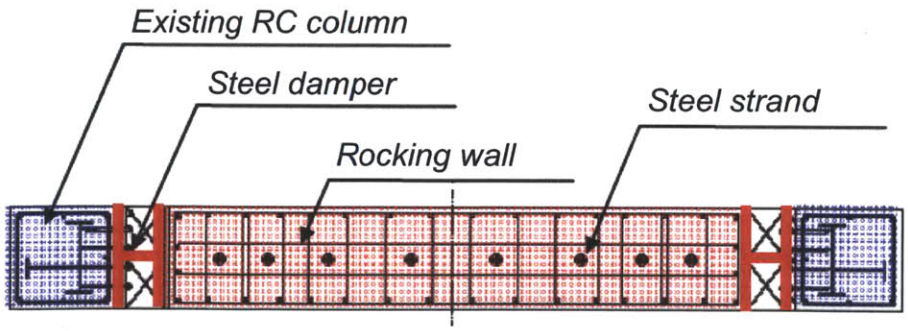

Figure 2.5.3. Cross-section of a rocking wall.[32(adapted)]

[28] *Wada et al. (2009)*
[29] *Wada et al. (2009), p6-7*
[30] *Wada et al. (2009), p5*

Professor Wada's report on the case study retrofit concludes by discussing that the upper-bound theorem is not easily applicable for a seismically controlled structure, which makes determining the ultimate strength and seismic performance of the structure highly difficult.[33]

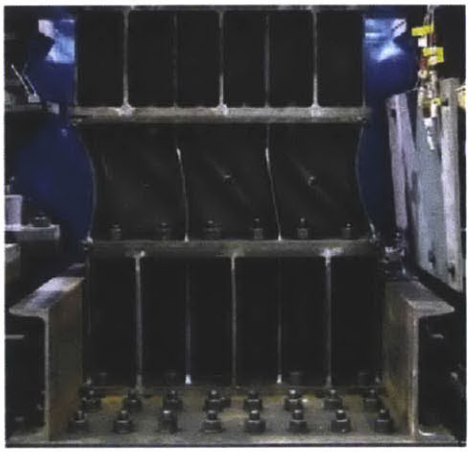

Figure 2.5.4. Testing of the steel dampers used in the case study retrofit project.[34]

2.5.1. Response of the Case Study Building to Seismic Loading in the Transverse Direction

The report on the retrofit of the case study building indicates that both directions of the building were below a seismic capacity of 0.7, and so were both required to be retrofitted.[35] However the report does not directly mention the effects of the rocking wall retrofit on the response of the building in the transverse y-direction, and only explicitly discusses the modeling of seismic performance evaluation in the longitudinal x-direction[36]. However, in a lecture, Professor Wada

[31] *Wada (2010), p7*
[32] *Wada et al. (2009), p7*
[33] *Wada et al. (2009), p11*
[34] *Qu and Wada (2011)*
[35] *Wada et al. (2009), p5*
[36] *Wada et al. (2009), p8*

mentioned the additional static shear walls which were added to the transverse direction[37], and which are seen in *figure 2.5.1*. When a student asked about this issue, Professor Wada remarked that the retrofitted building is adequately stiff in the transverse direction to resist severe damage, and that the project is designed for 225% of the code requirements.[38]

[37] *Wada (2010)(2), p7*
[38] *Wada (2010)(1)*

3. Rocking Wall Design

3.1. Problem Statement

Currently, each rocking wall design project requires an entirely new analysis from first principles, with expert-level oversight. Such high design requirements are prohibitive in the application of any new system. To aid in future maturation and acceptance of this structural system, it is required to provide tools that systematize the selection of rocking wall properties, based on the known parameters of the building to be retrofitted, to reduce the time required for the analysis phase, and provide a framework for design. This will allow engineers to better understand the structural system and aid discussion in this area of dynamic structures.

The most critical information to determine is the size of rocking wall that is required for a given building. Secondly, it is required to determine the lateral loads that the rocking wall applies to the building under code-determined seismic loading.

3.2. Method

In this work, the process of producing the tools alluded to in the problem statement is started with the development of a number of analytical models of the rocking wall system, in *sections 3.3 – 3.7* and *3.10*.

A method is developed which may generate benchmark discretized buildings of any number of stories, including story stiffnesses and story masses, such that the analytical model of the discretized building-rocking wall system may be applied to them, as discussed in *section 3.11*.

Seismic loads are applied to the analytical model, and the responses of the model to those loads are analyzed, as discussed in *sections 3.8 – 3.9*.

Example software is developed which implements those models programmatically, and returns the required information, as discussed in *sections 3.12 – 3.13*.

3.3. Introduction to Analytical Model

For low- to medium-rise structures, which are the primary focus of retrofitting rocking walls, buildings tend to deform approximately like a shear beam, under environmental loads. If the building deformation were exactly linear, as shown in *figure 3.3.1*, then clearly a rocking wall would add no stiffness to that particular deformation, only mass. In general this is close to the truth for fundamental mode deformations. Although for all buildings with stiffness profiles that are not parabolic, there will be some non-linearity in the deformation under seismic loading.[39]

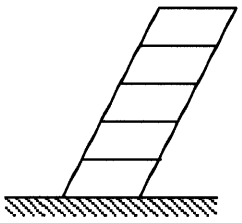

Figure 3.3.1. Low- to medium-rise buildings tend to deform like a shear beam

The principle of tributary areas can be used to model a low-rise building with an attached rocking wall as shown in *figure 3.3.2*.

[39] *Connor (2003)*

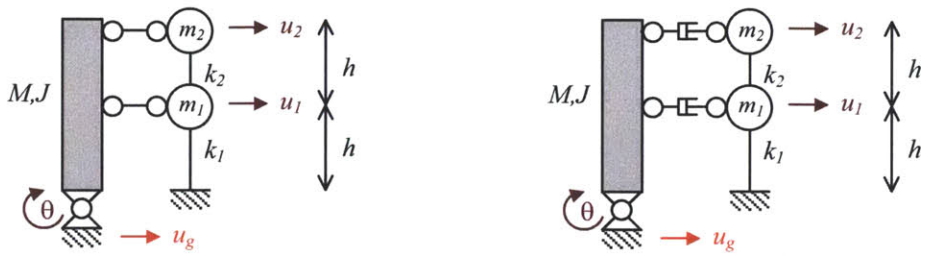

Figure 3.3.2. Schematic of a tributary two-story building model with rocking wall (a) without supplemental damping, (b) with supplemental damping

Initially, the rocking wall will be modeled as rigid. In subsequent models, the wall will be modeled as having finite rigidity, with the intent that an optimum rigidity will be found that maintains purely elastic deformation in the structure.

Initially, Lagrange's equation will be solved without taking the ground motion into account. Assuming deflections are small, a condition which the rocking wall is intended to enforce, changes in gravitational potential energy may be neglected, and the stiffness of the columns may be assumed to remain linear.

Three models of the rocking wall-building system are presented, of increasing complexity. First a model with a rigid wall is presented, then a model with a flexible wall, and finally the complete analytical stiffness matrix of the system will be presented.

3.4. Solving an Analytical Model without Rocking Wall

Before the model including the effect of the rocking wall is solved, the model without the rocking wall attached must be solved, so that the outputs of the two models can later be compared and contrasted, and so the benefit that the rocking wall has introduced can be clearly shown.

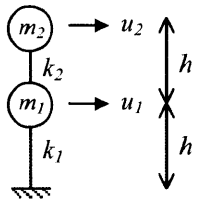

Figure 3.4.1. Lumped model of two-story building without rocking wall attached.

This system is of course trivial to solve,[40] with a characteristic equation and fundamental frequency of:

$$\begin{bmatrix} m_1 & 0 \\ 0 & m_2 \end{bmatrix}\begin{bmatrix} \ddot{u}_1 \\ \ddot{u}_2 \end{bmatrix}+\begin{bmatrix} k_1+k_2 & -k_2 \\ -k_2 & k_2 \end{bmatrix}\begin{bmatrix} u_1 \\ u_2 \end{bmatrix}=\underline{0} \qquad (3.1a)$$

$$\omega_n^2=\frac{k_1+k_2}{m_1+4m_2} \qquad (3.1b)$$

3.5. Solving an Analytical Model with Rigid Rocking Wall

The objective model is a model with ground motion, and flexible wall. But as a first model, the ground motion, damping, and the flexibility of the wall can be ignored. The kinetic and potential energies of the structure are thus:

$$K = \tfrac{1}{2}m_1\dot{u}_1^2 + \tfrac{1}{2}m_2\dot{u}_2^2 + \tfrac{1}{2}M\dot{u}_1^2 + \tfrac{1}{2}J\dot{\theta}^2 \qquad (3.2)$$

[40] *Chopra (2006)*

$$V = \tfrac{1}{2}k_2u_1^2 + \tfrac{1}{2}k_1(u_2 - u_1)^2 \tag{3.3}$$

However, since the rocking wall is initially being modeled as rigid, and small rotations are assumed, the geometric conditions exist:

$$u_2 = 2u_1 \tag{3.4}$$

$$\theta = \frac{u_1}{h} \tag{3.5}$$

and so without damping:

$$K = \tfrac{1}{2}m_1\dot{u}_1^2 + 2m_2\dot{u}_1^2 + \tfrac{1}{2}M\dot{u}_1^2 + \tfrac{1}{2}J(\frac{\dot{u}_1}{h})^2 = \tfrac{1}{2}(m_1 + 4m_2 + M + \frac{J}{h^2})\dot{u}_1^2 \tag{3.6}$$

$$V = \tfrac{1}{2}k_2u_1^2 + \tfrac{1}{2}k_1u_1^2 = \tfrac{1}{2}(k_1 + k_2)u_1^2 \tag{3.7}$$

$$\frac{\partial}{\partial t}(\frac{\partial K}{\partial \dot{u}_1}) = (m_1 + 4m_2 + M + \frac{J}{h^2})\ddot{u}_1^2 \tag{3.8}$$

$$\frac{\partial K}{\partial u_1} = 0 \tag{3.9}$$

$$\frac{\partial V}{\partial u_1} = (k_1 + k_2)u_1 \tag{3.10}$$

Thus from Lagrange's equation, the unforced equation of motion and natural frequency of the structure are shown to be:

$$(m_1 + 4m_2 + M + \frac{J}{h^2})\ddot{u}_1 + (k_1 + k_2)u_1 = 0 \tag{3.11}$$

$$\omega_n^2 = \frac{k_1 + k_2}{m_1 + 4m_2 + M + \dfrac{J}{h^2}} \tag{3.12}$$

Thus, assuming an approximately linear mode both with and without the rocking wall, the rocking wall decreases the fundamental frequency by an amount equal to $1 + \dfrac{M + \dfrac{J}{h^2}}{m_1 + 4m_2}$.

3.6 Solving an Analytical Model with Flexible Wall, Assumed Modes

This model is somewhat more realistic, but significantly more complex. In addition to a rigid mode, an appropriate non-rigid mode shall be superposed. It is noted that the first non-rigid mode and frequency of an ideal pin-ended beam free at the other end are:[41]

$$\omega_1 = (\frac{5}{4})^2\sqrt{\frac{\pi^4 EI}{\rho AL^2}} \qquad (3.17)$$

$$\psi_1 = \sin \alpha x - \frac{1}{\sqrt{2}}\frac{\sinh \alpha x}{\sinh \alpha L} \text{ (where } \alpha = \frac{5\pi}{4L}) \qquad (3.18)$$

which, as *figure 3.6.1* shows, may be approximated as:

$$\psi_1 \approx \sin \alpha x \qquad (3.19)$$

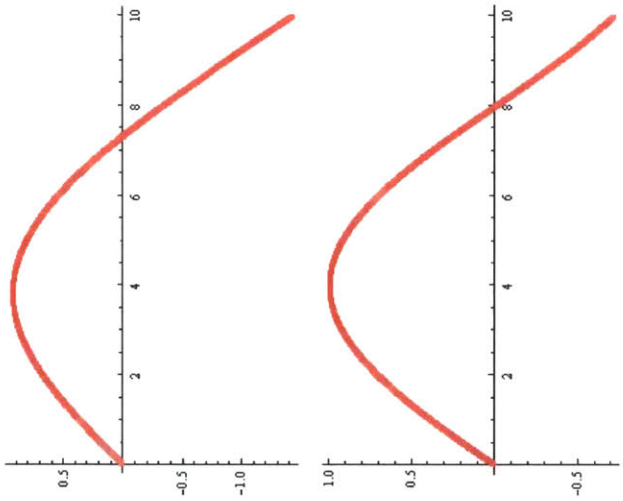

Figure 3.6.1. The non-rigid trial mode (a) $\psi_1 = \sin \alpha x - \frac{1}{\sqrt{2}}\frac{\sinh \alpha x}{\sinh \alpha L}$ *(b)* $\psi_1 \approx \sin \alpha x$

Clearly, the rigid body mode is:

$$\psi_0 = \frac{x}{L} \qquad (3.20)$$

Thus, if the following deformation form is assumed:

$$u = \psi_0 q_0(t) + \psi_1 q_1(t) \qquad (3.21)$$

[41] *Kausel (2010)*

Lagrange's equation may be applied to this problem, using the assumed modes method.

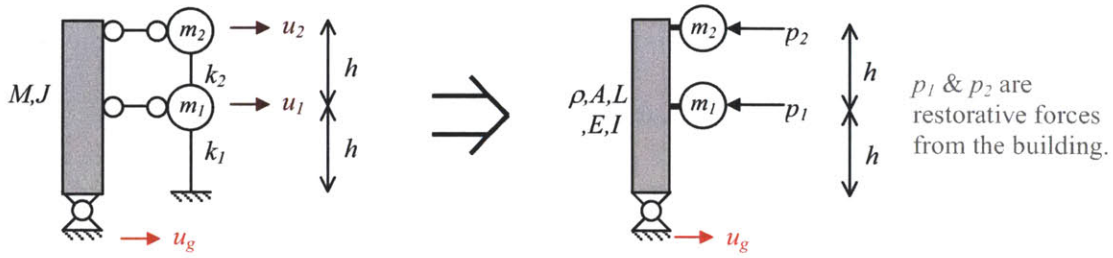

Figure 3.6.1. Further simplified rocking wall model

A model for the system may be presented as shown in *figure 3.6.1*. The building may be replaced by external restorative loads on the wall, which may be found by solving:

$$\underline{p} = \boldsymbol{K_b}\underline{u} \qquad (3.22)$$

where $\boldsymbol{K_b}$ is the stiffness matrix of the building.

The method used to solve the above system is extensive, though programmatically relatively straightforward. The *MATLAB* code that was used to solve the above system using Lagrange's equations may be found in *Appendix C*.

3.7. Solving an Analytical Model with Flexible Wall, Assumed Modes, Full Analysis

A third method to apply the seismic action is to solve the continuous system problem using the assumed modes method. This method requires a number of modes to be assumed, and increases in accuracy as the number of assumed modes is increased. This method is not subsequently used in the final formulation presented in this work, but is included for completeness. This method is similar to that presented in *section 3.6*, but does not simplify the problem by modelling the building force as an external load and requiring a computational solution.

In this formulation, two modes are considered: a linear mode ψ_0, and a chosen mode ψ_1, for which a good choice would be either of the modes shown in *figure 3.6.1*. In the following derivation, u represents the absolute displacement and v the relative displacement to the ground.

Consider the general problem as shown in *figure 3.7.1*:

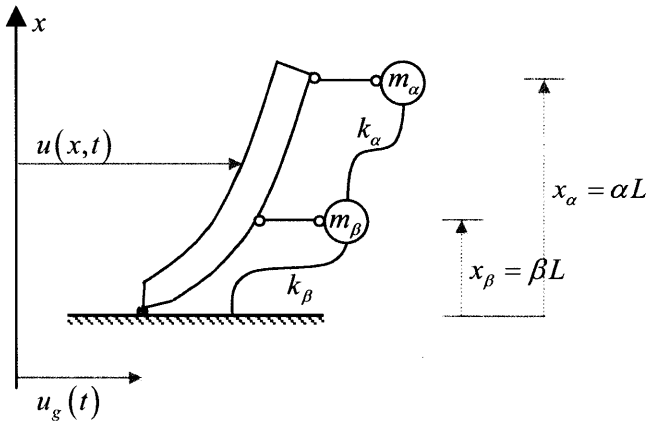

Figure 3.7.1. The rocking wall problem generalized.

From *figure 3.7.1*, it is observed that:

$$u(x,t)=v(x,t)+u_g,\ u_\alpha(t)=u(x_\alpha,t)=u(\alpha L,t), \tag{3.23}$$

$$u_\beta(t)=u(x_\beta,t)=u(\beta L,t) \tag{3.24}$$

Now define:

$$\psi_1(\alpha L)\equiv\psi_{1\alpha},\ \psi_1(\beta L)\equiv\psi_{1\beta}, \tag{3.25}$$

then:

$$\begin{aligned} K &= \tfrac{1}{2}\int_0^L \dot{u}^2\rho A dx+\tfrac{1}{2}m_\alpha\dot{u}_\alpha^2+\tfrac{1}{2}m_\beta\dot{u}_\beta^2 \\ &= \tfrac{1}{2}\left\{\int_0^L\left(\dot{v}+\dot{u}_g\right)^2\rho A dx+m_\alpha\left(\dot{v}_\alpha+\dot{u}_g\right)^2+m_\beta\left(\dot{v}_\beta+\dot{u}_g\right)^2\right\} \\ &= \tfrac{1}{2}\left\{\int_0^L\left(\tfrac{x}{L}\dot{q}_0+\psi_1\dot{q}_1+\dot{u}_g\right)^2\rho A dx+m_\alpha\left(\alpha\dot{q}_0+\psi_{1\alpha}\dot{q}_1+\dot{u}_g\right)^2+m_\beta\left(\beta\dot{q}_0+\psi_{1\beta}\dot{q}_1+\dot{u}_g\right)^2\right\} \end{aligned} \tag{3.26}$$

$$\frac{\partial K}{\partial \dot{q}_0} = \rho A \int_0^L \left(\tfrac{x}{L}\dot{q}_0 + \psi_1 \dot{q}_1 + \dot{u}_g\right)\tfrac{x}{L}dx + m_\alpha \alpha\left[\alpha\,\dot{q}_0 + \psi_{1\alpha}\dot{q}_1 + \dot{u}_g\right] + m_\beta \beta\left[\beta\,\dot{q}_0 + \psi_{1\beta}\,\dot{q}_1 + \dot{u}_g\right]$$

$$= \rho A\left[\frac{\dot{q}_0}{L^2}\int_0^L x^2 dx + \frac{\dot{q}_1}{L}\int_0^L \psi_1 x\,dx + \frac{\dot{u}_g}{L}\int_0^L x\,dx\right] + \left(\alpha^2 m_\alpha + \beta^2 m_\beta\right)\dot{q}_0 \qquad (3.27)$$

$$+\left(\alpha\, m_\alpha \psi_{1\alpha} + \beta m_\beta \psi_{1\beta}\right)\dot{q}_1 + \left(m_\alpha \alpha + m_\beta \beta\right)\dot{u}_g$$

$$\frac{\partial K}{\partial \dot{q}_1} = \rho A \int_0^L \left(\tfrac{x}{L}\dot{q}_0 + \psi_1 \dot{q}_1 + \dot{u}_g\right)\psi_1 dx + m_\alpha \psi_{1\alpha}\left[\alpha\,\dot{q}_0 + \psi_{1\alpha}\dot{q}_1 + \dot{u}_g\right] + m_\beta \psi_{1\beta}\left[\beta\,\dot{q}_0 + \psi_{1\beta}\dot{q}_1 + \dot{u}_g\right]$$

$$= \rho A\left[\frac{\dot{q}_0}{L}\int_0^L x\psi_1\,dx + \dot{q}_1\int_0^L \psi_1^2\,dx + \dot{u}_g\int_0^L \psi_1\,dx\right] + \left(\alpha\psi_{1\alpha}m_\alpha + \beta\psi_{1\beta}m_\beta\right)\dot{q}_0 \qquad (3.28)$$

$$+\left(\psi_{1\alpha}^2\, m_\alpha + \psi_{1\beta}^2 m_\beta\right)\dot{q}_1 + \left(\psi_{1\alpha} m_\alpha + \psi_{1\beta} m_\beta\right)\dot{u}_g$$

Hence differentiate these to find:

$$\frac{d}{dt}\left(\frac{\partial K}{\partial \dot{q}_0}\right) = \left(\tfrac{1}{3}\rho AL + \alpha^2 m_\alpha + \beta^2 m_\beta\right)\ddot{q}_0$$

$$+\left(\tfrac{1}{L}\rho A\int_0^L \psi_1 x\,dx + \alpha\, m_\alpha\psi_{1\alpha} + \beta m_\beta\psi_{1\beta}\right)\ddot{q}_1 + \left(\tfrac{1}{2}\rho AL + m_\alpha\alpha + m_\beta\beta\right)\ddot{u}_g \qquad (3.29)$$

$$\frac{d}{dt}\left(\frac{\partial K}{\partial \dot{q}_1}\right) = \left[\tfrac{1}{L}\rho A\int_0^L x\psi_1\,dx + \alpha\psi_{1\alpha}m_\alpha + \beta\psi_{1\beta}m_\beta\right]\ddot{q}_0$$

$$+\left[\rho A\int_0^L \psi_1^2\,dx + \psi_{1\alpha}^2\, m_\alpha + \psi_{1\beta}^2 m_\beta\right]\ddot{q}_1 + \left[\rho A\int_0^L \psi_1\,dx + \psi_{1\alpha}m_\alpha + \psi_{1\beta}m_\beta\right]\ddot{u}_g \qquad (3.30)$$

Also:

$$V = \tfrac{1}{2}\int_0^L EI\left(v''\right)^2 dx + \tfrac{1}{2}k_\alpha\left(v_\alpha - v_\beta\right)^2 + \tfrac{1}{2}k_\beta {v_\beta}^2$$

$$= \tfrac{1}{2}EI\int_0^L \left(\psi_1'' q_1\right)^2 dx + \tfrac{1}{2}k_\alpha\left(\left(\alpha-\beta\right)q_0 + \left(\psi_{1\alpha} - \psi_{1\beta}\right)q_1\right)^2 + \tfrac{1}{2}k_\beta\left(\beta q_0 + \psi_{1\beta}q_1\right)^2 \qquad (3.31)$$

$$\frac{\partial V}{\partial q_0} = k_\alpha\left(\alpha-\beta\right)\left[\left(\alpha-\beta\right)q_0 + \left(\psi_{1\alpha} - \psi_{1\beta}\right)q_1\right] + k_\beta\beta\left(\beta q_0 + \psi_{1\beta}q_1\right)$$

$$= \left[\left(\alpha-\beta\right)^2 k_\alpha + \beta^2 k_\beta\right]q_0 + \left[\left(\alpha-\beta\right)\left(\psi_{1\alpha} - \psi_{1\beta}\right)k_\alpha + \beta\psi_{1\beta}k_\beta\right]q_1 \qquad (3.32)$$

$$\frac{\partial V}{\partial q_1} = q_1 EI \int_0^L (\psi_1'')^2 \, dx + k_\alpha (\psi_{1\alpha} - \psi_{1\beta}) \left[(\alpha - \beta) q_0 + (\psi_{1\alpha} - \psi_{1\beta}) q_1 \right] + k_\beta \psi_{1\beta} (\beta q_0 + \psi_{1\beta} q_1)$$
$$= \left[(\alpha - \beta)(\psi_{1\alpha} - \psi_{1\beta}) k_\alpha + \beta \psi_{1\beta} k_\beta \right] q_0 + \left[EI \int_0^L (\psi_1'')^2 \, dx + (\psi_{1\alpha} - \psi_{1\beta})^2 k_\alpha + \psi_{1\beta}^2 k_\beta \right] q_1 \qquad (3.33)$$

Finally, applying Lagrange's equations:

$$\boldsymbol{M}\underline{\ddot{u}} + \boldsymbol{K}\underline{q} = -\underline{m}\ddot{u}_g$$

where:

$$\mathbf{M} = \begin{Bmatrix} \frac{1}{3}\rho AL + \alpha^2 m_\alpha + \beta^2 m_\beta & \frac{1}{L}\rho A \int_0^L \psi_1 x \, dx + \alpha m_\alpha \psi_{1\alpha} + \beta m_\beta \psi_{1\beta} \\ \frac{1}{L}\rho A \int_0^L x\psi_1 \, dx + \alpha \psi_{1\alpha} m_\alpha + \beta \psi_{1\beta} m_\beta & \rho A \int_0^L \psi_1^2 \, dx + \psi_{1\alpha}^2 m_\alpha + \psi_{1\beta}^2 m_\beta \end{Bmatrix} \qquad (3.34)$$

$$\mathbf{K} = \begin{Bmatrix} (\alpha - \beta)^2 k_\alpha + \beta^2 k_\beta & (\alpha - \beta)(\psi_{1\alpha} - \psi_{1\beta}) k_\alpha + \beta \psi_{1\beta} k_\beta \\ (\alpha - \beta)(\psi_{1\alpha} - \psi_{1\beta}) k_\alpha + \beta \psi_{1\beta} k_\beta & EI \int_0^L (\psi_1'')^2 \, dx + (\psi_{1\alpha} - \psi_{1\beta})^2 k_\alpha + \psi_{1\beta}^2 k_\beta \end{Bmatrix} \qquad (3.35)$$

$$\underline{m} = \begin{Bmatrix} \frac{1}{2}\rho AL + m_\alpha \alpha + m_\beta \beta \\ \rho A \int_0^L \psi_1 \, dx + \psi_{1\alpha} m_\alpha + \psi_{1\beta} m_\beta \end{Bmatrix}, \quad \underline{q} = \begin{Bmatrix} q_0 \\ q_1 \end{Bmatrix} \qquad (3.36)$$

Thus using the above formulation, the ground acceleration $\ddot{u}_g$ may be set to be the maximum ground acceleration S_a for a certain considered earthquake, and the system solved for that case.

3.8. Applying Seismic Action to the Analytical Model

Applying seismic action to a model can be achieved a number of ways. To solve discrete systems, the mass and stiffness matrices of the whole system $\boldsymbol{M}$ & $\boldsymbol{K}$ may be found, and the system solved for an earthquake ground acceleration $\ddot{u}_g$:[42]

$$\boldsymbol{M}\ddot{\underline{v}} + \boldsymbol{C}\dot{\underline{v}} + \boldsymbol{K}\underline{v} = -\boldsymbol{M}\underline{e}\ddot{u}_g \qquad (3.37)$$

where $\underline{e}$ is the unit constant rigid body vector, and $\underline{v}$ is the relative displacement:

$$\underline{v} = \underline{u} - \underline{e}u_g \qquad (3.38)$$

However, in order to model the rocking wall, a continuous element, another approach must be taken. One option is to discretize the rocking wall into lumped masses, and solve the problem as a discrete dynamic system. The other is to solve the flexible wall problem fully analytically as in *section 3.7*.

The quasi-static approach to applying seismic action is to apply forces, which are proportional to the square of the height, to the masses of the building. The values of these forces may be found analytically, and guides to aid their calculation are found in building codes. To solve the rocking wall as a statics problem, these loads may be applied to the analytical model, and find the resultant displacements.

To achieve either of the above methods of applying the seismic action, the stiffness matrix for the rocking wall-building system must be determined. This may be found empirically, for example using a finite element approach for a specific system under consideration.[43] However, it

[42] *Chopra (2006)*
[43] *Bathe (1996)*

would be far more valuable to determine the general analytical stiffness matrix of this system, for any given system parameters. That stiffness matrix is derived in *Section 3.10.*

3.9. Applying Static Equivalent Seismic Action

There are various methods of force-based design and analysis, such as equivalent lateral force method, response spectrum method, nonlinear static analysis, and nonlinear time-history analysis. The equivalent lateral force method is valid for modeling linear systems in 2D and considers the fundamental mode. This is particularly appropriate for the rocking wall-building system, since the system is intentionally constrained to primarily fundamental mode action.

The equivalent lateral force method involves representing the seismic activity as forces applied at each story by the equation:

$$F_j = \frac{V h_j^2 m_j}{\sum_i h_i^2 m_i} \qquad (3.39)$$

where V is the base shear, j, i are the floor number starting from the first floor above ground, h is the height of the floor from ground, and m is the mass of the floor.

The procedure for determining the equivalent lateral forces follows.[44]

The seismic base shear V, is determined by:

$$V = C_s W \qquad (3.40^{45})$$

where C_s is the seismic response coefficient, and W is the effective seismic weight.

[44] *ASCE (2006)*

The effective seismic weight of the building W, is defined by the code.[46] C_s is given by:

$$C_s = \frac{S_{DS}}{\left(\frac{R}{I}\right)} \qquad (3.41^{47})$$

where S_{DS} is the design spectral response acceleration at short period, R is the response modification factor, and I is the occupancy importance factor.

The design earthquake spectral response acceleration parameter at short period, S_{DS}, is given by:

$$S_{DS} = \frac{2}{3} S_{MS} \qquad (3.42^{48})$$

where S_{MS}, the Maximum Considered Earthquake (MCE) spectral response acceleration for short periods, is given by:

$$S_{MS} = F_a S_s \qquad (3.43^{49})$$

Here, S_s is the mapped MCE spectral response acceleration at short periods and F_a is a site coefficient. F_a is dependent on the Site Class and S_s. S_s is determined from the *0.2s* spectral response accelerations as shown by a contour map of the Unites States given in a specified figure.[50]

The code states that "Where the soil properties are not known in sufficient detail to determine the site class, Site Class D shall be used.".[51] In that case, F_a is found to be *1.6*.[52]

[45] *ASCE (2006), Eqn. 12.8-1*
[46] *ASCE (2006), Section 12.7.2*
[47] *ASCE (2006), Eqn. 12.8-2*
[48] *ASCE (2006), Eqn. 11.4-3*
[49] *ASCE (2006), Eqn. 11.4-1*
[50] *ASCE (2006), Figure 22-1*
[51] *ASCE (2006), Section 20.1*

Assuming an Occupancy Category of *III*,[53] the importance factor, *I*, is determined to be *1.25*.[54]

The response modification factor *R* is determined to be *4*, assuming an ordinary reinforced concrete shear wall.[55]

The value of C_s must not exceed:

$$C_s = \frac{S_{D1}}{T\left(\frac{R}{I}\right)} \quad for \quad T \le T_L \qquad (3.45^{56})$$

$$C_s = \frac{S_{D1}T_L}{T^2\left(\frac{R}{I}\right)} \quad for\ T > T_L \qquad (3.46^{57})$$

Additionally, C_s must not be less than 0.01.[58]

For structures located where $S_1 \geq 0.6$g, C_s must not be less than:

$$C_s = \frac{0.5S_1}{\left(\frac{R}{I}\right)} \qquad (3.47^{59})$$

In the above formulae, S_{D1}, T_L, T, and S_1 are to be evaluated.

S_{D1} is the design earthquake spectral response acceleration parameter at 1s period, and it is determined by:

[52] *ASCE (2006), Table 11.4-1*
[53] *ASCE (2006), Table 1-1*
[54] *ASCE (2006), Table 11.5-1*
[55] *ASCE (2006), Table 12.2-1*
[56] *ASCE (2006), Eqn. 12.8-3*
[57] *ASCE (2006), Eqn. 12.8-4*
[58] *ASCE (2006), Eqn. 12.8-5*
[59] *ASCE (2006), Eqn. 12.8-6*

$$S_{D1} = \frac{2}{3} S_{M1} \qquad (3.48^{60})$$

S_{M1}, the MCE spectral response acceleration at *1s* period, is determined by:

$$S_{M1} = F_v S_1 \qquad (3.49^{61})$$

S_1, the mapped MCE spectral response acceleration at a period of *1s*, is determined from a specified figure,[62] and F_v, a site coefficient, is determined from a specified table.[63]

T is the fundamental period of the structure. The approximate period T_a is found by the formula:

$$T_a = C_t h_n^x \qquad (3.50^{64})$$

where h_n is the height in feet above the base to the highest level of the structure and the coefficients C_t and x are determined from a specified table.[65]

3.10. Solving an Analytical Model with Flexible Wall, with Full Stiffness Matrix

The full analytical model of the rocking wall-discretized building system, concluding with the definition of the general stiffness matrix for this system, is first derived in this section.

[60] *ASCE (2006), Eqn. 11.4-4*
[61] *ASCE (2006), Eqn. 11.4-2*
[62] *ASCE (2006), Figure 22-2*
[63] *ASCE (2006), Table 11.4-2*
[64] *ASCE (2006), Eqn. 12.8-7*

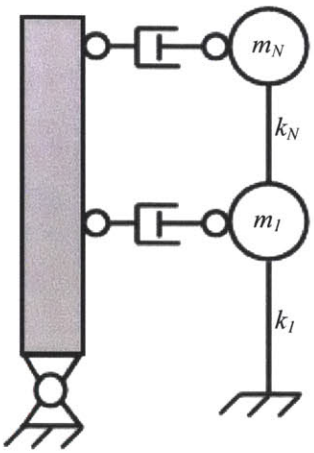

Figure 3.10.1. The statically condensed rocking wall-building system to be modeled.

The rocking wall-structure system is illustrated in *figure 3.10.1*, in which k_i and m_i represent the stiffness and tributary mass respectively of the i^{th} story. The development of the model begins by representing the rocking wall as a hinged beam, as shown in *figure 3.10.2*, in which F_i represent any loading on the beam that is constrained to static equilibrium.

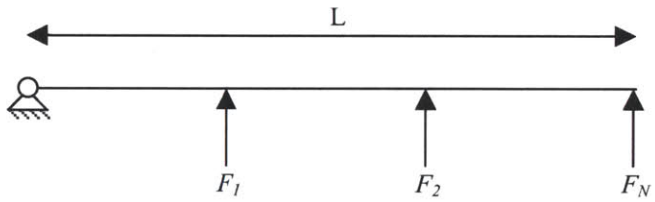

Figure 3.10.2. Model of the free rocking wall.

Computing moments about the pin, assuming constant inter-story height for simplicity, and setting the lowermost force to be a function of the others, an expression to describe the link forces F_i is obtained,

$$F_1 = -2F_2 - 3F_3 \ldots - NF_N \qquad (3.51)$$

[65] *ASCE (2006), Table 12.8-2*

These forces may be applied to the beam model in balanced pairs. First F_N at node N with a reaction of $-NF_N$ at position *1*, illustrated in *figure 3.10.3*, followed by F_{N-1} at node *N-1* with a reaction of $-(N-1)F_{N-1}$ at position *1*, and so on.

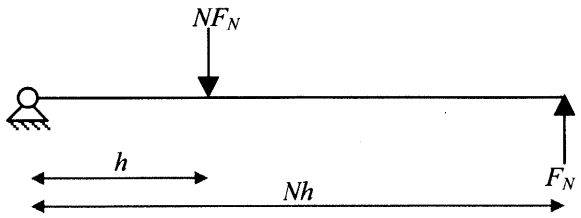

Figure 3.10.3. Loads applied to the mechanism in pairs, maintaining static equilibrium

It is shown readily that the order *N–1 pseudo*-flexibility matrix $\boldsymbol{F}_{wall}$ consists of elements:

$$\{\boldsymbol{F}_{wall}\}_{ij} = \frac{aL}{3NEI}x + \frac{x^2}{6EI}(-x + 3a) \quad (i \leq j;\ 1 \leq i,j \leq N\text{-}1;\ \text{i.e. } x \leq a) \tag{3.52}$$

$$\{\boldsymbol{F}_{wall}\}_{ij} = \frac{aL}{3NEI}x + \frac{a^2}{6EI}(3x - a) \quad (i > j;\ 1 \leq i,j \leq N\text{-}1;\ \text{i.e. } x > a) \tag{3.53}$$

which consist of a rotational term and a cantilever term, and where x and a are *distance to point of measurement* and *distance to point of application of load* from the pin respectively, and obtained as:

$$x = \frac{i\text{-}2}{N}L \tag{3.54}$$

$$a = \frac{j\text{-}2}{N}L \tag{3.55}$$

Thus rather than providing the displacements, $\boldsymbol{F}_{wall}$ provides the relative shape, $\underline{W} = \boldsymbol{F}_{wall}\,\underline{F}_w$, of the wall, under the statically-balanced loading $\underline{F}_w$, where the zero reference line is projected from the pin, through the lowest load-position on the beam, as illustrated in *figure 3.10.4*.

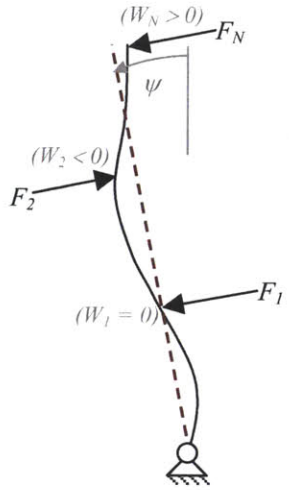

Figure 3.10.4. The model beam under an arbitrary loading and deformation. The reference line, shown dashed, coincides with the lowest beam reference position, requiring that the relative displacement W_1=0. ψ is the small angle through which the reference line is displaced.

A vector of displacements relative to the reference line may be defined as $\underline{W}$. The total displacement of the wall is given by $\underline{W}$, plus a rigid body rotation. For now, let $\underline{W}$ be of size *N-1*, omitting the lowest relative displacement $W_1 = 0$. The analysis may be continued by recognizing that since the beam is a mechanism, it may be rotated to any arbitrary small angle ψ under an arbitrary balanced loading, such that the absolute positions of the beam are a rigid body rotation displacement $\underline{\psi}$, plus the deviations from that line, $\underline{W}$. Additional information is required to fix the beam in space. Consider the model in *figure 3.10.5*, where $\underline{U}$, $\underline{V}$, $\underline{P}$, $\underline{Q}$, and $\underline{F}$ are vectors of displacements of the building and wall, loading on the building and wall, and link forces respectively.

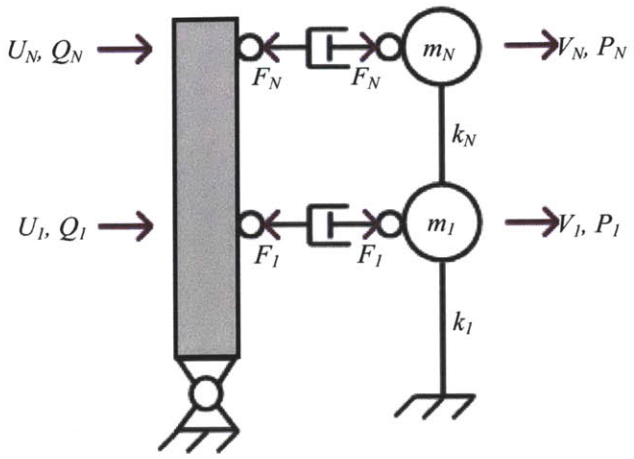

Figure 3.10.5. The rocking wall-building system model with forces and displacements required to complete the analysis

From the previous discussion, a matrix $\boldsymbol{F_{wall}}$ that uniquely maps the upper *N-1* net forces to the relative displacements of the wall $\underline{W}$ is determined. Since this mapping is clearly unique, $\boldsymbol{F_{wall}}$ may be inverted to $\boldsymbol{K_{wall}}$. Thus the order of $\boldsymbol{K_{wall}}$ may be incremented to N, by temporarily adding a leftmost zero column and topmost zero row. Thus $\boldsymbol{K_{wall}}$ now uniquely maps all N relative displacements $\underline{W}$, including the lowest relative displacement W_1 which is always zero, to the *upper N-1* forces $\underline{F_w}'$ on the wall:

$$\underline{F_w}' = \boldsymbol{K_{wall}}\underline{W} \tag{3.56}$$

The vector $\underline{F_w}'$ is denoted prime since it is incomplete: it incorrectly records the force applied to the lowest position on the wall as zero. That force may be determined by applying moments at the pin. A matrix $\boldsymbol{M_o}$ may be formulated which enforces the principle of moments, such that:

$$\underline{F_{w,1}} = \begin{bmatrix} F_{w,1} \\ 0 \\ \vdots \\ 0 \end{bmatrix} = \boldsymbol{M_o}\underline{F_w}' \tag{3.57}$$

where:

$$\boldsymbol{M_o} = \begin{bmatrix} 0 & \cdots & -(N-1) & -N \\ \vdots & & & 0 \\ \vdots & & & \vdots \\ 0 & \cdots & \cdots & 0 \end{bmatrix} \tag{3.58}$$

Thus, the complete net force on the wall is found to be:

$$\underline{F_w} = \underline{F_w}' + \boldsymbol{M_o}\underline{F_w}' = (\boldsymbol{M_o} + \boldsymbol{I})\underline{F_w}' = (\boldsymbol{M_o} + \boldsymbol{I})\boldsymbol{K_{wall}}\underline{W} \tag{3.59}$$

Since the total forces on the wall and on the building are defined as:

$$\underline{F_w} = \underline{Q} - \underline{F} \tag{3.60}$$

$$\underline{F_b} = \underline{P} + \underline{F} \tag{3.61}$$

These may be rearranged to:

$$\underline{F} = \underline{Q} - \underline{F_w} = \underline{Q} - (\boldsymbol{M_o} + \boldsymbol{I})\boldsymbol{K_{wall}}\underline{W} \tag{3.62}$$

$$\underline{F} = \underline{F_b} - \underline{P} = \boldsymbol{K_{bldg}}\underline{U} - \underline{P} \tag{3.63}$$

Applying Newton's third axiom, the above two formulae may be equated and rearranged:

$$\boldsymbol{K_{bldg}}\underline{U} + (\boldsymbol{M_o} + \boldsymbol{I})\boldsymbol{K_{wall}}\underline{W} = \underline{P} + \underline{Q} \tag{3.64}$$

As discussed, the absolute displacement of the wall is given as:

$$\underline{V} = \underline{\psi} + \underline{W} \tag{3.65}$$

where $\underline{\psi}$ is the arbitrary rigid body rotation vector, and $\underline{W}$ is the relative displacement of each point about that rigid body rotation. If ψ is the scalar angle of rotation, then:

$$\underline{\psi} = \psi \begin{bmatrix} h \\ 2h \\ \vdots \\ Nh \end{bmatrix} \tag{3.66}$$

And since the lowest position lies on the line by definition:

$$\psi = \frac{V_1}{h} \tag{3.67}$$

Thus *equation 3.65* becomes:

$$\underline{\Psi} = V_1 \begin{bmatrix} 1 \\ 2 \\ \vdots \\ N \end{bmatrix} \tag{3.68}$$

or:

$$\underline{\Psi} = \boldsymbol{L_1}\underline{V} \tag{3.69}$$

where $\boldsymbol{L_1}$ is a linear matrix that acts on the 1st term of a vector:

$$\boldsymbol{L_1} = \begin{bmatrix} 1 & 0 & \dots & 0 \\ 2 & & & \vdots \\ \vdots & & & \vdots \\ N & 0 & \dots & 0 \end{bmatrix} \tag{3.70}$$

Substituting *equation 3.69* into *equation 3.65*, it is found that:

$$\underline{W} = \underline{V} - \boldsymbol{L_1}\underline{V} = (\boldsymbol{I} - \boldsymbol{L_1})\underline{V} \tag{3.71}$$

which may be substituted into *equation 3.64* to yield:

$$\boldsymbol{K_{bldg}}\underline{U} + (\boldsymbol{M_o} + \boldsymbol{I})\boldsymbol{K_{wall}}(\boldsymbol{I} - \boldsymbol{L_1})\underline{V} = \underline{P} + \underline{Q} \tag{3.72}$$

If damping is to be added between the wall and the building, $\underline{U}$ and $\underline{V}$ must be considered independent. However, damping is outside of the scope of this work, where only quasi-static loading is considered. Without damping, it may be assumed that the links are rigid, and thus that the building displacements $\underline{U}$ are equal to the wall displacements $\underline{V}$. Thus the stiffness matrix of the undamped system is finally shown:

$$[\boldsymbol{K_{bldg}} + (\boldsymbol{M_o} + \boldsymbol{I})\boldsymbol{K_{wall}}(\boldsymbol{I} - \boldsymbol{L_1})]\underline{U} = \underline{P} + \underline{Q} \tag{3.73}$$

where $\underline{P} + \underline{Q}$ are the combined loads on the system, and the matrices are as previously defined. A *MATLAB* code that performs these calculations, returning the full stiffness numerical matrix of any given rocking wall-building system may be found in *Appendix D*.

Using the displacements $\underline{U}$ found with *equation 3.73*, *equation 3.61* may be rearranged to find $\underline{F}$, the forces in the links:

$$\underline{F} = \underline{F}_b - \underline{P} = \boldsymbol{K}_{bldg}\underline{U} - \underline{P} \qquad (3.74)$$

If a structure makes use of supplemental damping systems, and the seismic loads are to be applied in a quasi-static fashion, this measure of the link forces should be considered as an upper bound, since that method of applying seismic loads implicitly discounts any supplemental damping that may be added to a system.

This general model matches a good linear finite element analysis exactly, as illustrated in *figure 3.10.6*.

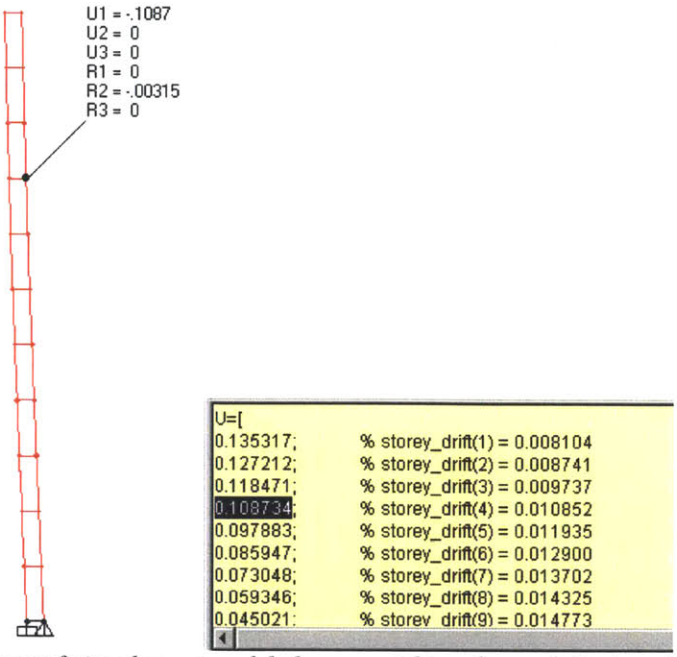

Figure 3.10.6 (a) & (b) A linear finite element model shown matching the analytical model derived above to every significant figure returned. In this case the structure is loaded under seismic equivalent loading.

3.11. Benchmark Buildings

In order to illustrate some of the ways in which the methods presented in this work may be applied, it was required to develop a set of benchmark buildings, which could reasonably represent buildings that might be found in practice. The benchmark buildings were to consist of stiffness profiles, mass profiles, and varying numbers of stories.

This requirement is a common one for structural research, and yet to the best of my knowledge, no qualified set of benchmark buildings, or method for producing a qualified benchmark building, is readily available to students and researchers.

As a significant sub-project of this work, a fully comprehensive method was developed, using principles from widely accepted building codes, to generate the stiffness and mass matrices to

define benchmark buildings. Using that method, 56 benchmark buildings were developed, ranging from 2 to 15 stories in height. These benchmark buildings were tested with 116 different rocking wall configurations, and the rocking wall design graph, as shown in *sections 4.4 – 4.6*, for each benchmark building was found.

The method of creating benchmark buildings, the data for the benchmark buildings generated, and the associated rocking wall design graphs, may be found in *Appendix B*.

The intent of the tables in *Appendix B* is that an engineer implementing a rocking wall project would be able to find a close approximation of the building under consideration, and in a matter of minutes determine the approximate size and number of rocking walls that would be appropriate, and whether rocking wall retrofit would be appropriate at all.

It is seen from the tables, for example, that for the benchmark (and thus intended to be representative) buildings of only two stories, there is no possible rocking wall configuration that will reduce the maximum story drift. And many other similarly interesting conclusions may also be drawn from the tables.

The entire sub-project relating to benchmark buildings is presented in *Appendix B*.

3.12. Software Implementation

Software has been developed which solves the entire process described in *section 3.10*, and offers many functions that will be useful for structural engineers who are designing a rocking wall installation, and also for those working on a standard design project.

The software developed finds the stiffness matrix of the building based on the stiffness distribution and a single story stiffness, if available. Otherwise, the software finds the stiffness matrix by extrapolation of the *ASCE 7-05* code, given whatever information the engineer has available, such as the number of stories and lateral load resisting system, or the measured natural period of the building. In the process of finding the stiffness matrix, the software also determines the natural mode. The software then determines the total stiffness matrix of the building-rocking wall system, and the equivalent seismic loads including the additional inertia of rocking wall. The software then incrementally increases the size of the rocking wall, finding the maximum story displacement under seismic loading for each rocking wall size, and reports the minimum of those story displacements, and the rocking wall size that causes it, providing the engineer with an optimization technique.

In order to apply the seismic loads including the inertia of the rocking wall (which is critical to finding the minimum story drift), the mass of the rocking wall is discretized. *Figure 3.12.1* illustrates this, and also illustrates the point that the rocking wall may rotate, but the building floors do not.

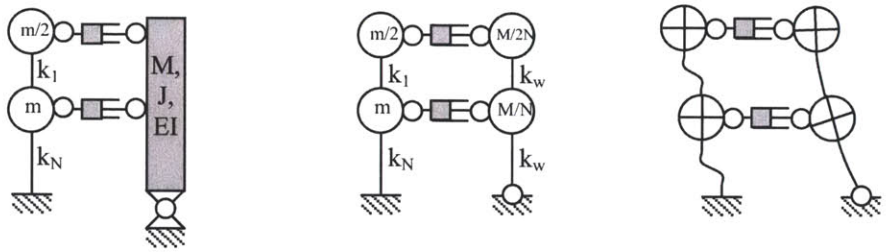

Figure 3.12.1. (a) The building-rocking wall system with the building discretized, (b) with the rocking wall also discretized, (c) the system in a displaced state.

Based on 11 basic pieces of information about the building and its locality, the software provides:

- The code-determined period T_n
- The maximum story drift without rocking wall
- The building stiffness vector without rocking wall
- The building natural mode without rocking wall
- The fundamental period T_n without any rocking wall from the Rayleigh Quotient formula (this matches the code-derived period, as it has been re-derived from the mass matrix and stiffness matrix derived from the code)
- Spreadsheet-ready tab-delimited data relating wall width to maximum story drift for many wall widths
- The wall width that allows the minimum maximum story drift

Also, for the width that gives the minimum story drift, and also any chosen wall width (e.g. no wall), the software provides:

- The code-determined base shear V
- The equivalent seismic loads P_j

- The natural mode for the building with the rocking wall
- The total flexibility matrix including the rocking wall
- The forces in the links joining the building to the rocking wall
- The displacements of the structure under seismic equivalent loading, and the story drifts
- The story at which the maximum story drift occurs

All of the data is returned in *MATLAB*-ready syntax, which may be copied from the software, should the engineer wish to perform further calculations with it.

Figure 3.12.2. Website with illustrative software created for this work.

3.13. Software to Implement ASCE 7-05 Equivalent Seismic Loads

Through careful interpretation of the *ASCE 7-05* code, it was possible to develop software that would accurately determine the equivalent seismic loads for any given structure. It was vital to develop this independently, firstly since it would be the foundation for developing further software that would automate the process of applying those loads to structures. In addition, the code is highly complex, and it is very easy to make mistakes in its application. For example, a popular online calculator tool, by Buildings Guide[66], makes an error in determining the approximate period of the structure. In applying the formula:

$$T_a = C_T h_n^x \qquad (3.75^{67})$$

that calculator neglects the fact that the above formula is only for moment frame systems, not for shear wall systems,[68] even though that calculator's default setting is a shear wall system. The ASCE code does give the formula for calculating the approximate period for a shear wall building, but it is complex, requiring summation terms. Another common mistake is to use the geographical short period acceleration S_s for buildings under six stories tall, but the code requires a fixed S_s of *1.5* in that case. The software developed for this work takes all of these factors into account, and allows for up to 19 shear walls (the limitation is only there to prevent the interface from being too large).

[66] *Buildings Guide (2012)*
[67] *ASCE (2006), p129*
[68] *ASCE (2006), p129*

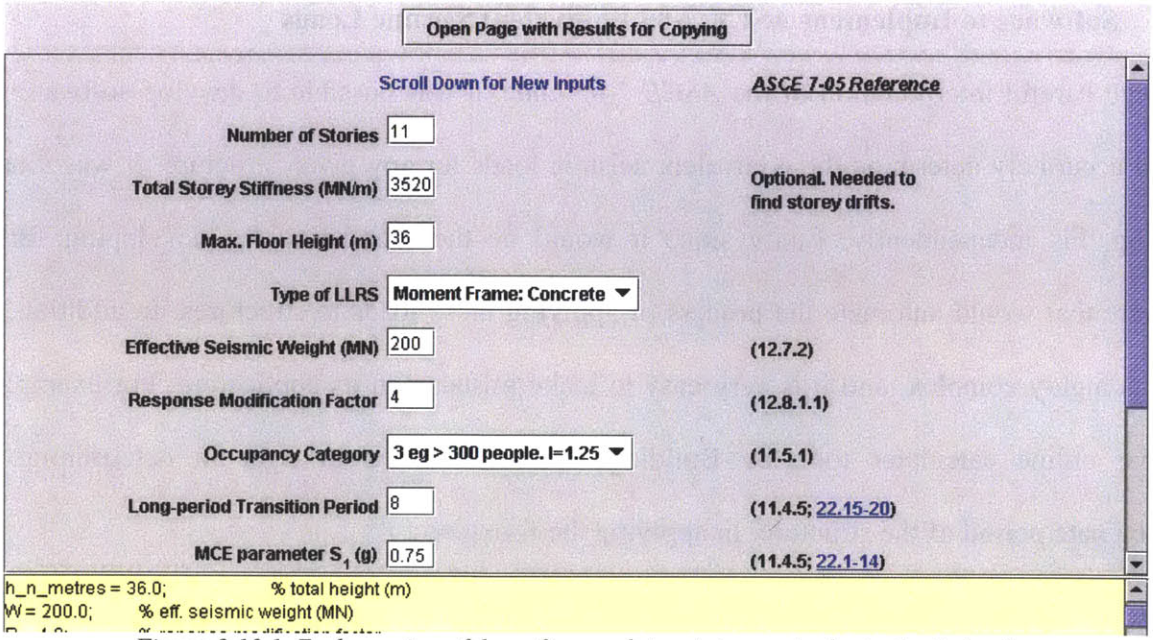

Figure 3.13.1. Early version of the software, determining equivalent seismic loads.

Developing software that reliably implemented the ASCE code was significantly more tractable after first translating the ASCE earthquake code to a graphical form. The software is available as an unsigned Java applet, so any researcher or engineer can use it. Every step of the calculation is reported to the user, in *MATLAB*-ready format. The software also calculates the equivalent seismic loads for the user, which no known online calculator currently does.

4. Analysis of Rocking Wall Design

4.1. Natural Frequencies of the Simulations

The analytical model with flexible wall using assumed modes, given in *section 3.6*, solved with *MATLAB* code given in *Appendix C*, using a rocking wall with the dimensions used in the case study retrofit (*14.4ft* wide by *2ft* deep, as shown in *section 2.5*), and a two-story test model, produces a period of *0.363s* for the first natural mode, and *0.0106s* for the second natural mode. The finite element model, with *SAP2000* used to perform the calculations, produces a period of *0.369s* for the first natural mode, and *0.0181s* for the second natural mode, for the same model. The analytical model thus produces a first period that is only *1.7%* less than the finite element model, and a second period which is *41%* less than the finite element method.

It should be expected that the first mode is the most accurate for the analytical model, since currently only two trial modes have been applied to the system. As the number of trial modes is increased, the accuracy of the higher modes improves.[69]

A natural period within *1.7%* of the finite element model is a very good start to the modelling process. The accuracy of this result is an indicator that the analytical model is good and that appropriate trial modes were chosen to represent the system.

[69] *Chopra (2006)*

4.2. Natural Frequencies of the System With and Without Rocking Wall

The analytical model without the rocking wall, solved in *MATLAB*, procuces natural periods of *0.33118s*, and *0.13718s* for the two story test model. The finite element model produces natural periods of *0.33117s*, and *0.13718s* for the same model. This virtually exact match should be expected, and confirms that the basic principles of the analytical model are good.

As expected, adding the rocking wall increases the period of the first mode by *11%*, making the structure less stiff in that mode, while decreasing the period of the second mode (considering the finite element result) by a notional *87%*, making the structure much stiffer in that mode. Both of these effects are generally good for the seismic response of a building, as illustrated in *figure 1.3*.

4.3. Modes of the System with Varying Stiffness of Rocking Wall

The stiffening effect of the rocking wall on the fundamental mode may be illustrated by solving the analytical model using the *MATLAB* code in *Appendix C*, and finding the modes of the system quantitatively, with varying stiffness of rocking wall, and with the rocking wall removed entirely. The following figures illustrate these results for the first mode of the same two-story test model.

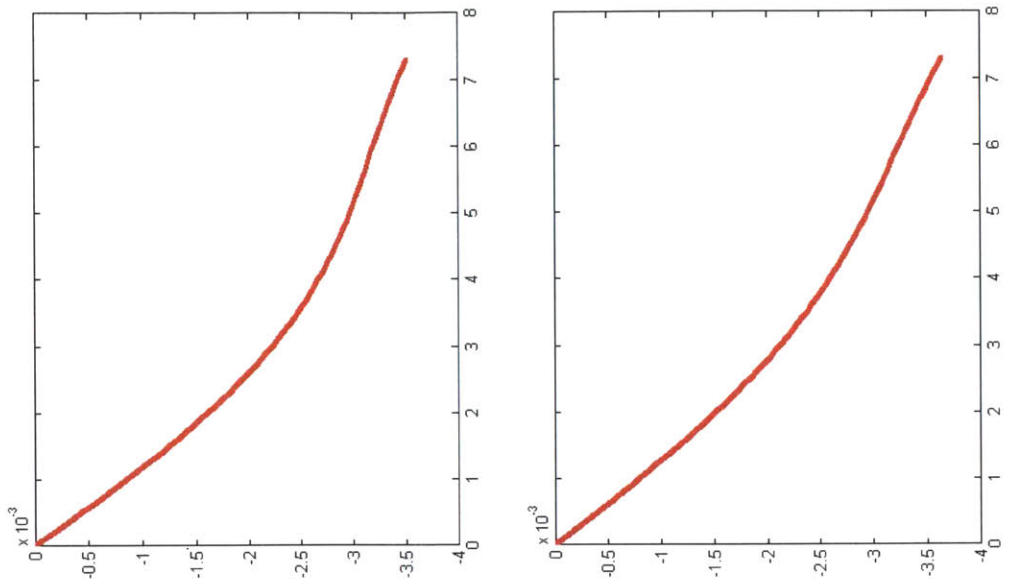

Figure 4.3.1. The rocking wall-building system first natural mode displacement against height/meters with (a) with no rocking wall stiffness (b) rocking wall stiffness 1000 times less than the case study retrofit project

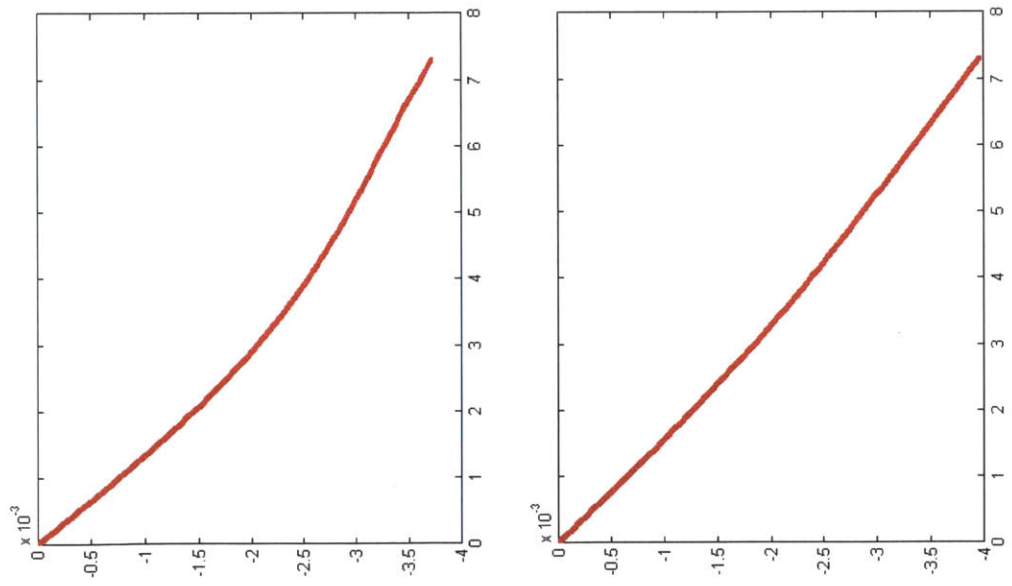

Figure 4.3.1. The rocking wall-building system first natural mode displacement against height/meters with rocking wall stiffness (c) 500 times more flexible (d) 100 times more flexible

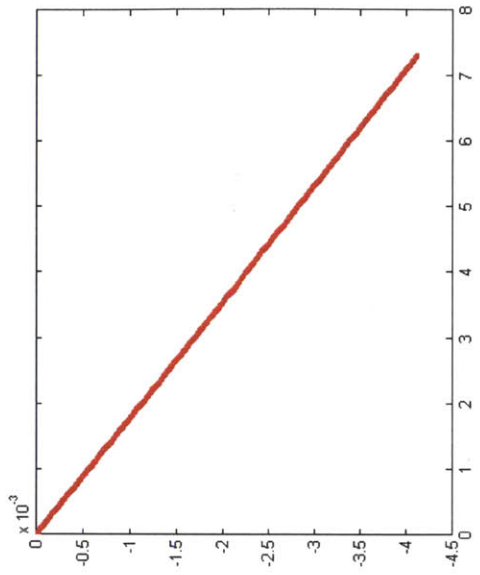

Figure 4.3.1. The rocking wall-building system first natural mode displacement against height/meters (e) with full rocking wall stiffness as used in the case study retrofit project (section 2.5)

4.4. Maximum Story Drift Angle With Varying Rocking Wall Width

A number of tests of the analytical building-rocking wall stiffness matrix, derived in *section 3.10*, against the output given by the *SAP2000* linear finite element software package have shown that the two have always matched to as many significant figures as *SAP2000* has returned. This is a very good indication of the efficacy of that analytical model.

As discussed briefly in *section 3.11*, the 116 graphs of maximum story drift plotted as a function of rocking wall width, for 56 model buildings given in *Appendix B* show some very interesting results. First, it is clear that the presence of multiple counteracting effects in rocking wall installations consistently provides for minima and maxima in these data. It is observed that there may be multiple turning points in these data, and that these turning points may be smooth, or abrupt. It appears that there may be many opportunities to design optimum rocking walls that

take advantage of the minima, and also points of diminishing returns that occur before the minima, in these data. An example of one of these design graphs is shown in *figure 4.4.1*. The graph displays Maximum Story Drift Angle vs. Rocking Wall Width (m), produced by the method developed in this work, for a benchmark building of 8 stories, with a linear stiffness profile increasing by a factor *d* of *50%* per story, a top story stiffness k_N of *92MN/m*, a story mass of *230 tonnes*, and utilizing 2 rocking walls. The graph shows an optimum design point of two rocking walls that are each *2.7m* wide, assuming a rocking wall depth of *0.6m*. However, an engineer might reasonably conclude from this graph that there are significantly diminishing returns after around *1.7m*. Although the graph is still decreasing at *1.7m*, the gradient indicates that the benefits may not outweigh the cost of increasing the wall size beyond about *1.7m*.

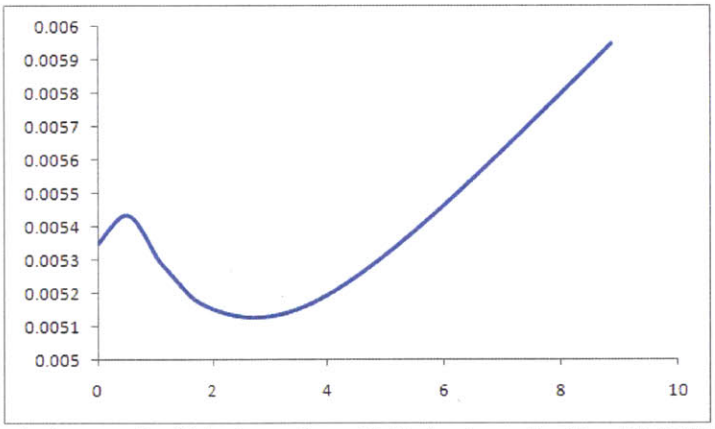

Figure 4.4.1. An example design graph of Maximum Story Drift Angle vs. Rocking Wall Width (m), for the particular benchmark building and rocking wall arrangement described.

The model produced in this report gives every indication of being robust. For example, the data produced may be used in reverse. For example, if a model of a building is generated in which the stiffness is specified but not the period, then a model is generated in which the period returned by the first model is specified as the period, and the stiffness is allowed to be determined by the model, then the stiffness returned by the second model matches exactly that which was specified for the first model.

4.5. Forces Applied to the Building by the Rocking Wall Inertia

By applying the model derived in *section 3.10*, the total maximum force in the building-rocking wall links, under the code-specified seismic loading, is found to be approximately *8.2MN*, or *1800 kips*, for the case study building, occurring at the top story. This force is due to the inertia of the building combined with that of the heavy rocking wall, and can be thought of as the effect of the rocking wall trying to straighten the deformation of the building, while the building is trying to bend under the lateral loading. This total load is distributed between 6 rocking walls each with 2 lateral connectors per story, resulting in a maximum undamped load of about *680kN*, or *150kips* per connector. However, the connections to the static shear walls, at the ends of the building, are less stiff than the others are, so should be considered as attracting less load.

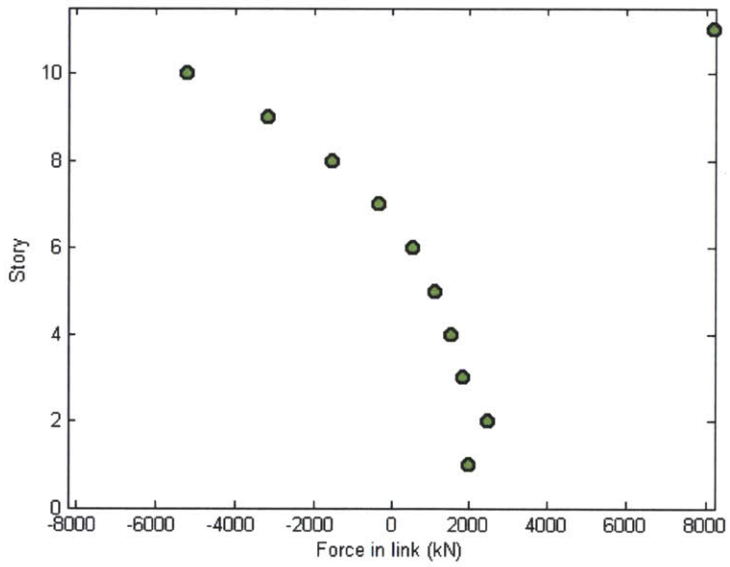

Figure 4.5.1. The forces in the building-rocking wall links, under code specified seismic loading, for the case study building, as predicted by the static equivalent method presented.

This is a useful figure, since it illuminates the loading on the rocking wall itself, and thus could allow further optimization of the rocking wall stiffness along its length.

At the lower stories, the wall is pushing the building further than it would ordinarily go under this loading, to maintain the straight profile. Around the middle stories, the force in each link is low. This can be thought of as being due to the natural position of the building under this loading, approximately matching the wall-reinforced position, at that location. At the higher stories, the wall is pulling the building back, less far than it would ordinarily go, to maintain the straight profile. At the top story, the wall is once again pushing the building further than it would go. This is due to the half-story mass associated with the top story in the model, and since the seismic load is correlated with mass, the top story drift would usually be lower than other story drifts. The top story drift is then forced to the near-constant story drift by the rocking wall.

One design strategy for a rocking wall, and later a rocking column, may be to design the wall or column to stop short of the top story, if the weight of the top story were low, since otherwise the wall may actually be applying greater stress to that story than is necessary.

The maximum link force is of the order of magnitude of the total weight of a story, and may also be equated to the thrust produced by a jet engine, by order of magnitude. As discussed previously, this figure is an upper bound, due to not taking account of supplemental damping. *Section 5* contains an analysis of whether the case study structure was sufficient to sustain these lateral forces.

4.6. Comparison with Given Case Study Building Data

The team who designed the case study rocking wall installation were kind enough to share the actual case study building data to aid with this work. It has thus been possible to compare the simulation against experimentally confirmed data.

If the discretized case study story stiffnesses for each of the *11* stories is plotted against a linear stiffness form where the incremental increase of the top stiffness is $d=0.25$, a very reasonable match is found:

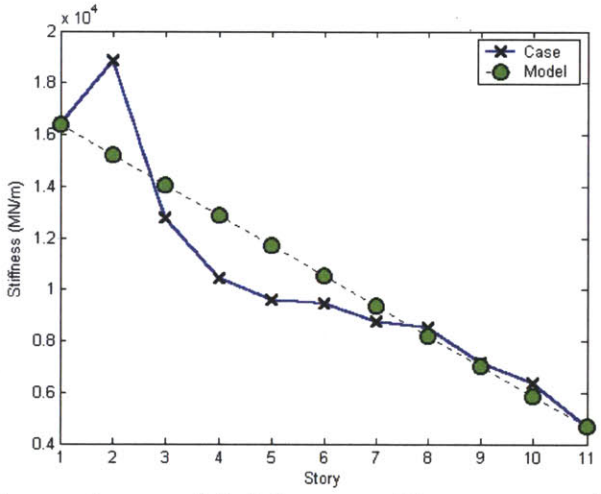

Figure 4.6.1. The actual case study building story stiffnesses compared to a linear model.

The mass model that has been used divides the total mass by the number of stories, and distributes the mass equally between the stories, except for the top floor, to which it apportions half the mass of the other floors. The comparison with the real case study data is again reasonably good:

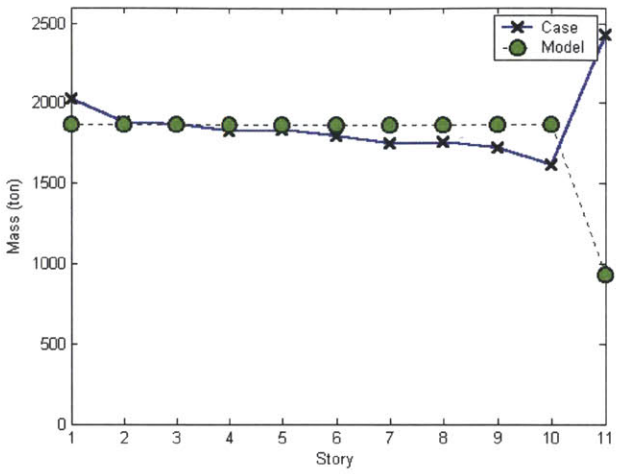

Figure 4.6.2. The given case study building story masses compared to a linear top-light model.

However, the mass model presented here (*Fig 4.6.2, green dots*) may be a more accurate discretization of the case study building, as the mass for the top floor given by the case study design team appears to be the combined mass of that floor, which is not the commonly accepted method of building discretization.[70]

The actual value for natural period in the building x direction was given as *0.589s*, and this is confirmed to 2 decimal places by applying the iterated Rayleigh quotient formula to the given information of stiffness and mass.

In a further illustration of robustness, if this given period of *0.589s* is inputted into the formulae developed for this work (as in *Appendix B*), using a stiffness increase factor $d=0.25$ as in *figure 4.6.1*, the stiffnesses generated are a reasonable approximation of the actual, with k_N just 15% less than the actual given value for k_N.

[70] *Kausel (2010)*

Similarly, given the true k_N and a factor $d=0.25$, the linearized model developed provides a first period of *0.539s*, which is just *8.7%* less than the period given. Applying this closely-matching model of the case study building, and using six rocking walls with a wall depth of *0.61m*, a top story stiffness of *4.68GN/m*, a user-specified stiffness profile of $d=25\%$, applying the factored earthquake intensity parameters for Tokyo[71], considering an effective seismic weight W of *200MN*, *11* stories of *3.27m* each, and a natural period of *0.589s*, the following design graph, tailored for the case study building, is found.

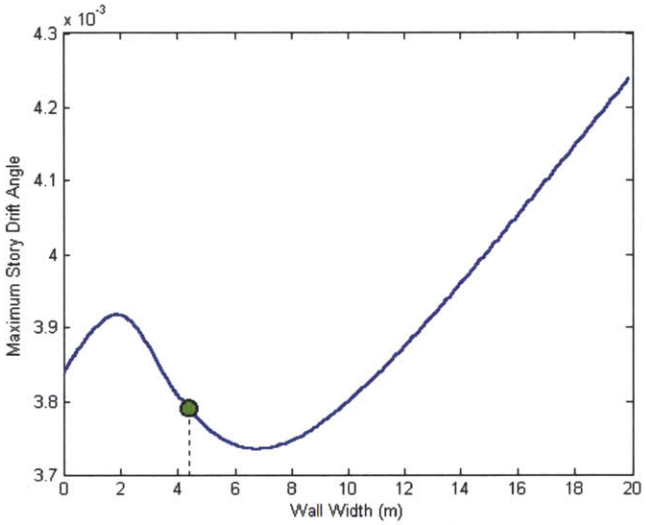

Figure 4.6.3. The Rocking Wall Design Graph for the case study building, showing maximum story drift angle of the modeled case study building, against rocking wall width (m), using 6 rocking walls. The location of the 4.39m-wide walls actually used in the case study is marked.

It is seen from *figure 4.6.3*, that based on the design graphs produced by this analysis method, the *4.4m*-wide walls, that were chosen through an exhaustive experimental testing process, were a highly appropriate choice for the case study building retrofit project. Although the actual optimal minimum of the data is at *6.7m*, it is seen from the figure that the returns obtained for adding further wall size begin to diminish significantly after around *4.5m*.

[71] *Kinetics (2008)*

The fact that the suggested wall size given by the method presented in this work matches closely that chosen for a fully experimentally-tested rocking wall installation is a useful confirmation of this method.

It is thus clearly seen, that the models developed in this work suggest that for example *2m*-wide walls, or *12m*-wide walls, would actually make the case study building's seismic response worse, rather than better. This is a counter-intuitive, and thus very useful result.

It is also interesting to note that in this case the maximum story drift occurs at the sixth story from the ground. Although some might expect the highest building stresses due to environmental loads to always be at ground level, the maximum story drift only occurs at the lowest story in the case where the story stiffness profile is close to constant. When the story stiffnesses are linearly increasing, the maximum story drift due to the seismic equivalent loading often occurs as the middle stories, according to the data produced by this model, as shown in *figure 4.6.4*. Since it is usually seen in practice that buildings fail at a middle story during an earthquake, this is another useful confirmation that the equivalent seismic loading method used here is a good tool to predict and prevent such middle story failure. If the correct parabolic stiffness were used, then the drift profile under seismic loading would be linear[72], and thus optimal, as previously discussed.

[72] *Connor (2003)*

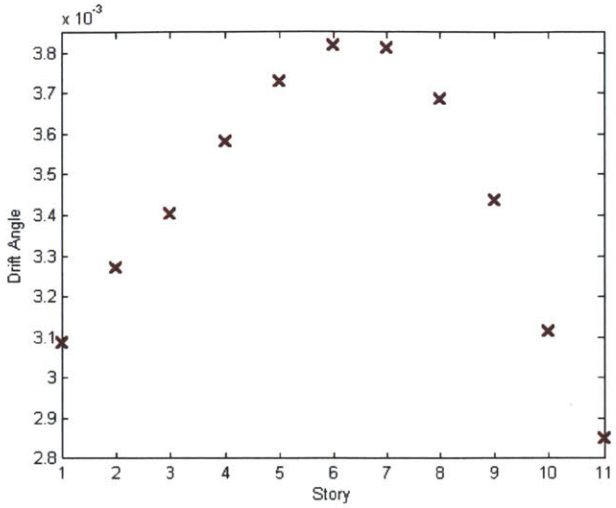

Figure 4.6.4. The story drift angles of the case study building under seismic equivalent loading, with the maximum occurring at the middle stories.

Another helpful result is that the output design parameter of the method presented is especially robust. If the story stiffnesses or masses are changed by some reasonable amount, the overall shape of the graph remains very similar, with very little movement of the minimum or the point of diminishing returns, as shown in *figure 4.6.5*. And so although a number of approximations have been incorporated to the model of the building (*figures 4.6.1 – 4.6.2*), there can be confidence that the result returned for most useful size of rocking wall would be very similar even if the fully analytical mass and stiffness matrix of the building had been used. The same is true if the loads are scaled, for example by changing the location of the building and thus the magnitude of the equivalent seismic loads. Thus it appears that the primary aim of this work, which was to offer a useful starting point for rocking wall size for rocking wall installations, has been achieved.

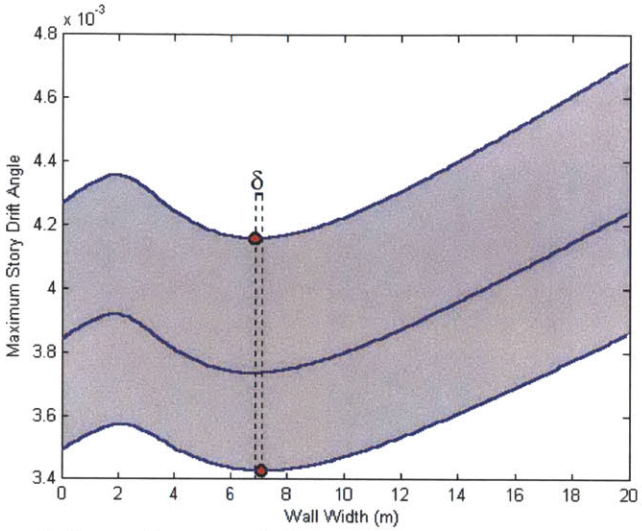

Figure 4.6.5. The rocking wall design function of the case study building compared to cases where all story stiffnesses are modified by ±10%. The central line is the case study, the upper with stiffnesses decreased by 10%, and the lower with stiffnesses increased by 10%. The change in the minimal width δ is only 0.2m, illustrating the robustness of the output.

5. Study to Determine whether the Case Study Rocking Wall Caused Damage During the Tōhoku Earthquake

Figure 5.0.1. The case study building model, as retrofitted with rocking walls. The arrow indicates a static shear wall that was damaged during the 2011 earthquake, which was of relatively light intensity in Tokyo.

It is noted during the Tōhoku Earthquake of March 2011, that a shear wall adjacent and perpendicular to the case study rocking wall installation was damaged. Based on the work culminating with *section 4.5*, which suggests very high inertial forces from the rocking wall, it is theorized that the inertial forces exerted by the adjacent rocking wall were responsible for the damage to the static shear wall. The inertial forces that rocking walls exert on surrounding structure will be studied, and it will be demonstrated that the stresses experienced by the static shear wall due to the rocking wall inertial forces were sufficient to cause the damage that was observed.

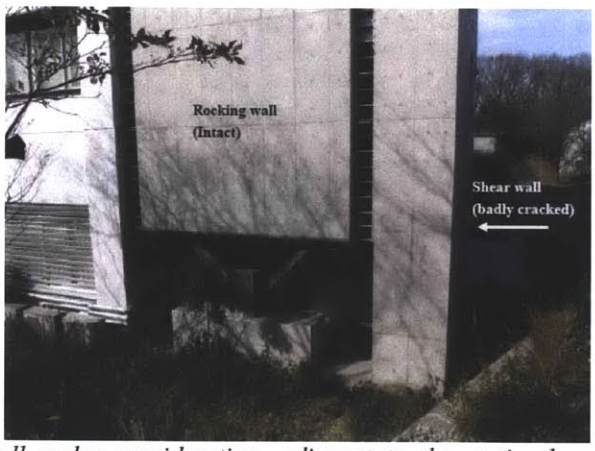

Figure 5.0.2. The rocking wall under consideration, adjacent to the static shear wall that sustained damage (courtesy Dr. Z. Qu, March 15th 2011)

This structure will be modeled in the finite element modeling package *ADINA*, with the exact dynamic earthquake loading that was felt in Tokyo during the earthquake, and the forces in the links joining the rocking wall to the building will be determined, as a function of time. Those link forces will then be combined, to find the overturning moment as a function of time that the rocking wall exerted on the building. It will then be determined that the overturning moment was sufficient to cause the cracking that was observed in the static shear wall.

The rocking walls for the *11*-story case study building are $0.61m \times 4.39m$ in plan, and each story is $3.27m$.

5.1. The Mathematical Model of the Building

The physical rocking wall-building system will be modeled as a bending planar beam hinged at the base, hinge-connected at each story to a building that is idealized as a set of shear springs.

Due to assistance from the team that designed the case study building, the story stiffnesses of the building are known, and can be approximated with a stiffness profile that starts at $4.68GN/m$ at

the top story, and increases by a factor $d=25\%$ of the top story stiffness for each lower story, as shown in *figure 4.6.1.*

5.2. Finite Element Modeling

It is desired to determine the forces that are generated in the building-wall links, and thus that the wall exerts on the building, under seismic loading.

The stiffnesses and corresponding section size for the building floors is given in *table 5.2.1.*

Story	Stiffness k (GN/m)	Side dimension b using steel (m)
1	*16.38*	*1.301759*
2	*15.21*	*1.277863*
3	*14.04*	*1.252546*
4	*12.87*	*1.225594*
5	*11.7*	*1.196736*
6	*10.53*	*1.165626*
7	*9.36*	*1.131803*
8	*8.19*	*1.094644*
9	*7.02*	*1.053262*
10	*5.85*	*1.006331*
11	*4.68*	*0.951729*

Table 5.2.1. Building story stiffnesses, and corresponding square section size required, when modeled with steel, with rotational fixity at both ends

For the finite element model, the building will be fully attached to the rocking wall by the pinned truss members, as illustrated in *figure 5.2.1.*

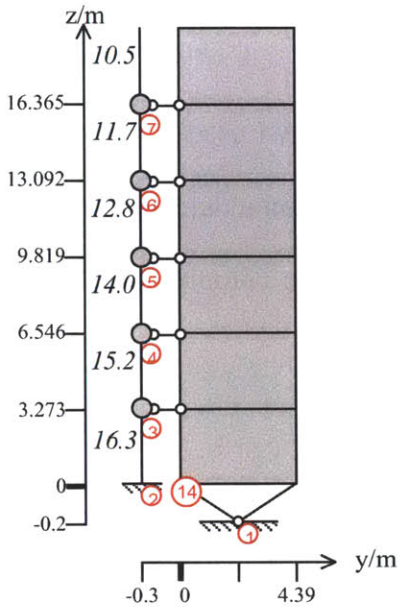

Figure 5.2.1. The third mathematical model, showing only 6 of the 11 stories for clarity.

The analytical stiffness matrix for the arrangement shown in *figure 5.2.1* has previously been defined in *section 3.10*, and tested against the *SAP2000* software package, as illustrated in *figure 3.10.6*. The analytical stiffness matrix may now be further tested using the *ADINA* finite element software package.

Story	Finite Element Model 3 (m)	Mathematical Model 3 (m)	Difference (m)	Difference (%)
1	*0.061933*	*0.061766*	*-0.000167*	*-0.270*
2	*0.127870*	*0.128206*	*0.000336*	*0.263*
3	*0.199264*	*0.199569*	*0.000305*	*0.153*
4	*0.277259*	*0.277641*	*0.000382*	*0.138*
5	*0.363213*	*0.363681*	*0.000468*	*0.129*
6	*0.458948*	*0.459534*	*0.000586*	*0.128*
7	*0.566977*	*0.567801*	*0.000824*	*0.145*
8	*0.690692*	*0.692168*	*0.001476*	*0.214*
9	*0.834341*	*0.837533*	*0.003192*	*0.383*
10	*1.002660*	*1.008431*	*0.005771*	*0.576*
11	*1.204450*	*1.201345*	*-0.003105*	*-0.258*

Table 5.2.2. The results of the third finite element model compared with the results of the third mathematical model

The maximum difference in the results between the finite element model and the mathematical model is *0.6%*, but are mostly around *0.2%*. Clearly this is a very good match. The reason for the slight difference is that the version of *ADINA* used is limited to 900 finite element nodes. While *SAP2000* performs all element meshing automatically, meshing is chosen by the engineer in ADINA to allow the engineer to optimize complex problems, and in the version available is limited to 900 nodes.

To fully compare the analytical stiffness matrix against the finite element model, the stiffness matrix can be found directly from the finite element model by setting each degree of freedom to unity in turn, while holding the others fixed and finding the reactions will give one row of the stiffness matrix. However this is a laborious process to accomplish by hand, and checking the displacements in this way is sufficient.

The model includes 2-D elements, which only approaches the exact theoretical solution as the number of elements increases.[73]

[73] *Bathe (1996)*

5.3. Dynamics

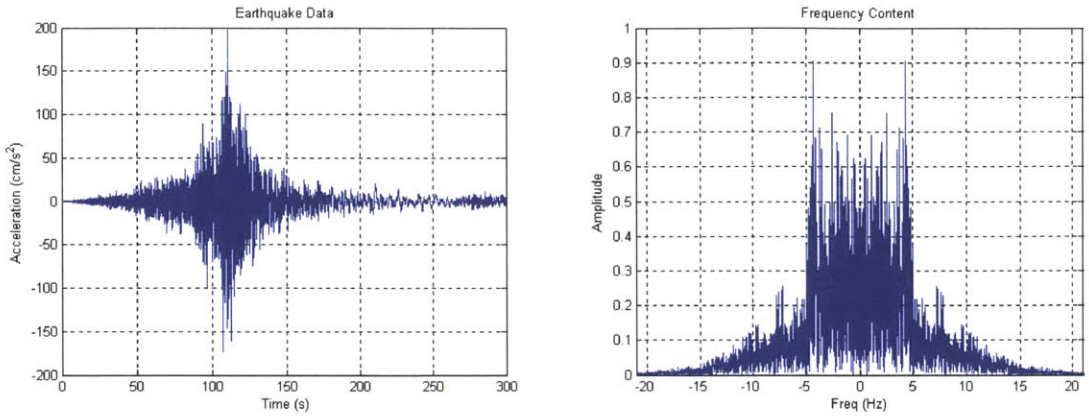

Figure 5.3.1. (a) The Tōhoku Earthquake data, as felt in Tokyo at an angle of 348° east from north, and (b) the central span of its Fourier Transform.

As is seen in *figure 5.3.1(a)*, The magnitude of the horizontal accelerations in Tokyo peaked at only a fifth of gravity, which is not a high acceleration value for a modern city to withstand. There was not significant damage in Tokyo generally following the Tōhoku earthquake.

It is seen from *figure 5.3.1(b)* that the frequency content drops off significantly after 15Hz (below about *3%* of peak). This shall be considered the ultimate loading frequency f_u.[74] Thus the cutoff frequency $f_{co} = 4f_u = 60Hz$.

The frequencies of the model, to the first frequency above *60Hz*, are as shown in *table 5.3.1*:

[74] *Bathe (1996)*

Model	Mode 1	Mode 2	Mode 3
As described in 5.3	*14.1*	*38.37*	*63.48*
With the wall surfaces divided in 4	*13.59*	*36.77*	*60.77*
With the wall surfaces divided in 9	*13.38*	*36.11*	*59.64*

Table 5.3.1. Frequencies of the finite element model (in Hz), to find how much model detail is required for convergence

In finding these frequencies, it was required to restrain the building and wall nodes vertically to prevent erroneous axial modes.

The refinement of the frequencies of the modes of interest was less than *1%* when increasing the mesh detail from splitting the wall surfaces into 4 parts than when splitting the wall surfaces into 9 parts, so the model with the wall surfaces divided into 4 shall be used for the dynamic analysis. This represents a level of model refinement that is accurate enough to capture the details needed, but not so accurate that the processing is overly expensive.[75]

Implicit direct integration analysis shall be used as the earthquake load is over a long period of time it is reasonable to believe that implicit analysis would be more efficient than explicit, and has the added benefit of a consistent mass matrix. For accuracy a time step of $t = T_{cu}/40$ will be used, where $T_{cu} = 1/f_{cu}$. Thus $t = 0.0016\dot{s}$, and *180000* time steps are required for the *300s* of earthquake data.

[75] *Bathe (1996)*

However, this many time steps produces an *8.6GB ADINA* porthole file, which the software cannot open on the computer hardware available. In *ADINA*, the number of time steps recorded can be limited by going using the function *Control/Porthole/Timesteps (nodal results)*, setting the function to *Overwrite Any Existing Blocks*, and defining all of the *180000* time steps as being in one of these 'blocks'. The period of interest in the earthquake is *75s* to *150s*, which corresponds to time steps *45000-90000*. Additionally, it is chosen to not record any time steps for the blocks outside of this period, and only one in six time steps will be recorded for this period, which is one every $1/100^{th}$ of a second, the frequency of the acceleration data.

5.4. Units and Consistency

The acceleration load is applied in m/s^2, which is the consistent unit for SI, which the model has been constructed in. The acceleration loads that are to be used are for Tokyo, which was far from the epicenter of the Tōhoku earthquake. As such, this data is not high-priority and has not been processed, and has a non-zero mean. This means that in the video illustration of the finite element analysis, the building can be observed drifting to one side. Japan of course is known to have moved by 8 feet in the Tōhoku earthquake, and so to some degree that motion accurately represents the history, although drift observed in the illustration is greater than the *8 feet* that Japan is commonly understood to have moved during the earthquake. This fact is not detrimental to the present analysis, in which it is planned to find the forces in the links between the building and the rocking wall. Since the movement is gradual over *5 minutes*, the accuracy of the link forces will not be significantly affected.

5.5. Mass for Dynamic Analysis

Mass will be added to the finite element model at specific points, in *particular 2000 tonnes* will be added at points 3 to 12, and *1000 tonnes* at point 13, to match the mathematical model of the building. This is accomplished in *ADINA* with the function *Model/Element Properties/Concentrated Masses*. In addition, the material that the building was notionally constructed in the finite element model from has its density set to zero, matching the mathematical model of a lumped-mass building.

5.6. Finding and Processing the Link Axial Forces in ADINA

To find the axial forces in each link (represented in the finite element model by lines *48* to *58*), each one must be added to a different element group (element groups *14* through *24*), as although setting the zone to "element 1 of element group 2" and so on was accepted by *ADINA* as correct syntax, it did not function as expected. On time steps after the first, details for other elements were also printed. Also it was not immediately apparent which element was element *n*.

To solve that problem, the data were processed with text editing software to obtain 11 vectors of forces in *MATLAB*-ready syntax. These vectors were then multiplied by the height vector for the structure, and the results summed, to find the combined turning moment at the base of the building, as a function of time. The result is shown in *figure 5.6.1*, below.

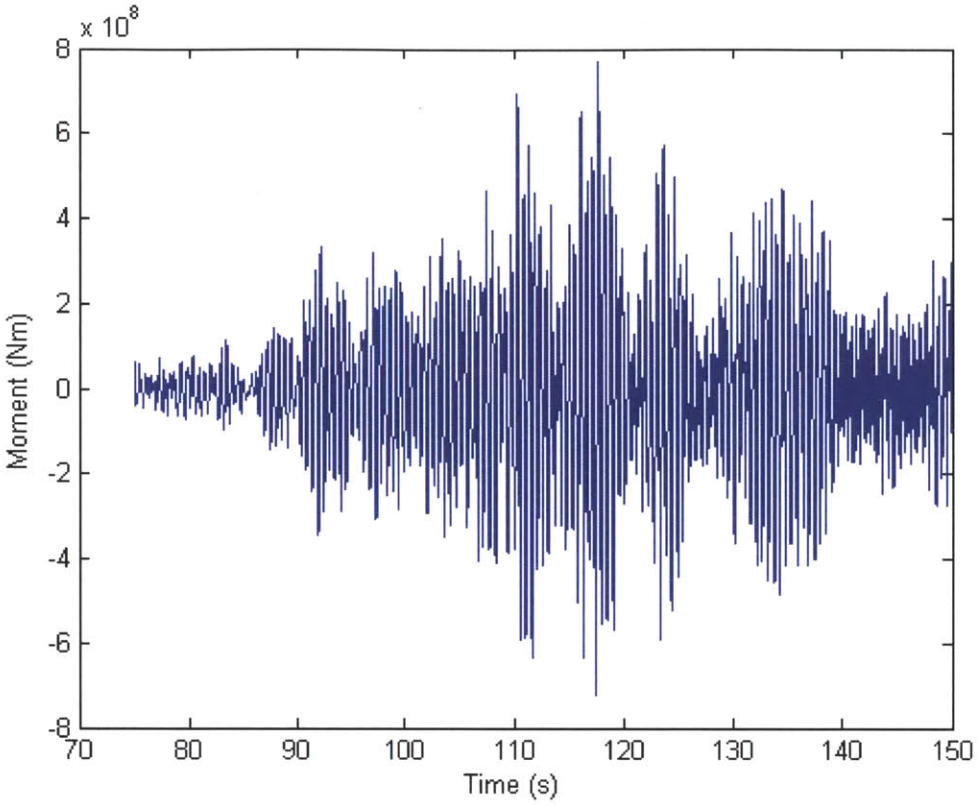

Figure 5.6.1. The overturning moment at the base of the building, as a function of time

5.7. The Addition of Damping to the Model

For the final model, *5%* Rayleigh Damping was added in *ADINA* using the commands *Control/Analysis Assumptions/Rayleigh Damping*, and setting the parameters α and β to *0.7225* and *1.67E-3* respectively.

As is seen from *figure 5.7.1*, the addition of *5%* damping to the model reduced the peak moment by nearly *30%*, and the sustained moment magnitude by even more.

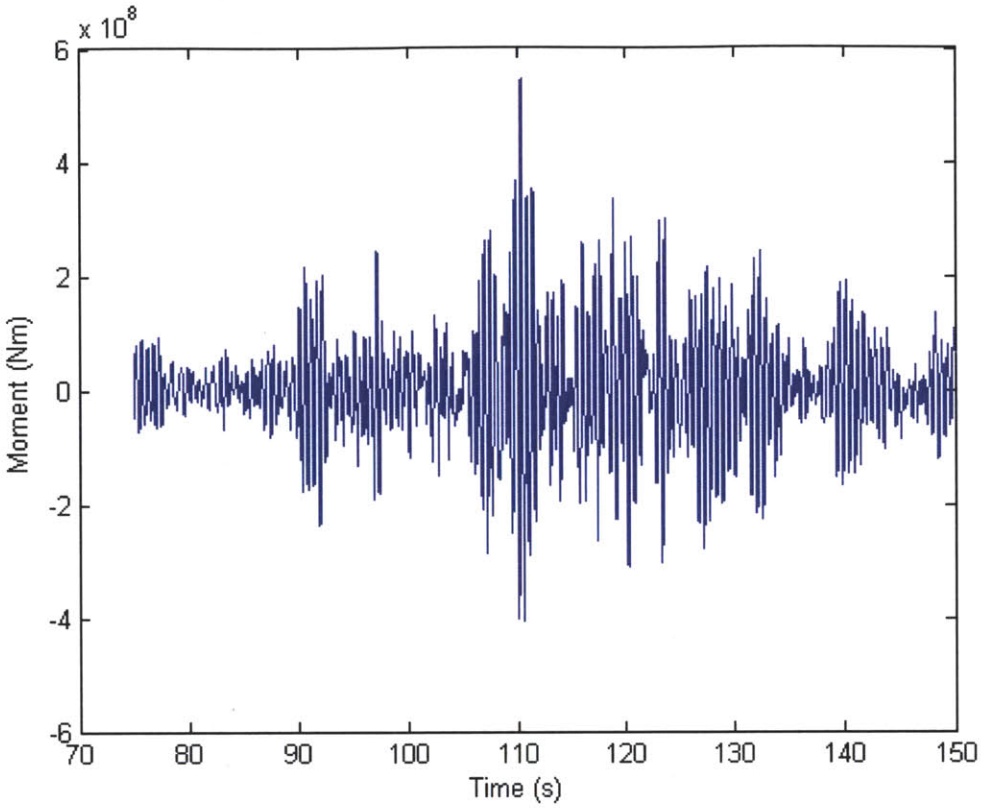

Figure 5.7.1. The overturning moment at the base of the building, as a function of time, with 5% Rayleigh damping

5.8. Calculation of the Static Shear Wall Cracking Moment

The size of the static shear wall as seen in *figure 5.0.2* is approximately *5.2ft* by *54.4ft*, and thus the second moment of area of the weak axis is *637.42 ft*^{4}. High strength *5 ksi* concrete is assumed.

The cracking moment may be found from the following formulae:[76]

$$f_r = 7.5\sqrt{f'_c} = M_{crack}y_{max}/I \qquad (5.1)$$

$$M_{crack} = 7.5I\sqrt{f'_c}/y_{max} \qquad (5.2)$$

[76] *Nilson et al. (2009)*

It is found that the cracking moment of the static shear wall is 2.247×10^8 *lb-in* or 2.5393×10^7 *Nm*. The first moment value recorded in the high-energy earthquake period from *75s* to *150s* is 4.8×10^7 *Nm*, almost twice the cracking moment. Thus it is seen that the cracking strength of the concrete was reached relatively early in this earthquake. The remaining earthquake cycles over the following minutes will have continued to crush the concrete around the cracks, making the cracks visible to the naked eye, as was observed. The peak overturning moment, approximately *2 minutes* into the earthquake, was approximately *20* times the cracking moment of the static shear wall.

5.9. Conclusions of the Finite Element Study

It is clear from the finite element analysis presented that the inertia force from the rocking wall was sufficient to cause, and most likely was the cause of the cracking in the adjacent static shear wall of the building studied.

The high inertial forces generated by rocking walls during an earthquake should be carefully considered by designers implementing this scheme. In this particular case, the rocking wall should not be attached to the static shear wall, and the static shear wall should not block the dynamic path of the rocking wall.

Connections from a rocking wall to a building should only be on the near side of the rocking wall, when the rocking wall is constructed on the edge of a building.

It may be noted that while the loads imposed by the rocking wall were substantial, they were not entirely unmanageable. *Equations 5.1 – 5.2* show that if the static shear wall were doubled in thickness, it could have sustained the loads without cracking.

6. Rocking Column Design

6.1. Rationale for Design

As a consequence of the research presented in this work, it has become apparent that the lateral inertial forces exerted by rocking walls on the surrounding structure during an earthquake are greater than was previously understood.

In addition to requiring additional care in the design process, regarding the kind of adjacent structures that should be supporting the inertial lateral loads from rocking walls, it emerges clearly from the presented research that when under full code-specified seismic loading, the total maximum load that rocking walls apply laterally is of the magnitude of one story weight. For the case study building presented, this total maximum lateral load occurs at the top story, and is *8.2MN*, or *1800 kips* in magnitude, which is *4* times more than the weight of the rocking wall itself. It is clear that the connections from the rocking wall to the building are required to be very significant to support such a load. Such connections are not readily available, and are costly. And although this load is the maximum load, the loads at other stories are also significant.

The above loads were calculated without the effect of supplemental damping systems, and so should be considered an upper bound. However, it would not generally be expected for even optimum damping to reduce the lateral loads by more than *50%*, and thus the remaining loads will still be very difficult to control.

In addition, the foundations required for rocking walls, and the pins required at their base, are very significant and costly. For the case study building, each of the six rocking walls are *3400*

cubic feet in volume, and *500 kips* of weight, not including the case iron base. As a reference, the case study retrofit project added *50%* to the existing reinforce concrete area, in plan.

Clearly, reinforced concrete rocking walls have been a highly commendable academic effort, and have taught the engineering community a lot about this kind of dynamic structure. However, there are practical difficulties inherent in their design that must still be overcome.

6.2. Introduction to Rocking Column Design

It is suggested that to overcome the difficulties observed with rocking walls, that a structure be designed from steel which maintains the desired properties of adding lateral stiffness to the structure, while being moment-released at the base, but without the high mass of a rocking wall.

Starting from the assumption that a wide flange section is most efficient in general bending, some initial calculations can be performed to determine the size of section that would be required to replace, for example, a rocking wall from the case study:

$$I_c E_c = I_s E_s \tag{6.1}$$

$$\frac{bd^3}{12} E_c = 2A_f \left(\frac{d}{2}\right)^2 E_s \tag{6.2}$$

and thus:

$$A_f = \frac{bdE_c}{6E_s} \approx \frac{bd}{40} \tag{6.3}$$

where I_c, I_s, E_c, E_s are the strong second moment of area and modulus, of the concrete and steel respectively, A_f is the area of the flange, and d, b are the dimensions of the rocking wall in plan.

Thus for the same stiffness, the total area of steel flange is *95%* less than the area of concrete. Steel is approximately *3.25* more dense than concrete, and so the weight of the steel flanges is approximately *84%* less than the weight of the concrete.

The web of the wide-flange section need not be continuous, but rather should most likely be designed as a truss. In particular, a concentric braced frame, as illustrated in *figure 6.2.1* is a popular form of deep supporting section in steel construction.[77] For total steel weight, a reasonable conservative first estimate is that for the deep section considered for the case study building, the web be an inch thick. Ultimately, the web design would be a much lighter truss of course, so this would be a gross overestimate of the web area A_w. If applied consistently for any size section, this would suggest a web area of:

$$A_w \approx \frac{bd}{24} \tag{6.4}$$

This upper bound estimate would then suggest a total steel area of *91%* less than the equivalent concrete system, and a total weight of *70%* less. This corresponds to a rocking column weighing approximately *150 kips*, for the case study example, compared to the rocking wall with a weight of *500 kips*.

[77] *McCormac and Csernak (2012)*

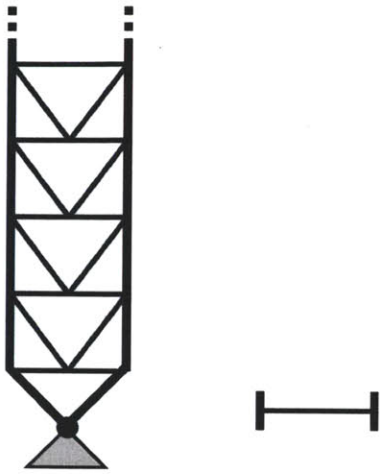

Figure 6.2.1. Schematic (a) lower elevation, and (b) plan, of a rocking column, with trussed web

6.3. Further Rocking Column Design

For the case study building, the flange size required is $104in^2$, which is *4.3 in.* wide over the *24 in.* depth of the available space. Such sizes of steel plate are not commonly available.

One possible solution would be to build up a thicker section from thinner plates, which may be desirable in certain architectural situations. Architectural considerations are addressed further in *section 6.5*. The most realistic structural approach is to use a standard wide-flange or *WT* section for the flange of the rocking column.

The most likely candidate wide flange sections for the case study example are given in *Table 6.3.1*.

Section	Area A, in^2	Overall depth d, in	flange width b_f, in	flange thickness t_f, in
W40x362	107	40.6	16.0	2.01
W36x361	106	38.0	16.7	2.01
W33x354	104	35.6	16.1	2.09
W30x357	105	32.8	15.5	2.24
W27x368	108	30.4	14.7	2.48
W24x370	109	28.0	13.7	2.72
W14x370	109	17.9	16.5	2.66

Table 6.3.1. Candidate wide flange sections for the flange of a rocking column for use in the case study building[78]. All shapes are considered heavy shapes, with a flange thickness greater than 2", so AISC A3.1(c) applies.

The least wide section is most desirable, since it is required to get the rocking column flange area as far from the middle of the rocking wall as possible. This requirement would lead to *W24x370* being chosen. However, the depth of the section is *4 in.* more than the current rocking wall. Possibly this would be within tolerances. However, *W14x370* will be chosen, with a web thickness of *1.66 in.*, to ensure that the rocking column design would fit within the existing space allocated for the rocking wall. This is illustrated in plan, to approximate scale, in *figure 6.3.1.*

Figure 6.3.1. A schematic plan of a rocking column, using standard structural steel wide flange shapes, designed for the case study building, to approximate scale, assuming 4 in. members for the truss web.

An alternative approach would be to use a *WT* shape for the flanges. These are more expensive per unit mass of steel, since they consist of a wide flange shape that has been cut in half along the web, and are not as common as wide flange shapes. However, they would offer a more efficient use of steel, since the steel would be as far as possible from the center of the rocking column.

There are only two standard *WT* sections that meet the area requirement, as shown in *table 6.3.2.*

Section	Area A, in^2	Overall depth d, in	flange width b_f, in	flange thickness t_f, in
WT18x400	118	21.3	18.0	4.29
WT7x365	107	11.2	17.9	4.91

Table 6.3.2. Candidate WT *sections for the flange of a rocking column for use in the case study building*[79]*. All shapes are considered heavy shapes, with a flange thickness greater than 2".*

As is seen from *table 6.3.2*, the net effect of using a wide flange section for this purpose would be simply to split the flange of the rocking column into two halves.

Both of the possible *WT* sections meet the depth requirement of *24 in*. However, the *WT7x365* is the better choice in this case, with a flange thickness of 4.*91 in.*, placing the maximum area away from the center of the rocking column, and the lightest possible, with a stem thickness of 3.07 in. This yields an ideal rocking column, as illustrated in *figure 6.3.2*.

Figure 6.3.2. A schematic plan of a rocking column, using standard structural steel WT shapes, designed for the case study building, to approximate scale, assuming 4 in. members for the truss web.

6.4. Detail Design

The open-face cast iron pin presented by Wada *et al.*, illustrated in *figure 2.1.2* and pictured in *figure 6.4.1* is a proven design, behaving as intended during the 2011 earthquake. A smaller version of that pin might be used for this purpose.

[78] *AISC (2005)*
[79] *AISC (2005)*

Figure 6.4.1. Open cast pin (photograph courtesy Prof. Simon Laflamme)

6.5. Architectural Considerations

For certain contemporary buildings, a set of visible rocking columns may be a desirable architectural feature, particularly for architects who desire a structurally descriptive style.

For many buildings, such a feature may not be architecturally appropriate, and will require covering, as is common for most structural systems. A model illustrating how a rocking column installation for the case study building might look, at three stages, is shown in *figure 6.5.1.*

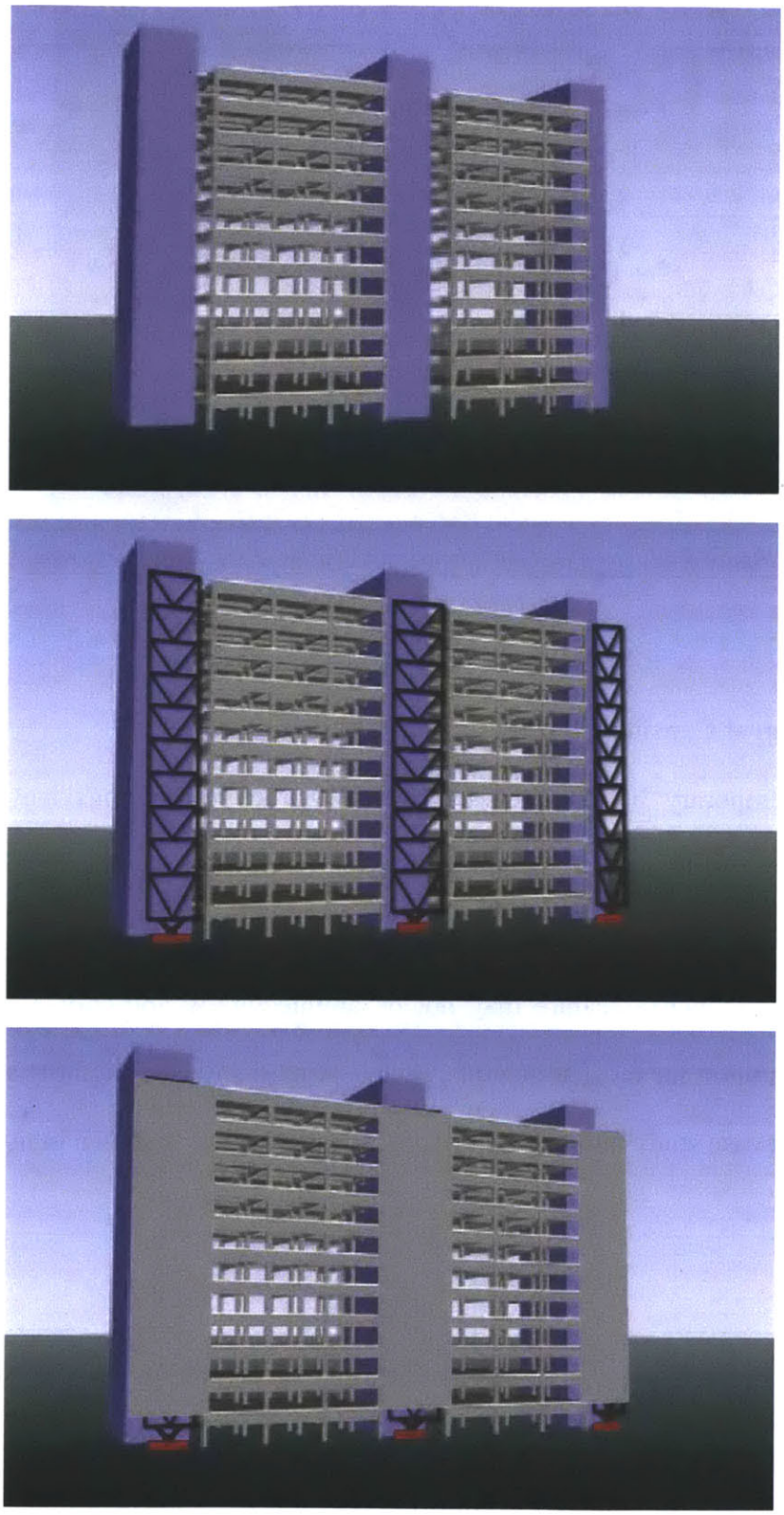

Figure 6.5.1. A model of the case study building (a) as it was before retrofit, (b) with rocking columns installed, (c) with architectural cover

6.6. Analysis of the Benefits of Rocking Columns

6.6.1 Lateral Force Reduction

The software developed for rocking wall analysis was modified to allow both rocking wall analysis and rocking column analysis.

Based on a new full analysis of the case study building, it is found for the case study building that the maximum lateral force in the wall-building links is projected to drop by 7.5% with a rocking column, corresponding to the drop in mass of the new system.

The case study building is very massive, due to being long in one direction. The reduction in lateral force from using a rocking wall is greater for a less massive building, since the rocking wall represents a greater fraction of the total mass of the building. For a very massive building, the majority of the lateral link load may be attributed directly to the action of the stiffness of the rocking wall or column.

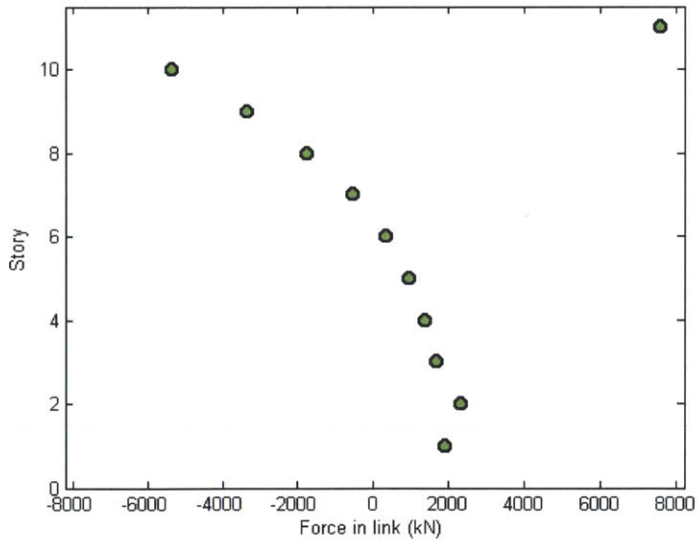

Figure 6.6.1.1. The forces in the building-rocking column links, under code specified seismic loading, for the case study building, as predicted by the static equivalent method presented.

6.6.2 Foundations Reduction

As discussed in section 6.2, the weight of rocking columns is predicted to be *70%* less than that of rocking walls. It is thus reasonable to consider that the foundations required for rocking columns will be *50%* to *70%* less substantial than those required rocking walls, with significant cost savings.

6.6.3 Cost Effective Connections

As has been established, substantial lateral connections are required between the rocking wall and the building, for either rocking walls, or rocking columns. Such connections are predicted to be more cost effective for rocking columns, since steel-to-steel connections are significantly less expensive than steel-to-concrete connections.[80]

6.6.4 Greater Story Drift Reduction, with Potential for Further Reductions

As is seen from *figure 6.6.4.1*, since the use of steel rather than concrete reduces the system density by *70%*, a significant reduction in maximum story drift is achieved for the case study building, using the same size column as the wall that was used: *4.39m* wide by *0.61m* deep.

[80] *McCormac and Csernak (2012)*

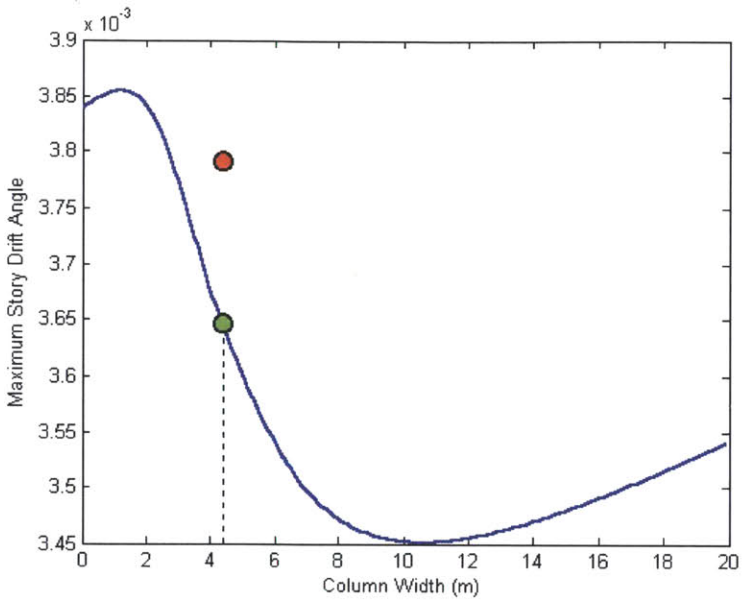

Figure 6.6.4.1. The Rocking Column Design Graph for the case study building, showing maximum story drift angle of the modeled case study building, against rocking column width (m), using 6 rocking columns. The location of the 4.39m-wide walls actually used in the case study is marked red, and the reduction in maximum story drift that is predicted to be achieved with rocking columns is marked with green.

As is also seen from the figure, there is significantly capacity to reduce the maximum story drift even further, by using a rocking column rather than a rocking wall. The point of diminishing returns occurs at about *7m*, and the gradient before this point is very steep, indicating a high incentive to increase the width of the column if possible.

6.6.5 Overall Comparative Effectiveness

Due to their use in dynamic motion, concrete rocking walls are highly reinforced members. Of course, concrete is not generally a material that is considered for dynamic applications.

There have been no negative indications found of using steel rocking columns rather than concrete rocking walls, and several substantial positive indications. It seems highly advisable to use steel rather than concrete in future projects of this type.

7. Suggested Extensions

There is much that could be extended in this work. A number of possible extensions to this work are suggested:

- Use the link forces to determine the stresses in the wall & thus indicate the amount of pre/poststress required in the wall.
- Apply a dynamic load application approach to these issues.
- Consider that seismic damage to columns may decrease the story stiffnesses during an earthquake.[81]
- Add to the software the ability to take an input of zip code and to derive the design spectral acceleration values S_s and S_1 from the zip code.
- Add supplemental damping to the model, which the analytical model is designed to allow, since it allows the wall to move independently from the building.
- Allow for a fully specified stiffness, mass, and height vectors in the software.

[81] *Koh et al. (1995)*

8. Conclusions

Retrofitting certain sizes of rocking walls to older buildings is an effective method of reducing structural response during a seismic event. It is thus an effective method of reducing the structural damage caused, thus reduces the potential for loss of life and societal disorder.

Care must be taken in the rocking wall design process, however, to ensure that adjacent systems are capable of supporting the high lateral loads that the rocking wall will exert during a seismic event. Those forces are primarily due to the stiffness of the rocking wall, but also increase with the mass of the rocking wall. In addition, as also shown in this work, care must be taken that useful sizes of rocking wall are chosen, and not sizes that will worsen the structural response.

If the top story of a retrofitted building is significantly lighter than other stories, the research presented implies that rocking walls and columns may be stopped short of the top story without negative consequence.

Current rocking walls designs consume significant area on a building plan, and may not be the most effective option for a modern newly constructed building that requires maximum available light and access. However, the latest buildings use all available technologies to deal with extreme load cases, and rocking walls may form part of a comprehensive damage reduction strategy for new buildings, particularly if optimized rocking wall sizes for given applications can be identified.

The quasi-static approach to applying seismic loads to structures is an effective way of determining the maximum story drift when the building is excited in its first mode. The frequencies of higher modes are increased significantly by rocking columns or rocking walls, often well beyond excitation frequencies, reducing the need to analyse those modes.

The general stiffness matrix derived for a discretized shear spring-mass system pin-connected to a flexible pinned column (a simplified building-rocking wall system) provides an accurate description of the simplified building-rocking wall system under arbitrary loading.

The total maximum forces in the links joining the rocking wall to the building in the case of the case study building rocking wall retrofit have an upper bound of the order of one story weight, and occur at the top stories of an installation. Supplemental damping may reduce these forces.

The representative discretized building models presented are a useful tool by which to simulate structural ideas against a broad background of representative buildings.

Based on comparison with the case study rocking wall retrofit, the method presented of using an analytical model to produce a design graph of maximum story drift against rocking wall size is an effective way to optimize the size of rocking wall required for a rocking wall installation project.

The use of steel rocking columns, as presented in *section 6*, is an effective way to reduce the difficulties associated with concrete rocking walls. They show evidence of reducing the maximum story drift further than rocking walls for the same volume of wall, and have potential for greater story drift reductions than rocking walls. They require smaller foundations, and smaller lateral connections. Rocking columns have a greater potential to be commercially viable than rocking walls have so far been.

9. References

Ajrab *et al.* (2004) *Rocking Wall–Frame Structures with Supplemental Tendon Systems.* *Available at: http://dx.doi.org/10.1061/(ASCE)0733-9445(2004)130:6(895)* (Accessed: 16 January 2012)

American Institute of Steel Construction (AISC) (2005) *Specifications for Structural Steel Buildings., ASCE/SEI 7-05.*

American Society of Civil Engineers (ASCE) (2006) *Minimum Design Loads for Buildings and Other Structures, ASCE/SEI 7-05.*

Bathe, K-J. (1996) *Finite Element Procedures.*, Prentice-Hall

Buildings Guide (2012) *Seismic Base Shear Calculator.* *Available at: http://www.buildingsguide.com/calculators/structural/IBC2006E/* (Accessed: 16 January 2012)

Chopra, A. (2006) *Dynamics of Structures.*, Prentice-Hall

Connor, J. (2003) *Introduction to Structural Motion Control.* Pearson Education, Upper Saddle River

Deierlein, G. (2010) *Presentation: Damage Resistant Braced Frames with Controlled Rocking and Energy Dissipating Fuses.* *Available at:* http://peer.berkeley.edu/events/2010/semm_seminar_deierlein.html (Accessed: 16 January 2012)

Federal Emergency Management Agency (FEMA) (1997) *NEHRP Guidelines for the Seismic Rehabilitation of Buildings.* *Available at:* http://www.wbdg.org/ccb/FEMA/ARCHIVES/fema273.pdf (Accessed: 16 January 2012)

Housner, G. W. (1963) *The behavior of inverted pendulum structures during earthquakes.* Bulletin of the Seismological Society of America, 53 (2), 403–417.

Kausel, E. (2010) *Advanced Structural Dynamics and Vibrations, Course Materials.* Massachusetts Institute of Technology, Cambridge, Massachusetts, Nov 2010

Kinetics (2008) *Understanding IBC Seismic for MEP.*
Available at: http://www.kineticsnoise.com/seismic/pdf/Understanding%20IBC%20Seismic%20for%20MEP.pdf (Accessed: 16 January 2012)

Kishiki, S. and Wada, A. (2009) *New Dynamic Testing Method on Braced-Frame Subassemblies.*
Available at: http://peer.berkeley.edu/events/2009/icaese3/cd/files/pdf/KISHIKI_WADA_21.pdf (Accessed: 16 January 2012)

Koh *et al.* (1995) *Determination of story stiffness of three-dimensional frame buildings*
Available at: http://linkinghub.elsevier.com/retrieve/pii/014102969500055C (Accessed: 16 January 2012)

Mander, J. and Cheng, C-T., (1997). *Seismic resistance of bridge piers based on damage avoidance design. Tech. Rep. NCEER-97-0014*, National Center for Earthquake Engineering Research, Buffalo, N.Y.

Mander, J. B., Contreras R., and Garcia, R. (1998) *Rocking columns: An effective means of seismically isolating a bridge.* U.S.-Italy Workshop on Seismic Protective Systems for Bridges, Colombia, N.Y.

Marriott *et al.* (2008) *Dynamic Testing of Precast, Post-Tensioned Rocking Wall Systems with Alternative Dissipating Solutions.*
Available at: http://hdl.handle.net/10092/2676 (Accessed: 16 January 2012)

McCormac, J. and Csernak, S. (2012) *Structural Steel Design.* 5th Edition, Prentice Hall

Nilson A.H., Darwin D., and Dolan C.W. (2009) *Design of Concrete Structures.*, 14th Edition, McGraw-Hill

Pekcan, G., Mander, J., and Chen, S. (2000). *Balancing lateral loads using tendon-based supplemental damping system. Journal of Structural Engineering,* 126 (8), 896–905.

Percassi, S. J. (2000). *Rocking column structures with supplemental damping devices.* MS thesis, State Univ. of New York at Buffalo, Buffalo, N.Y.

Qu Z., Wada A. (2011), *Rocking Walls for Enhancing the Seismic Performance of Building Structures.*

Wada *et al.* (2009) *Seismic Retrofit Using Rocking Walls and Steel Dampers.*
Available at: http://www.quzhe.net/Resource/Struct/2009_ATC-SEI_G3Bld.pdf (Accessed: 16 January 2012)

Wada, A. (2010) *Talk on the rocking wall installation project at the Tokyo Institute of Technology.* Massachusetts Institute of Technology, Cambridge, Massachusetts, 22 Oct 2010

Wada, A. (2010) *Strength, Deformability, Integrity and Strong Columns in Seismic Design of Multi-Story Structures.*
Available at: http://www.bridge.t.u-tokyo.ac.jp/apss/lectures/Prof.Wada_July26_APSS2010.pdf (Accessed: 16 January 2012)

Design of Innovative Dynamic Systems for Seismic Response Mitigation

by

Douglas Seymour

Massachusetts Institute of Technology
Department of Civil and Environmental Engineering

Appendices

Appendix A. The 20 Significant United States Earthquakes 1933-2006

Appendix B. A Set of Benchmark Building Models for Use in Simulations

Appendix C. MATLAB Code for Solving the Rocking Wall as a Flexible Continuous System, using Lagrange

Appendix D. MATLAB Code to Find the Stiffness Matrix of Building-Rocking Wall System

Appendix A: The 20 Significant United States Earthquakes 1933-2006

This appendix presents the time histories and spectral acceleration plots of the 20 earthquakes that occurred in the United States from *1933* to *2006* that are considered significant.[A1] This information was combined to create *figure 1.2.3*, which illustrates that the most damaging earthquake frequencies are in the approximate range *2* to *6 Hz*, and that moving structural response frequencies away from this region is a good way to control structural response.

The Spectral Acceleration plots are calculated with a damping of *5%* of critical.

Earthquake	Year	Date	Time	Latitude	Longitude	Mag.	Fatalities	Peak Accn. Period Low (s)	Peak Accn. Period High (s)
Hawaii Kiholo Bay	2006	10/15/06	07:07:48 HST	19.820	-156.027	6.7	0	0.1	0.6
Parkfield	2004	09/28/04	10:15:24 PDT	35.815	-120.374	6.0	0	0.1	0.6
San Simeon	2003	12/22/03	11:15:56 PST	35.706	-121.101	6.5	2	0.1	0.4
Hector Mine	1999	10/16/99	02:46:45 PDT	34.600	-116.270	7.1	0	0.1	1.0
Northridge	1994	01/17/94	04:30:00 PST	34.209	-118.541	6.4	57	0.1	0.8
Big Bear	1992	06/28/92	08:05:31 PDT	34.201	-116.826	6.5	0	0.1	0.3
Landers	1992	06/28/92	04:57:31 PDT	34.216	-116.433	7.3	3	0.2	1.3
Cape Mendocino	1992	04/25/92	11:06:05 PDT	40.380	-124.230	7.1	0	0.1	0.4
Sierra Madre	1991	06/28/91	07:43:00 PDT	34.262	-118.002	5.8	2	0.3	0.6
Loma Prieta	1989	10/17/89	17:04:00 PDT	37.037	-121.883	7.0	63	0.2	0.6
Whittier Narrows	1987	10/01/87	07:42:20 PDT	34.067	-118.078	6.1	8	0.1	0.4
Morgan Hill	1984	04/24/84	14:15:19 PDT	37.317	-121.680	6.2	0	0.2	0.6
Coalinga	1983	05/02/83	16:43:00 PDT	36.250	-120.300	6.5	0	0.2	0.7
Livermore	1980	01/26/80	18:33:35 PST	37.760	-121.700	5.8	0	0.2	0.6
Livermore	1980	01/24/80	11:00:09 PST	37.840	-121.800	5.9	0	0.2	0.7
Imperial Valley	1979	10/15/79	16:16:00 PDT	32.640	-115.330	6.6	0	0.1	0.6
San Fernando	1971	02/09/71	06:00:00 PST	34.400	-118.400	6.6	65	0.2	0.5
Kern County	1952	07/21/52	16:52:14 PDT	34.958	-118.998	7.5	14	0.3	0.4
El Centro	1940	05/18/40	20:36:40 PST	32.844	-115.381	6.9	9	0.2	0.6
Long Beach	1933	03/10/33	17:54:00 PST	33.700	-118.000	6.4	120	0.2	0.6

Table A1: Overview of the 20 significant earthquakes in the United States from 1933-2006

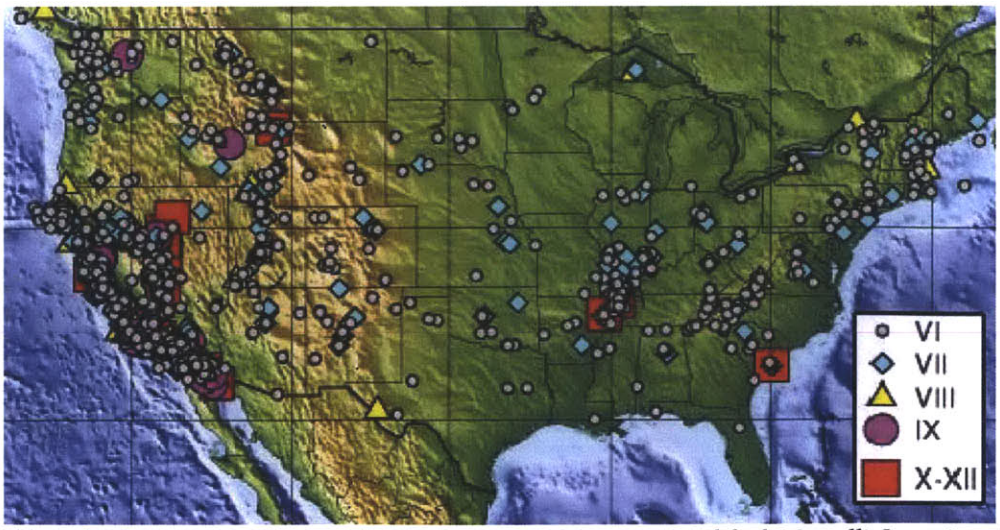

Figure A1. U.S. Earthquakes Causing Damage, 1750-1996, using Modified Mercalli Intensity. Adapted from USGS record of damaging US earthquakes[A5]

1) Long Beach 1933

Magnitude: 6.4
Recording station and instrument:
Long Beach, CA - Public Utilities Bldg - 215 W Broadway
Closest distance to fault: 0.8 km
188°

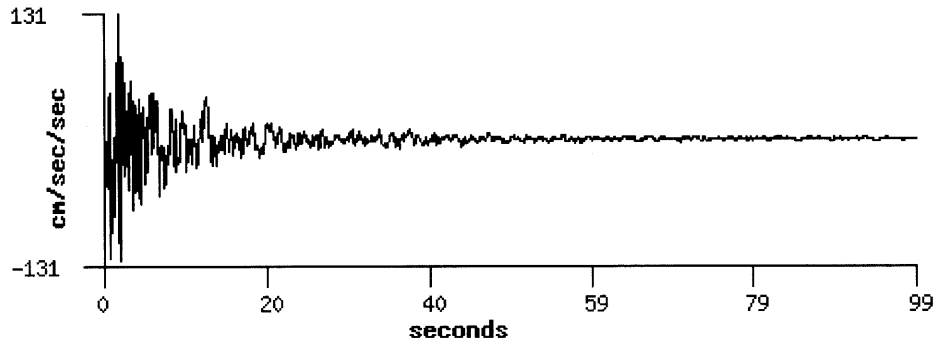

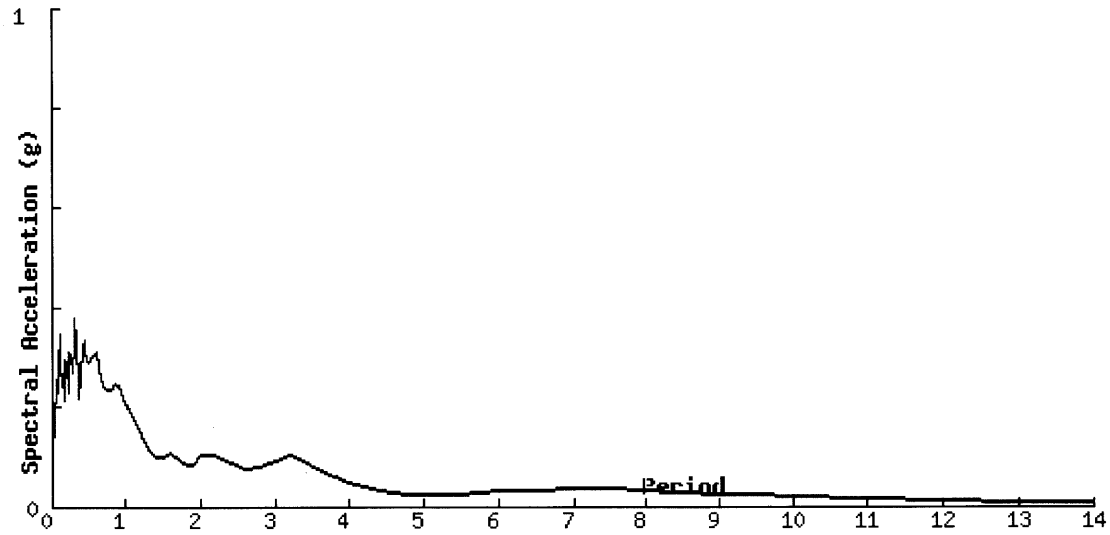

Wikipedia link: http://en.wikipedia.org/wiki/1933_Long_Beach_earthquake

2) El Centro 1940

Magnitude: 6.9
Recording station and instrument:
El Centro, CA - Array Sta 9; Imperial Valley Irrigation District - 302 Commercial
Hypocentral distance: 12.2 km
180°

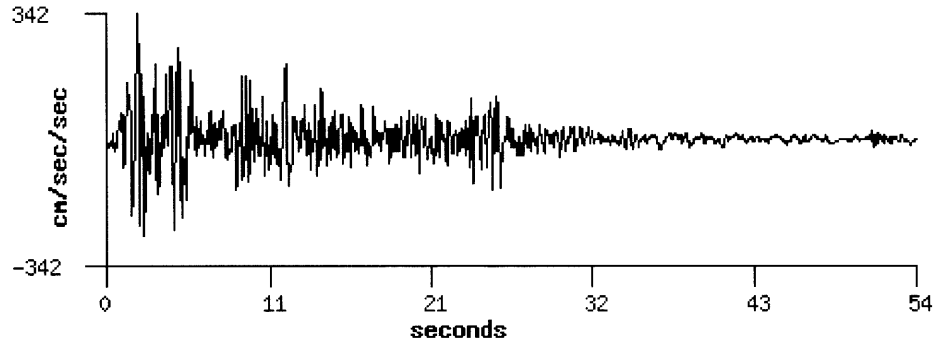

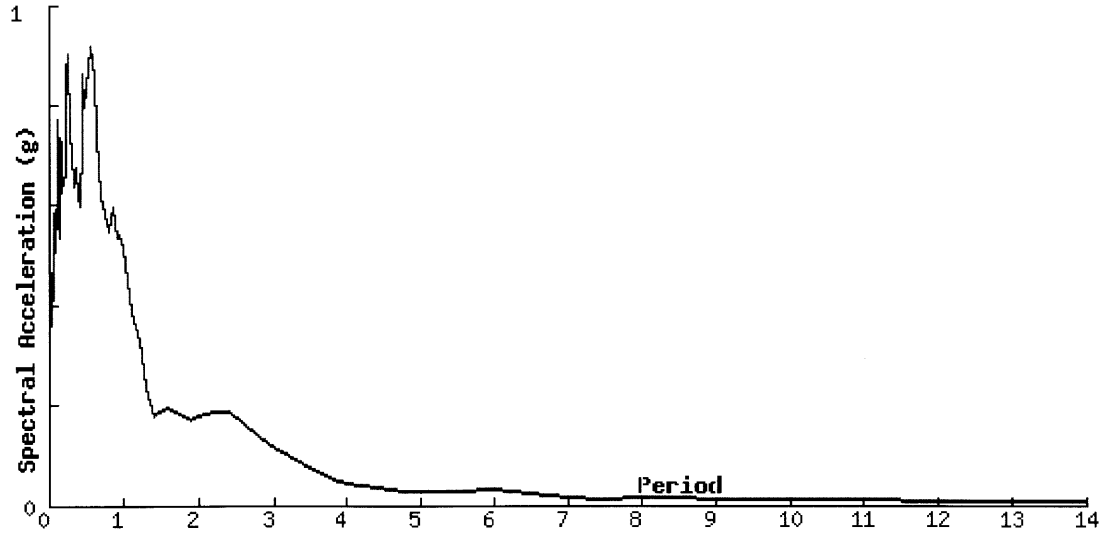

Wikipedia link: http://en.wikipedia.org/wiki/1940_El_Centro_earthquake

3) Kern County 1952

Magnitude: 7.5
Recording station and instrument:
Taft, CA - Lincoln School - 810 N Sixth
Closest distance to fault: 36.2 km
21°

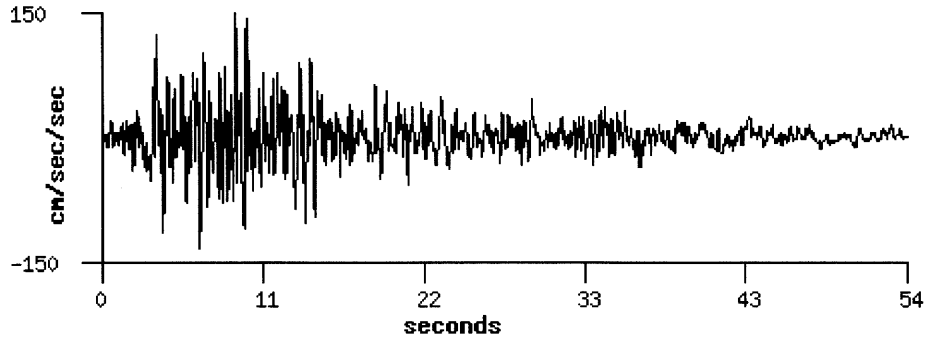

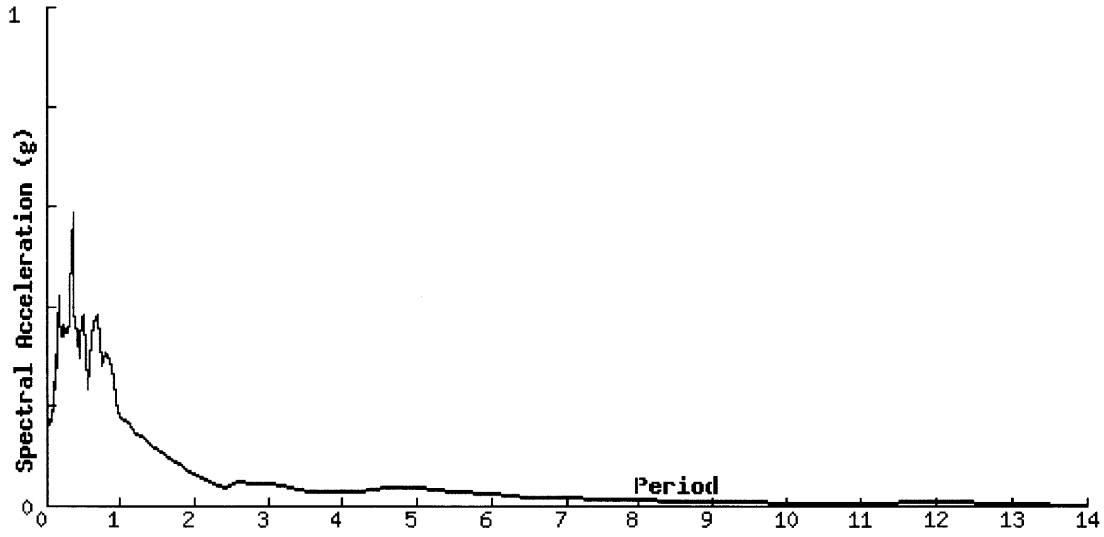

Wikipedia link: http://en.wikipedia.org/wiki/1952_Kern_County_earthquake

4) San Fernando 1971

Magnitude: 6.6
Recording station and instrument:
Pacoima Dam, CA
Closest distance to fault: 3.5 km
164°

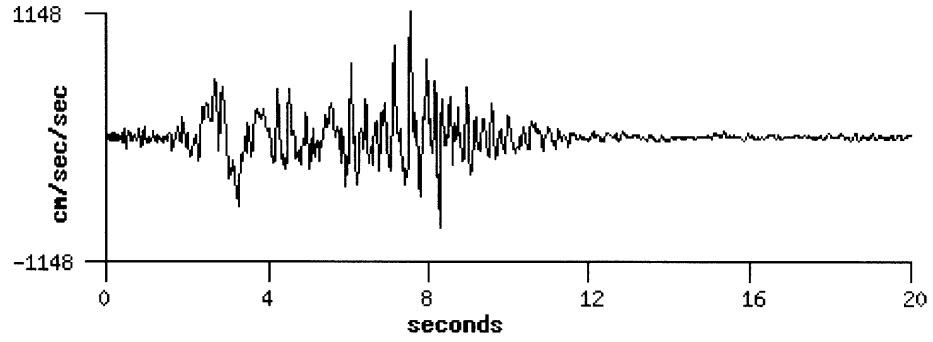

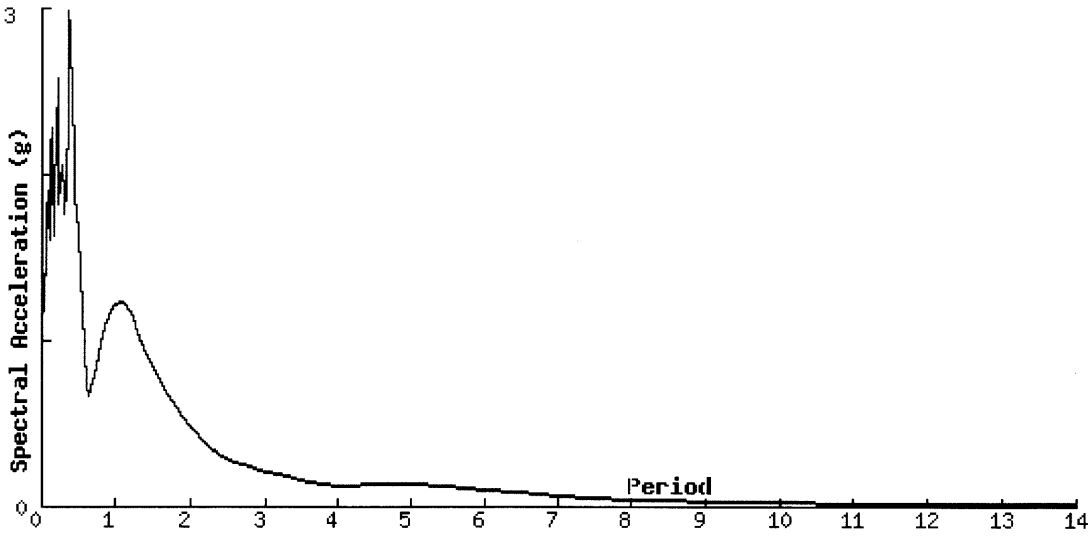

Wikipedia link: http://en.wikipedia.org/wiki/1971_San_Fernando_earthquake

5) Imperial Valley 1979

Magnitude: 6.6
Recording station and instrument:
Bonds Corner, CA - Omlim residence - Hwys 115 & 98
Closest distance to fault: 4.4 km
140°

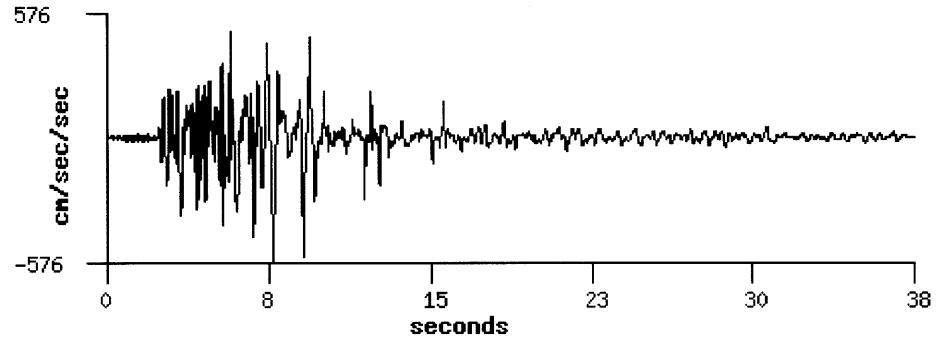

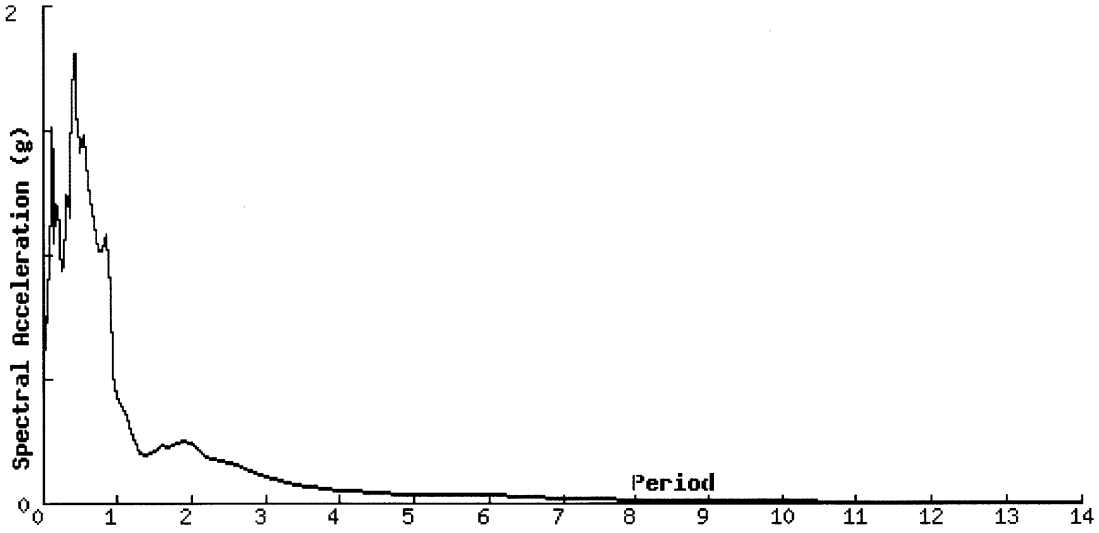

Wikipedia link: http://en.wikipedia.org/wiki/List_of_earthquakes_in_California

6) Livermore A 1980

Magnitude: 5.9
Recording station and instrument:
San Ramon, CA - Fire Station
Hypocentral distance: 19.5 km
340°

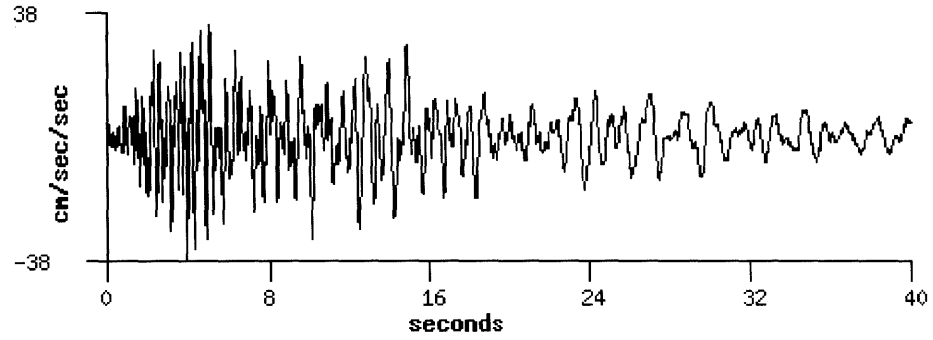

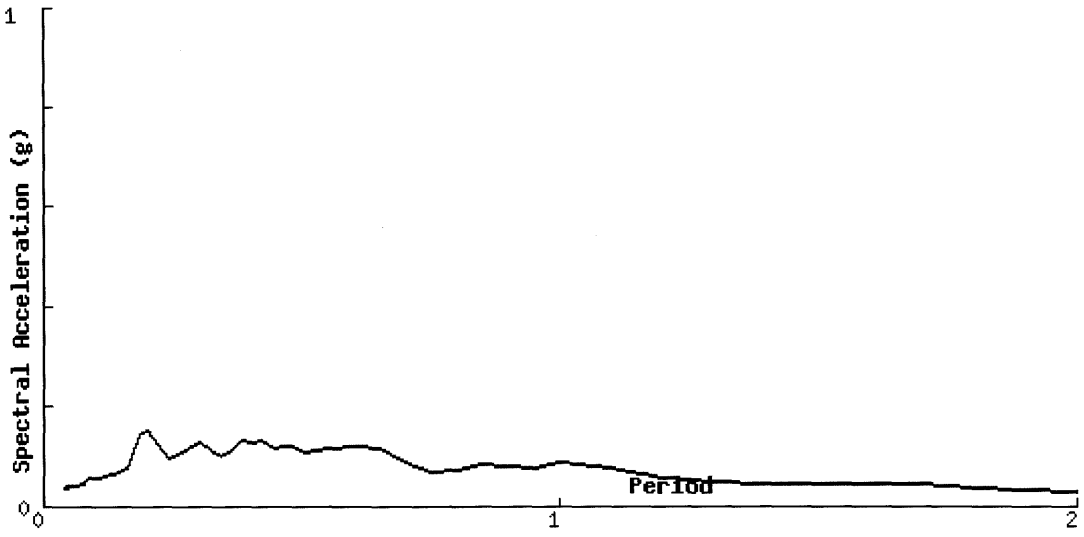

Wikipedia link: http://en.wikipedia.org/wiki/List_of_earthquakes_in_California

7) Livermore B 1980

Magnitude: 5.8
Recording station and instrument:
Livermore, CA - Fagundes Ranch
Hypocentral dist: 11.3 km
360°

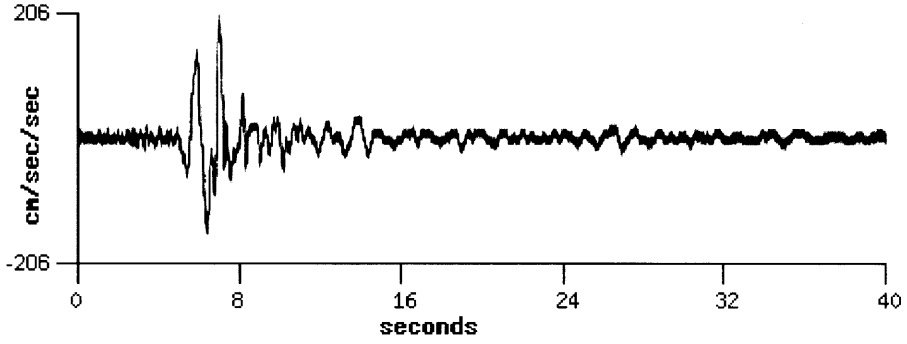

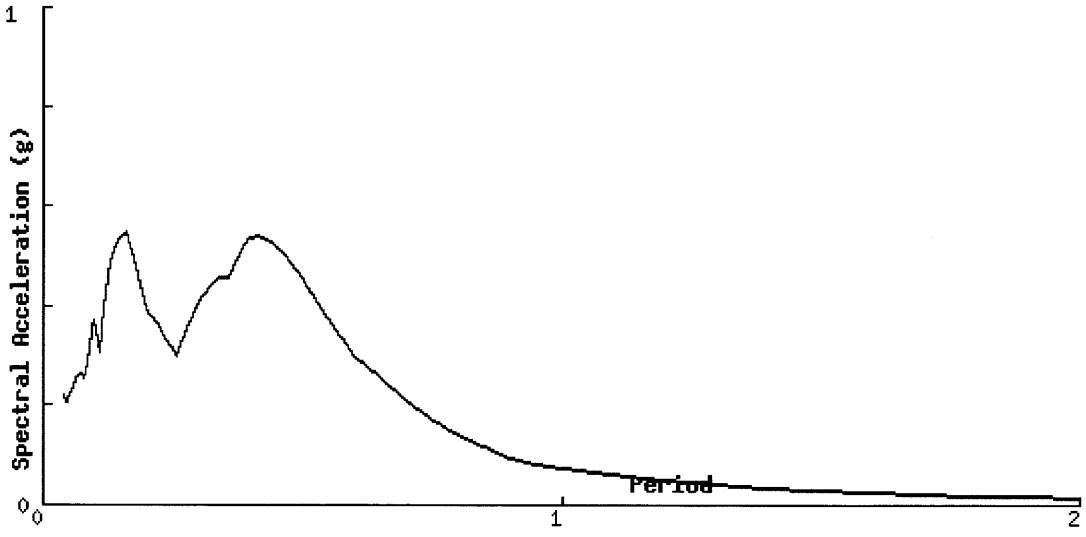

Wikipedia link: http://en.wikipedia.org/wiki/List_of_earthquakes_in_California

8) Coalinga 1980

Magnitude: 6.5
Recording station and instrument:
Pleasant Valley, CA - Pumping Plant
Hypocentral dist: 14.1 km
45°

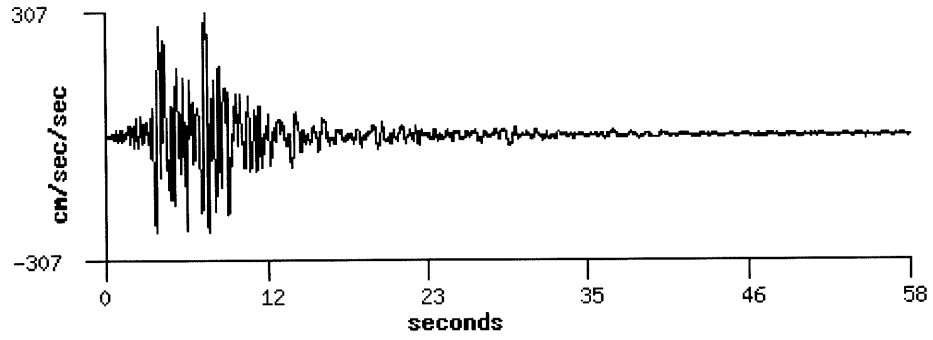

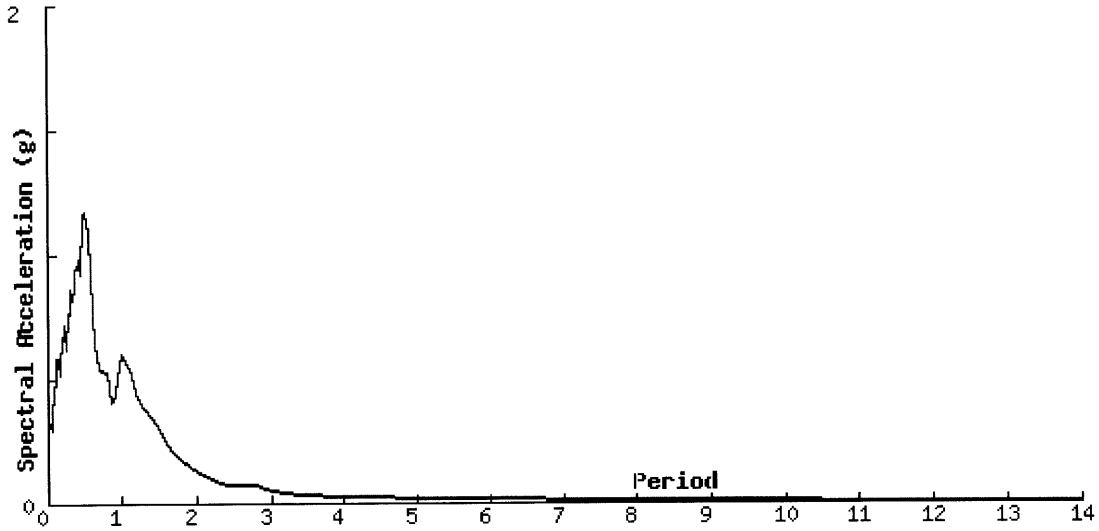

Wikipedia link: http://en.wikipedia.org/wiki/1983_Coalinga_earthquake

9) Morgan Hill 1984

Magnitude: 6.2
Recording station and instrument:
Halls Valley, CA - Grant Ranch
Closest distance to fault: 2.5 km
150°

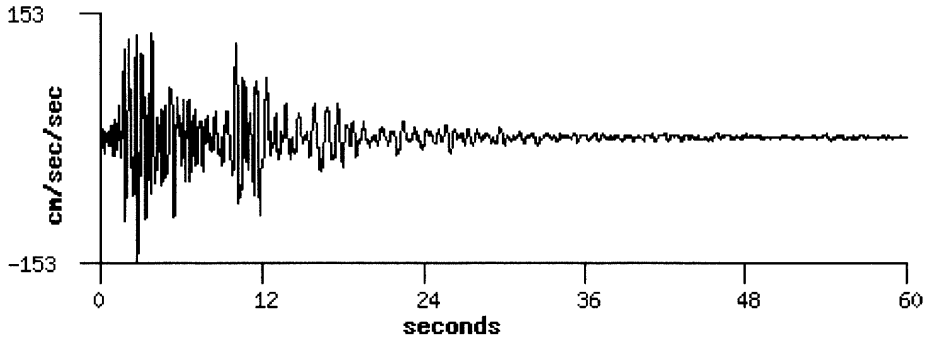

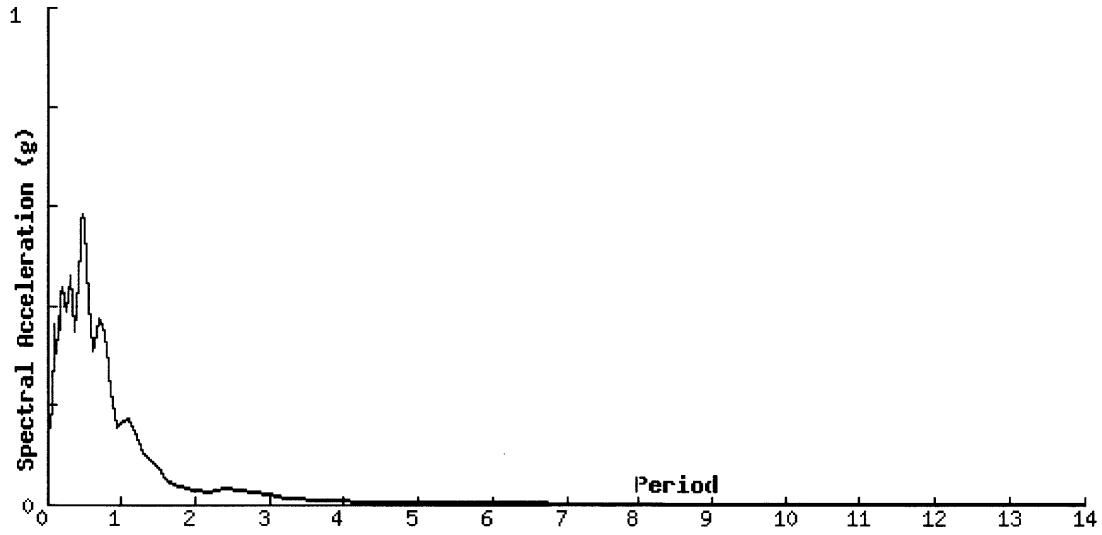

Wikipedia link: http://en.wikipedia.org/wiki/1984_Morgan_Hill_earthquake

10) Whittier 1987

Magnitude: 6.1
Recording station and instrument:
Monterey Park, CA - Garvey Reservoir
Closest distance to fault: 13.6 km
330°

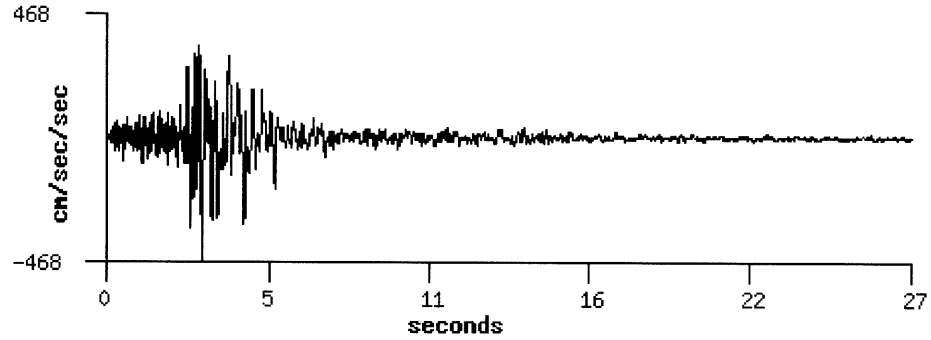

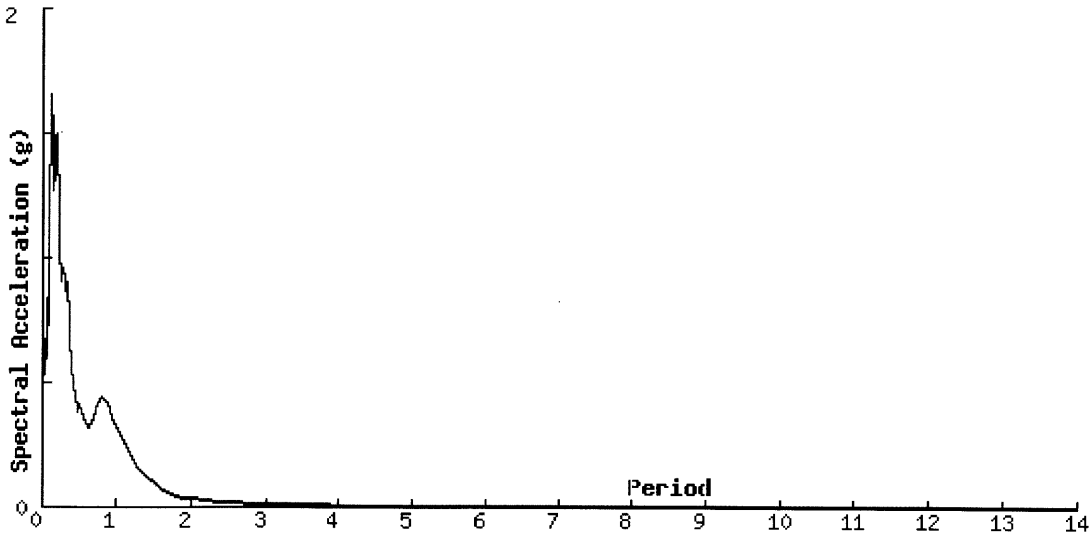

Wikipedia link: http://en.wikipedia.org/wiki/1987_Whittier_Narrows_earthquake

11) Loma Prieta 1989

Magnitude: 7.0
Recording station and instrument:
Corralitos, CA
Closest distance to fault: 2.8 km
0°

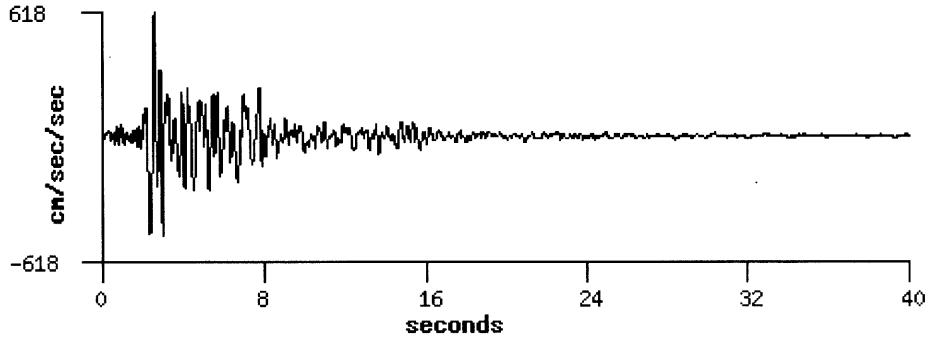

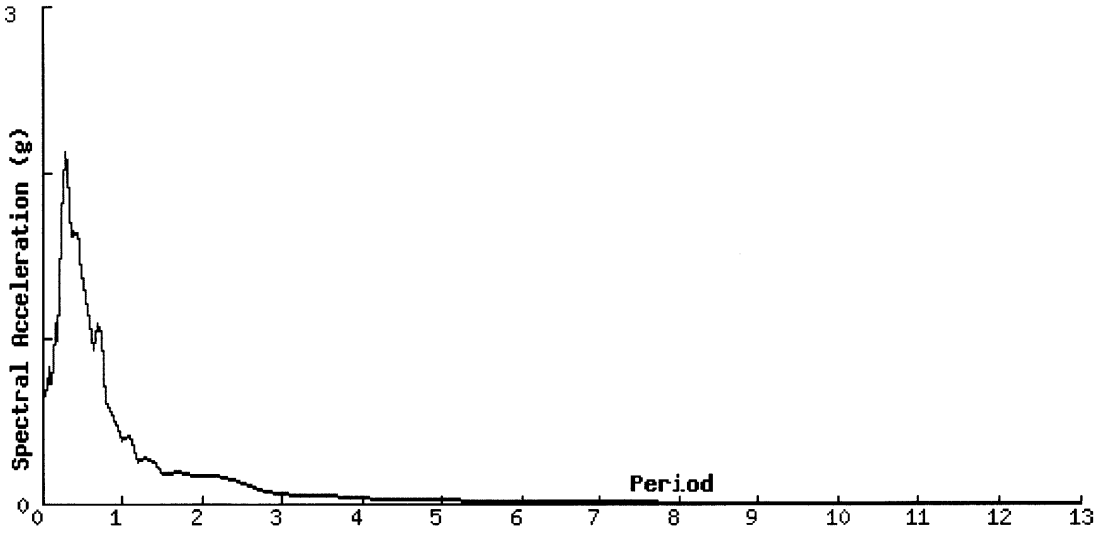

Wikipedia link: http://en.wikipedia.org/wiki/1989_Loma_Prieta_earthquake

12) Sierra Madre 1991

Magnitude: 5.8
Recording station and instrument:
Sierra Madre, CA - Cogswell Dam (Ctr Crest)
Hypocentral distance: 12.6 km
155°

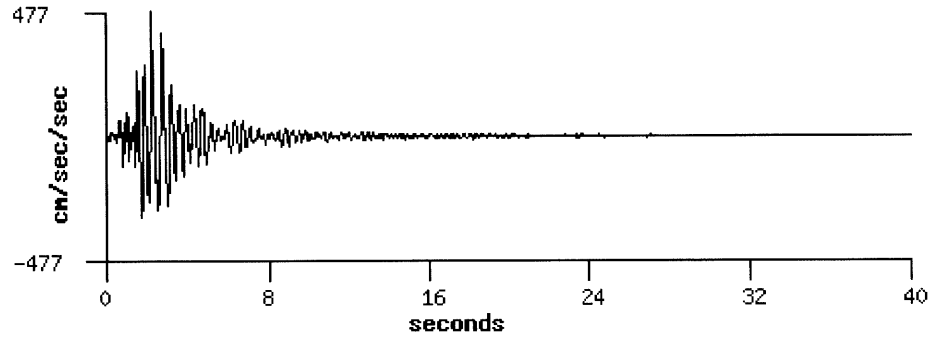

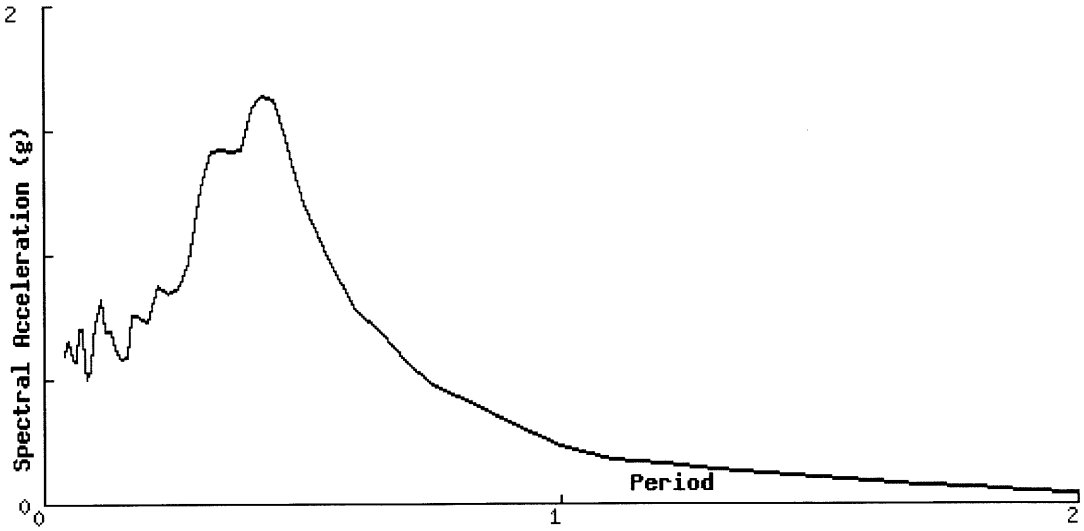

Wikipedia link: http://en.wikipedia.org/wiki/List_of_earthquakes_in_California

13) Petrolia 1992

Magnitude: 7.1
Recording station and instrument:
Cape Mendocino, CA - Petrolia
Hypocentral distance: 15.5 km
0°

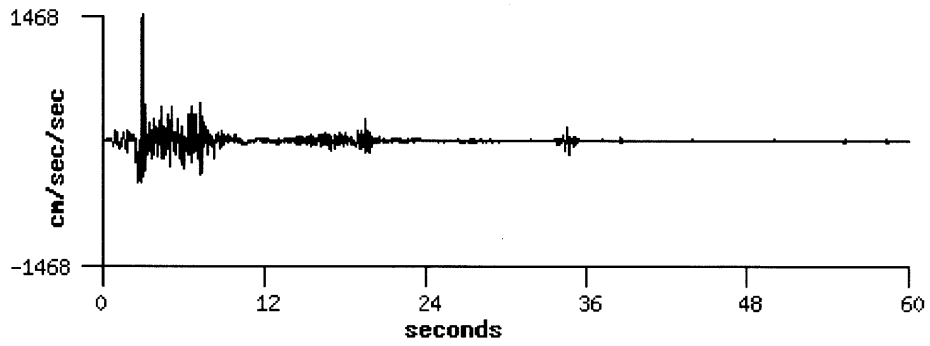

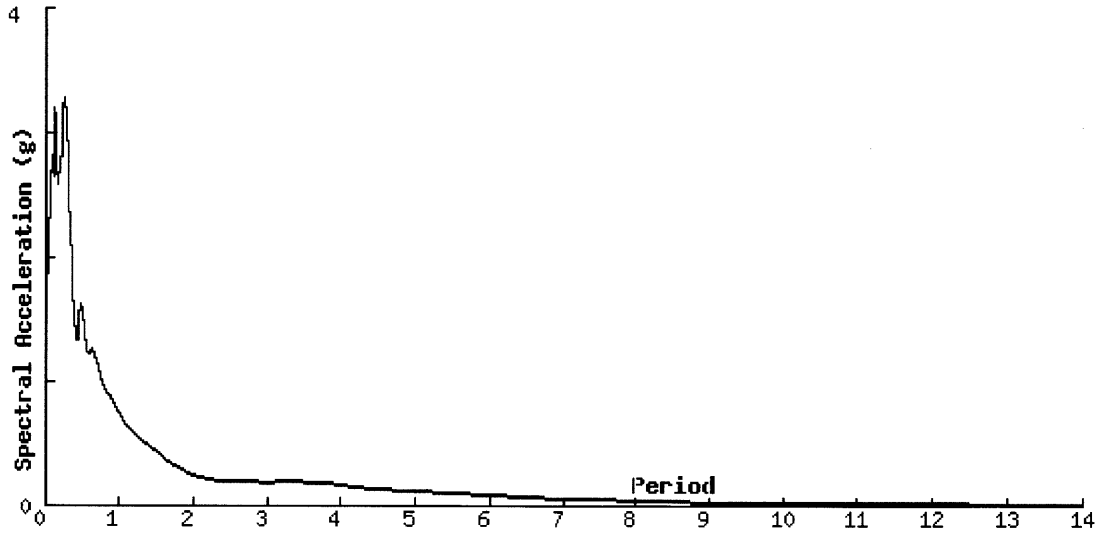

Wikipedia link: http://en.wikipedia.org/wiki/1992_Cape_Mendocino_earthquakes

14) Landers 1992

Magnitude: 7.3
Recording station and instrument:
Joshua Tree, CA - Fire Station
Closest distance to fault: 10.0 km
0°

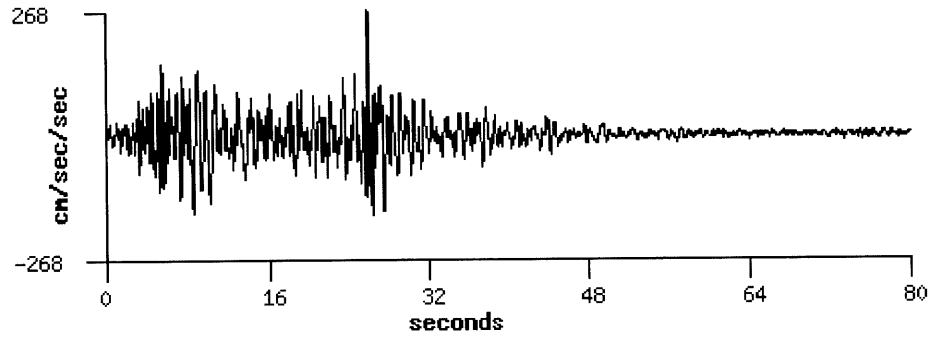

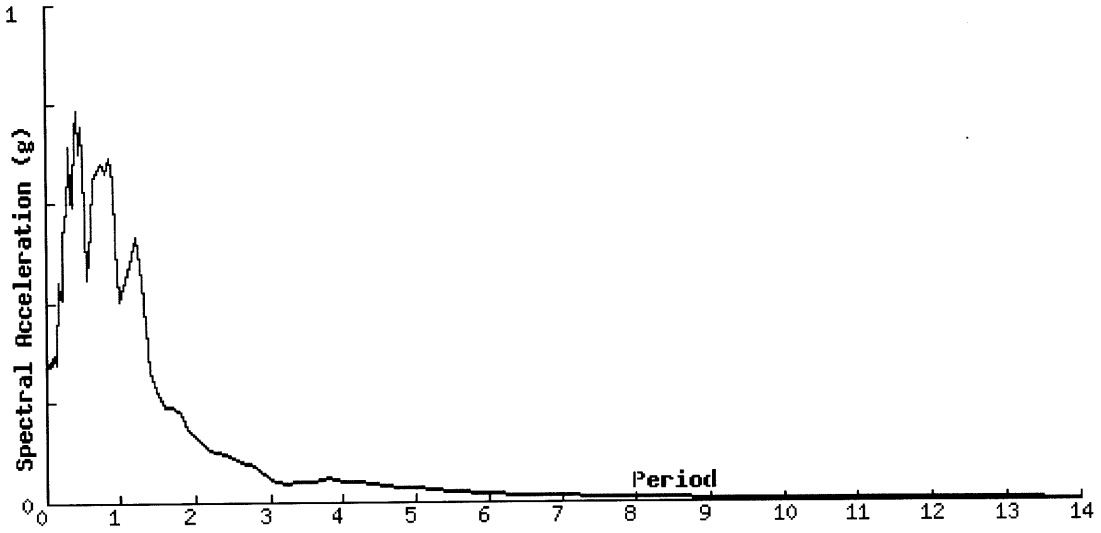

Wikipedia link: http://en.wikipedia.org/wiki/1992_Landers_earthquake

15) Big Bear 1992

Magnitude: 6.5
Recording station and instrument:
Snow Creek, CA
Hypocentral distance: 37.9 km
180°

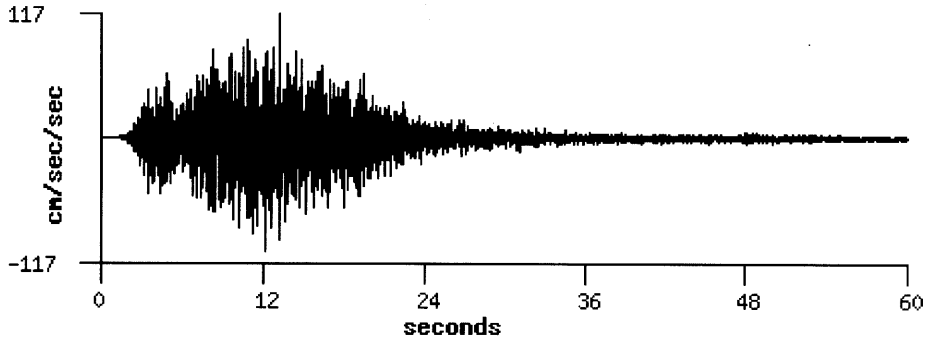

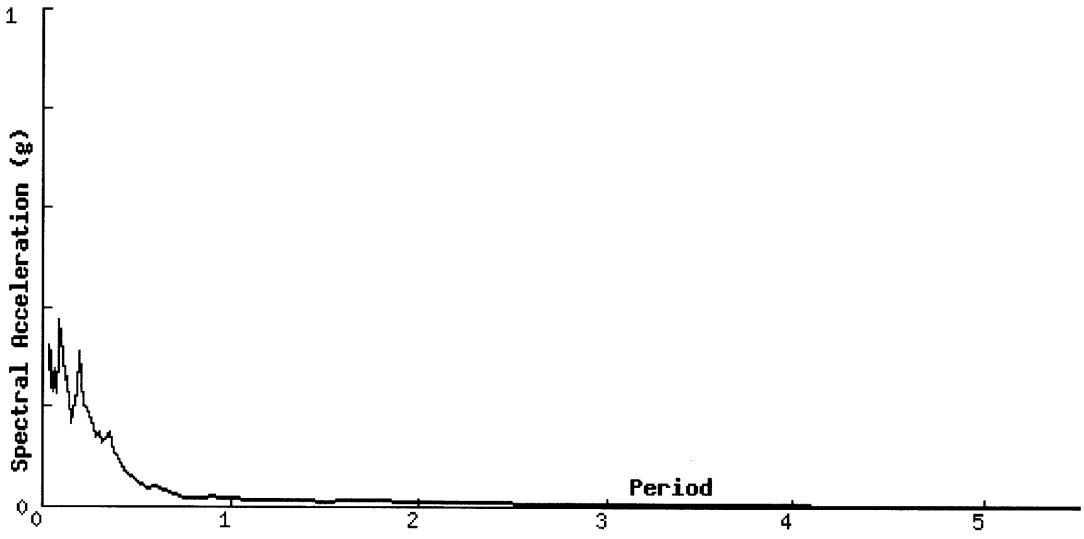

Wikipedia link: http://en.wikipedia.org/wiki/1992_Big_Bear_earthquake

16) Northridge 1994

Magnitude: 6.4
Recording station and instrument:
Tarzana, CA - Cedar Hill Nursery A
Closest distance to fault: 16.7 km
360°

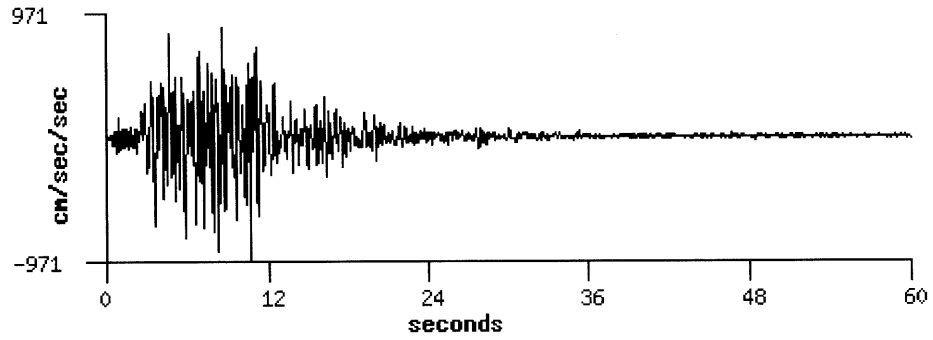

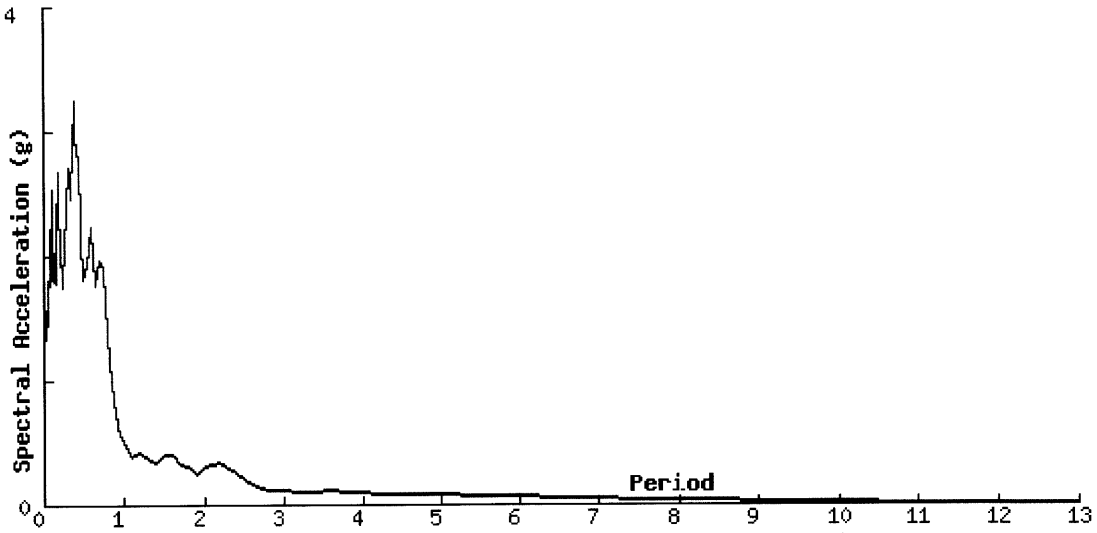

Wikipedia link: http://en.wikipedia.org/wiki/1994_Northridge_earthquake

17) Hector Mine 1999

Magnitude: 7.1
Recording station and instrument:
Amboy, CA
Hypocentral distance: 48.4 km
360°

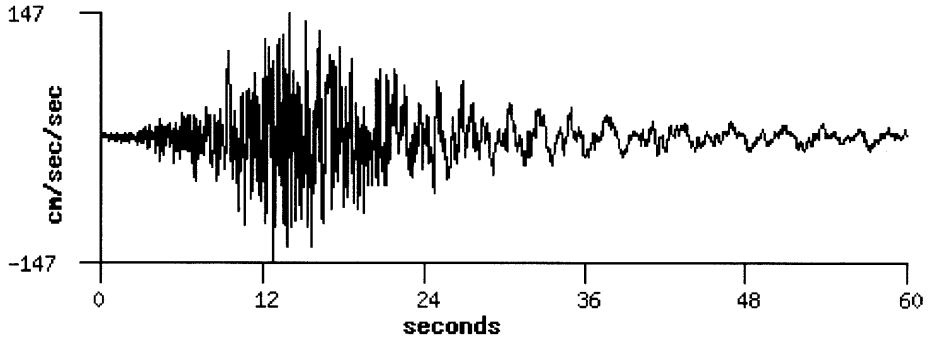

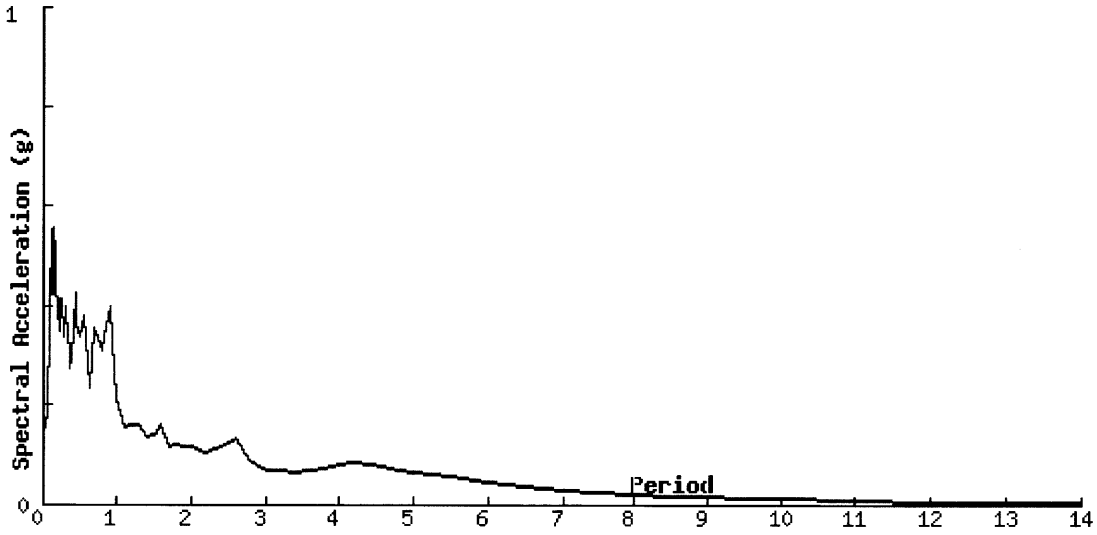

Wikipedia link: http://en.wikipedia.org/wiki/1999_Hector_Mine_earthquake

18) San Simeon 2003

Magnitude: 6.5
Recording station and instrument:
Cambria, CA - Hwy 1 Caltrans Bridge Grnds
Hypocentral distance: 14.8 km
360°

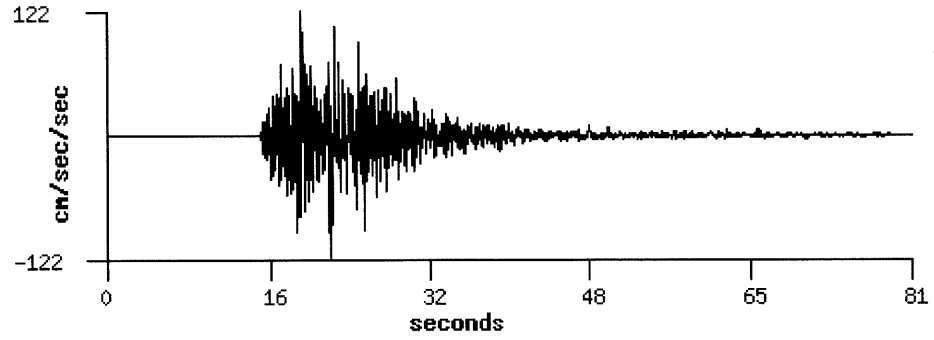

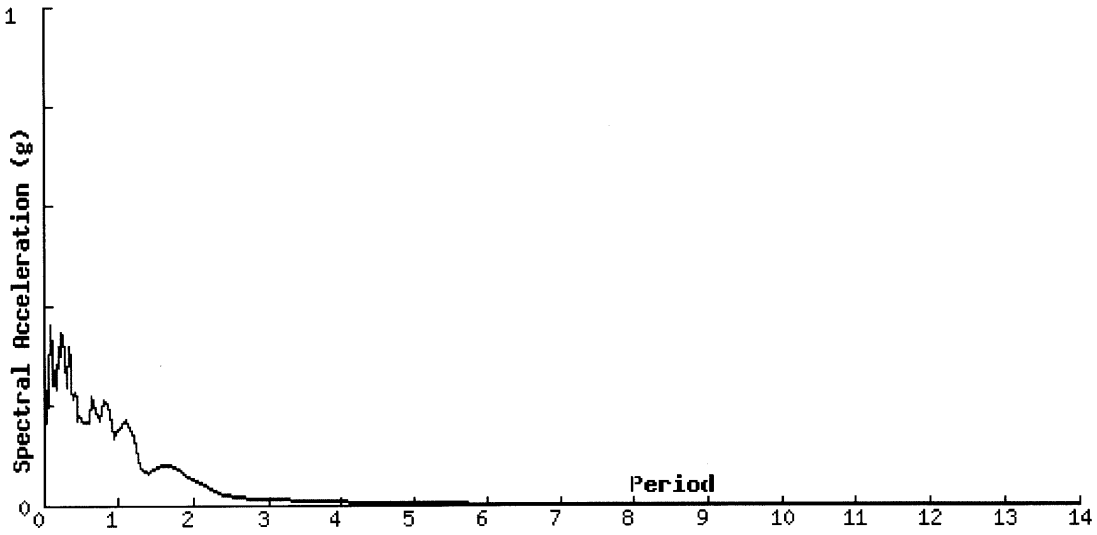

Wikipedia link: http://en.wikipedia.org/wiki/San_Simeon_earthquake

19) Parkfield 2004

Magnitude: 6.0
Recording station and instrument:
Parkfield, CA - Gold Hill 1W
Closest dist to fault: 0.5 km
360°

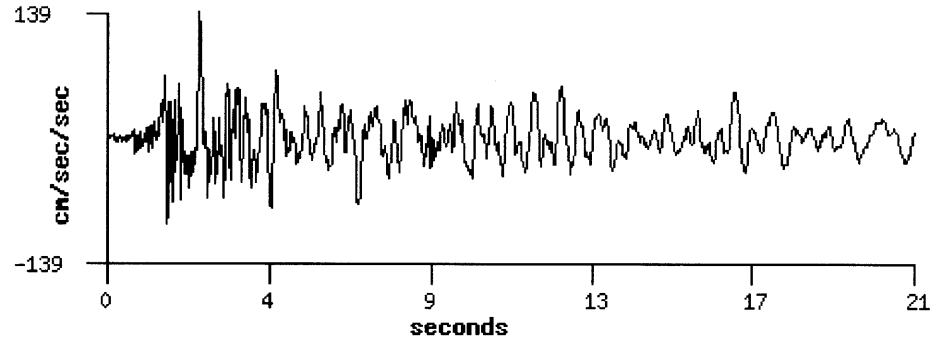

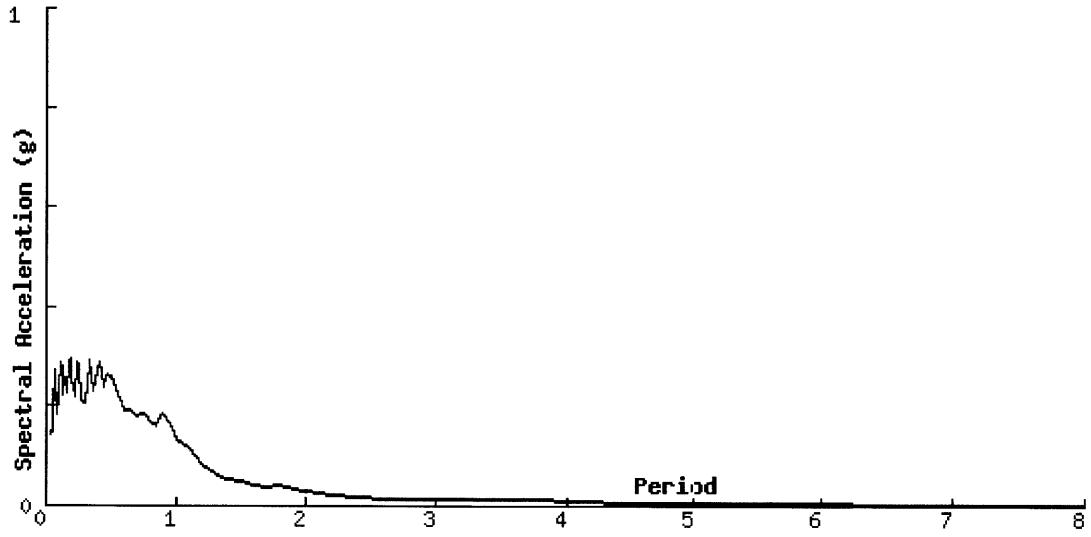

Wikipedia link: http://en.wikipedia.org/wiki/2004_Parkfield_earthquake

Notes:

High resolution data of this event is available from the Parkfield High Resolution Seismic Network.[A3] As part of the research operation at Parkfield, a hole was drilled near the fault to a depth of 8500 feet. Drilling was completed a week before this event.[A4]

20) Hawaii 2006

Magnitude: 6.7
Recording station and instrument:
Anaehoomalu, Hawaii Is, HI - Waikoloa Hotel
Hypocentral dist: 42.5 km
178°

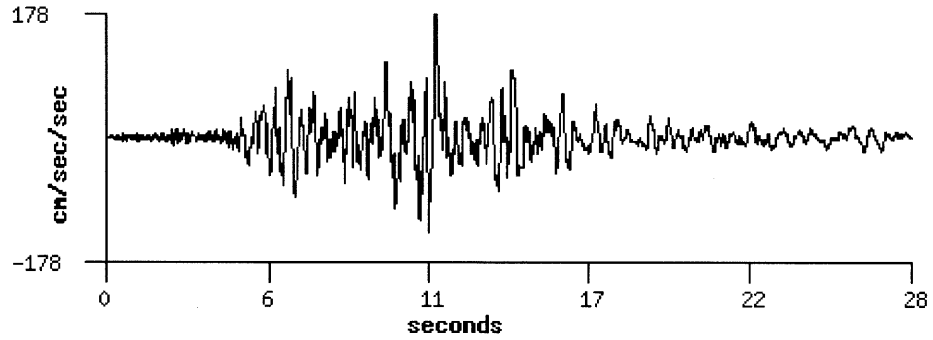

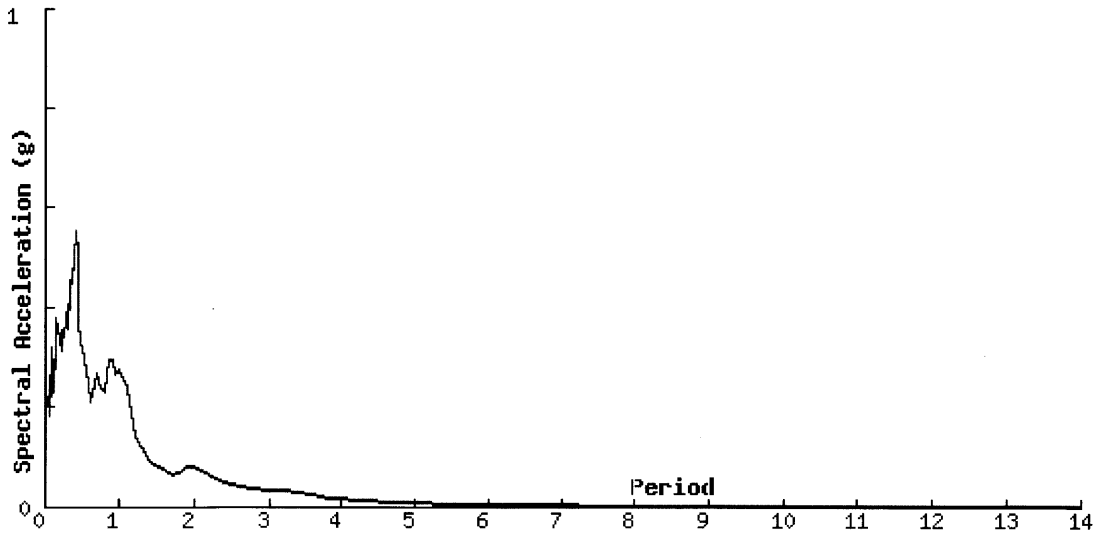

Wikipedia link: http://en.wikipedia.org/wiki/2006_Hawaii_earthquake

References

Earthquake data from the COSMOS Virtual Data Center[A2].
Magnitude information from the Strong Motion Center[A1].

[A1] http://www.strongmotioncenter.org/cgi-bin/CESMD/archive.pl?Archives=Significant (Jan 9th 2012)
[A2] http://db.cosmos-eq.org/scripts/earthquakes.plx (Jan 9th 2012)
[A3] http://www.ncedc.org//2004parkfield.html (Jan 9th 2012)
[A4] http://www.cisn.org/special/evt.04.09.28/ (Jan 9th 2012)
[A5] http://earthquake.usgs.gov/earthquakes/states/us_damage_eq.php (Jan 9th 2012)

Appendix B: A Set of Benchmark Building Models for Use in Simulations

B.1. Index of Symbols Used

Symbols are defined as they are used, and are also defined here for reference.

A	constant used to simplify the calculation of parabolic stiffness distribution. Defined in eqn B.53
C_T	variable used by the ASCE 7-05 code to find the approximate first natural period
D	the fractional increase in stiffness, of k_1, that defines a linearly-increasing stiffness distribution
d	The linear increment of lower story stiffnesses as a fraction of k_1. Defined in eqn B.11
δ	story drift
E	material stiffness modulus
$\underline{e}$	rigid body vector. Defined in eqn B.9
F_I	force on structure node i. In particular the forces in the wall-building links
$\underline{F}$	vector of forces F_i
$\underline{F_w}$	vector of the net loads on the wall
$\underline{F_w}'$	vector of the net loads on the wall but incomplete as $F_N = 0$
$\underline{F_b}$	vector of the net loads on the building
$\boldsymbol{F_{wall}}$	wall pseudo-flexibility matrix, determining shape from loads
$\boldsymbol{F_l}$	a 'flip' matrix. Defined in eqn B.28
H	total height of the building
h, h_s	single story height
$h_{i,j}$	the height of the i^{th}, j^{th} story
$\boldsymbol{I}$	the identity matrix
I	second moment of area, usually of the rocking wall
J	the rotational moment of inertia of the rocking wall
k_i	the story stiffness of the i^{th} story, where i=1 is the top story
k	story stiffness. If no subscript, then represents constant story stiffness
$\underline{k}$	stiffness vector of the building story stiffnesses
$\boldsymbol{K}$	stiffness matrix, either of the building, or of the whole building-rocking wall system ,depending on context
$\boldsymbol{K_{wall}}$	wall pseudo-stiffness matrix, determining loads from shape
$\boldsymbol{K_{bldg}}$	the stiffness matrix of the building
$\boldsymbol{L}$	a lower triangular matrix where the lower triangular elements are all unity. Defined in eqn B.16
L	length, either of a single story, or the total height of the rocking wall, depending on context
$\boldsymbol{M}$	diagonal matrix of the masses in a building. Defined for the standard top-light case in eqn B.3
M	total mass of the rocking wall
m	mass of any non-top story, when using the standard top-light mass distribution
m_i	the mass of the i^{th} story
N	the number of stories in the building
P_i	load on building position i
$\underline{P}$	vector of P_i
Q_i	load on wall position i

$\underline{Q}$	vector of Q_I
$\boldsymbol{S_{D/L}}$	a matrix that shifts elements down or left depending whether it pre- or post-multiplies. Defined in eqn B.5
$\boldsymbol{S_{U/R}}$	a matrix that shifts elements up or right depending whether it pre- or post-multiplies. Defined in eqn B.6
S_s	geographical short period acceleration
T, T_1	first natural period, usually of the building
T_a	approximate first natural period
u_i	displacement of building node i
$\underline{U}$	vector of u_i
$\boldsymbol{U}$	an upper triangular matrix where the upper triangular elements are all unity. Defined in eqn B.17
v_i	displacement of wall node i
$\underline{V}$	vector of v_i
$\underline{v}$	linear vector which is the standard initial guess for the building first mode.
V	the base shear in an equivalent seismic load calculation
$\boldsymbol{V}$	diag($\underline{v}$), a diagonal matrix of the linear vector $\underline{v}$. Defined in eqn B.58
$\underline{W}$	shape displacement vector for wall, as measured from some rotational datum line
W_i	i^{th} element of $\underline{W}$
ω_n, ω_1	first natural angular frequency, usually of the building
ψ	angle through which the datum line (projected through the hinge and position N) of the wall has rotated
$\underline{\psi}$	vector representing a rigid body rotation of ψ

B.2. Conventions

In this appendix, the top node of a discretized building is referred to as *node 1*, while the lowest node is referred to as *node N*. This is in contrast to the work body.

B.3. Introduction

In order to present details of the most useful rocking wall size for representative building types, those representative buildings must first be defined.

There are many ways in which this could be done. The method that seems most natural is to start with basic assumptions that a structural engineer would have about a building of a given size. One of the earliest appreciations that an engineer has is of the natural period of a building.

The natural period may be estimated with the familiar $T \approx 0.1N$. However, that is a very rough approximation, and can be considerably off, especially for certain kinds of structure. A better approach to approximate the period is to follow the guidelines in a widely accepted code, such as *ASCE 7-05*. *ASCE 7-05* considers almost all building types when calculating the natural period, and although it usually produces a result within 25% of $T \approx 0.1N$, is not constrained by the assumptions in that formula.

In addition to story masses, the only other piece of information needed to determine the story stiffnesses is the stiffness form. For example, it is required to know whether the story stiffnesses are uniform, or increase linearly from the top down, or increase parabolically from the top down. It is not possible to model every building, but rather a representative set of models may be determined, one of which will offer a reasonable approximation to most given rocking wall installations, and thus provide data which simplifies the analysis process.

It is important to understand that if, in addition to the mass distribution, the stiffness form (constant/linear/parabolic) is known, and code is used to determine the natural period, then the code fully implies the stiffness matrix. Developing a stiffness matrix in addition to using code to determine the natural period is redundant. Likewise, if the stiffness matrix is known, then using the code to find the period is redundant. And since code provides a very useful approximation of the natural period of buildings, it may also be extended to provide a useful set of representative building models. Making the leap from natural period to stiffness matrix, given the stiffness form, requires some careful algebra, which is presented here.

Based on the mass, mass form, and stiffness form, algebra may be applied that rearranges the Rayleigh quotient formula, including inverse iteration, to provide the building stiffnesses, to determine the story stiffnesses, and thus produce a set of representative discretized building models. An example will also be used to suggest that using five inverse iterations is equivalent for any reasonable purpose to a closed-form solution.

In the case where the story stiffnesses are uniform, the Rayleigh quotient is not required, since the closed-form solution may be applied:

$$\omega_1^2 = 4\frac{k}{m}\sin^2\frac{\pi}{4N} \qquad (B.1)^{(2,p139)}$$

where N is the number of stories, m is the story mass of a standard top-light building model, and k is the story stiffness.

B.4. Using the Rayleigh Quotient to Find the Building Stiffness

In order to find the stiffness from the natural period of a building, the logical formula to use is the Rayleigh quotient.

When the Rayleigh quotient is used with buildings, a very commonly used initial vector is the linear vector, $\underline{v} = [N, N-1, \ldots, 1]^T$.

If this vector is substituted into the denominator of the Rayleigh quotient formula, with a standard top-light mass matrix $\boldsymbol{M}$, it can be seen that:

$$\underline{v}^T \boldsymbol{M} \underline{v} = m\frac{N}{6}(2N^2 + 1) \qquad (B.2)^{(2,p138)}$$

where

$$\boldsymbol{M} = \begin{bmatrix} \frac{m}{2} & 0 & \cdots & 0 \\ 0 & m & & \vdots \\ \vdots & & \ddots & 0 \\ 0 & \cdots & 0 & m \end{bmatrix} \qquad (B.3)$$

For the numerator, a similar method may be applied in the case where k_i are constant:

$$\underline{v}^T \boldsymbol{K} \underline{v} = Nk \qquad (B.4)^{(2,p138)}$$

However, most buildings do not have a constant k_i, but rather are stiffer at the base, and become less stiff towards the top. Thus it would be useful to extend this idea to other distributions of k_i.

Let us define a matrix $\boldsymbol{S_{D/L}}$, that shifts elements down or left, and $\boldsymbol{S_{U/R}}$, that shifts elements up or right, depending respectively whether they pre- or post-multiply:

$$\boldsymbol{S}_{D/L} = \begin{bmatrix} 0 & 0 & \cdots & 0 \\ 1 & \ddots & \ddots & \vdots \\ 0 & \ddots & \ddots & 0 \\ 0 & 0 & 1 & 0 \end{bmatrix} \tag{B.5}$$

$$\boldsymbol{S}_{U/R} = \begin{bmatrix} 0 & 1 & \cdots & 0 \\ 0 & \ddots & \ddots & \vdots \\ 0 & \ddots & \ddots & 1 \\ 0 & 0 & 0 & 0 \end{bmatrix} \tag{B.6}$$

it is seen that

$$\underline{v}^T(\boldsymbol{I} - \boldsymbol{S}_{D/L}) = \underline{e}^T \tag{B.7}$$

$$(\boldsymbol{I} - \boldsymbol{S}_{U/R})\underline{v} = \underline{e} \tag{B.8}$$

where

$$\underline{e} = \begin{bmatrix} 1 \\ \vdots \\ \vdots \\ 1 \end{bmatrix} \tag{B.9}$$

If the output of the formula $\underline{v}^T\boldsymbol{K}\underline{v}$ is studied, it is observed that:

$$\underline{v}^T\boldsymbol{K}\underline{v} = \sum_{i=1}^{N} k_i \tag{B.10}$$

This is very useful, and this may be used with the uniterated Rayleigh quotient formula to determine k_i, for some predictable distribution of stiffness, given the natural period of a structure. However, it would be preferable to apply inverse iteration in the solution.

B.5. Using Inverse Iteration to Find the Building Stiffness

The next step is to incorporate inverse iteration to the method, to ensure that the values found for k_i are as close as possible to the true values.

However, the Rayleigh quotient formula only allows us to solve for one variable, so in order to use inverse iteration, a stiffness matrix must be formulated specifically for a given arrangement of stiffnesses, in terms of a fixed variable that defines the stiffness distribution, such as k_1.

When each story stiffness is a successive multiple of the top stiffness (i.e. in the following example, the increment $d=1$), the structure deforms linearly, under uniform loading.[3,p58] Let us consider the general linearly-increasing case, in which the increment d may be less than or greater than unity:

$$k_i = k_1 + (j-1)dk_1 \qquad (1 \leq j < N;\ d \in \mathbb{R}^+) \qquad (B.11)$$

It is required to solve the following for k_1, or some other variable that uniquely specifies the stiffness matrix, given the stiffness arrangement:

$$R_i = \frac{\underline{v}^T((K^{-1}M)^T)^n K(K^{-1}M)^n \underline{v}}{\underline{v}^T((K^{-1}M)^T)^n M(K^{-1}M)^n \underline{v}} \qquad (B.12)$$

Since it is known that:

$$\underline{v}^T \boldsymbol{K} \underline{v} = \sum_{i=1}^{N} k_i \qquad (B.13)$$

and by definition:

$$\underline{e}^T \underline{k} = \sum_{i=1}^{N} k_i \qquad (B.14)$$

it may be equated in the general case:

$$\underline{e}^T \underline{k} = \underline{v}^T \boldsymbol{K} \underline{v} \qquad (B.15)$$

It would be helpful if $\underline{k}$, a vector of story stiffnesses could be solved for, knowing $\boldsymbol{K}$. Define:

$$\boldsymbol{L} = \begin{bmatrix} 1 & 0 & \cdots & 0 \\ 1 & \ddots & \ddots & \vdots \\ \vdots & \ddots & \ddots & 0 \\ 1 & \cdots & 1 & 1 \end{bmatrix} \tag{B.16}$$

$$\boldsymbol{U} = \begin{bmatrix} 1 & 1 & \cdots & 1 \\ 0 & \ddots & \ddots & \vdots \\ 0 & \ddots & \ddots & 1 \\ 0 & 0 & 0 & 1 \end{bmatrix} \tag{B.17}$$

and thus:

$$\underline{v} = \boldsymbol{U}\underline{e} \tag{B.18}$$

$$v^T = \underline{e}^T\boldsymbol{L} \tag{B.19}$$

Also note that:

$$(\boldsymbol{I} - \boldsymbol{S}_{D/L}) = \mathbf{L}^{-1} \tag{B.10}$$

$$(\boldsymbol{I} - \boldsymbol{S}_{U/R}) = \mathbf{U}^{-1} \tag{B.21}$$

Thus *equation B.19* may be rearranged for $\underline{e}^T$, and substitute into *equation B.15*:

$$\underline{v}^T(\boldsymbol{I} - \boldsymbol{S}_{D/L})\underline{k} = \underline{v}^T\boldsymbol{K}\underline{v} \tag{B.22}$$

And so the following may be observed in the general case:

$$\underline{k} = \boldsymbol{L}\boldsymbol{K}\underline{v} \tag{B.23}$$

$$\boldsymbol{L}\boldsymbol{K}\boldsymbol{U} = diag(\underline{k}) \tag{B.24}$$

$$\underline{k} = \boldsymbol{L}\boldsymbol{K}\boldsymbol{U}\underline{e} \tag{B.25}$$

Thus, to find $\boldsymbol{K}$ as a multiple of k_1, or of some other variable that defines a specific arrangement of stiffnesses, first $diag(\underline{k})$ must be defined as a multiple of that variable.

B.5.1. Linear Stiffness

For the linear case,

$$\underline{k} = k_1 \begin{bmatrix} 1 \\ 1+d \\ 1+2d \\ \vdots \\ 1+(N-1)d \end{bmatrix} \tag{B.26}$$

so

$$diag(\underline{k}) = k_1(\boldsymbol{I} + d\boldsymbol{S_{D/L}F_lVF_lS_{U/R}}) \tag{B.27}$$

where $\boldsymbol{F_l}$ is a 'flip' matrix:

$$\boldsymbol{F_l} = \begin{bmatrix} 0 & \cdots & 0 & 1 \\ \vdots & & \iddots & 0 \\ 0 & \iddots & & \vdots \\ 1 & 0 & \cdots & 0 \end{bmatrix} \tag{B.28}$$

where it might be noted that $\boldsymbol{U} = \boldsymbol{F_lLF_l}$. $\boldsymbol{V}$ is the linear diagonal matrix:

$$\boldsymbol{V} = diag(\underline{v}) = \underline{v}\underline{e}^T .*\boldsymbol{I} = \begin{bmatrix} N & 0 & \cdots & 0 \\ 0 & N-1 & & \vdots \\ \vdots & & \ddots & 0 \\ 0 & \cdots & 0 & 1 \end{bmatrix} \tag{B.29}$$

thus substituting *equation B.27* into *equation B.24*,

$$k_1(\boldsymbol{I} + d\boldsymbol{S_{D/L}F_lVF_lS_{U/R}}) = \boldsymbol{LKU} \tag{B.30}$$

rearranging:

$$\boldsymbol{K} = k_1(\boldsymbol{I} - \boldsymbol{S_{D/L}})(\boldsymbol{I} + d\boldsymbol{S_{D/L}F_lVF_lS_{U/R}})(\boldsymbol{I} - \boldsymbol{S_{U/R}}) \tag{B.31}$$

and so

$$\boldsymbol{K^{-1}} = \frac{1}{k_1}\boldsymbol{U}(\boldsymbol{I} + d\boldsymbol{S_{D/L}F_lVF_lS_{U/R}})^{-1}\boldsymbol{L} \tag{B.32}$$

This linearly increasing $\boldsymbol{K}$ may thus also be substituted into the uniterated Rayleigh quotient formula as a simple multiple of k_1:

$$\underline{v}^T\boldsymbol{K}\underline{v} = k_1\underline{v}^T(\boldsymbol{I} - \boldsymbol{S_{D/L}})(\boldsymbol{I} + d\boldsymbol{S_{D/L}F_lVF_lS_{U/R}})(\boldsymbol{I} - \boldsymbol{S_{U/R}})\underline{v} \qquad (B.33)$$

simplifying:

$$\underline{v}^T\boldsymbol{K}\underline{v} = \underline{e}^T\underline{k} = k_1\underline{e}^T(\boldsymbol{I} + d\boldsymbol{S_{D/L}F_lVF_lS_{U/R}})\underline{e} \qquad (B.34)$$

The mass matrix may also be defined in terms of such standard matrices, multiplied by a constant:

$$\boldsymbol{M} = \frac{m}{2}(\boldsymbol{I} + \boldsymbol{S_{D/L}S_{U/R}}) \qquad (B.35)$$

and so:

$$\boldsymbol{K^{-1}M} = \frac{m}{2k_1}\boldsymbol{U}(\boldsymbol{I} + d\boldsymbol{S_{D/L}F_lVF_lS_{U/R}})^{-1}\boldsymbol{L}(\boldsymbol{I} + \boldsymbol{S_{D/L}S_{U/R}}) \qquad (B.36)$$

Thus, in the linear case, the n^{th} iteration of the first eigenvector is:

$$\underline{v}_n = (\boldsymbol{K^{-1}M})^n\underline{v} = \frac{m^n}{2^n k_1^{\,n}}[\boldsymbol{U}(\boldsymbol{I} + d\boldsymbol{S_{D/L}F_lVF_lS_{U/R}})^{-1}\boldsymbol{L}(\boldsymbol{I} + \boldsymbol{S_{D/L}S_{U/R}})]^n\underline{v} \qquad (B.37)$$

where high n may simply be chosen to very closely approximate the true eigenvector. The constants may be neglected of course. Thus the iterated Rayleigh quotient formula for k_1 may be evaluated:

$$k_1 = \frac{\omega_1^{\,2}\underline{v_n}^T M\underline{v_n}}{\left(\frac{\underline{v_n}^T K\underline{v_n}}{k_1}\right)} \qquad (B.38)$$

$$= \frac{\omega_1^{\,2}\frac{m}{2}\underline{v_n}^T(I + S_{D/L}S_{U/R})\underline{v_n}}{\underline{v_n}^T(I - S_{D/L})(I + dS_{D/L}F_lVF_lS_{U/R})(I - S_{U/R})\underline{v_n}} \qquad (B.39)$$

which may be found in non-dimensional form:

$$\frac{k_1}{m\omega_1^2} = \frac{\frac{1}{2}\underline{v_n}^T (I + S_{D/L}S_{U/R})\underline{v_n}}{\underline{v_n}^T (I - S_{D/L})(I + dS_{D/L}F_1VF_1S_{U/R})(I - S_{U/R})\underline{v_n}} \qquad (B.40)$$

where $\underline{v_n}$ is found in *equation B.37*. The constants multiplying $\underline{v_n}$ and $\underline{v_n}^T$ are not required.

B.5.2. Constant Stiffness

Now that the case of linearly increasing story stiffnesses has illuminated the issues, let the simpler case be considered, where k_i are constant.

E*quation B.1* may be rearranged to find k in the constant case, or $d=0$ may be set in *equation B.40*. But let the problem also be solved from scratch, in order to compare the results.

For the constant case,

$$diag(\underline{k}) = k\boldsymbol{I} \qquad (B.41)$$

substituting into *equation B.24*:

$$k\boldsymbol{I} = \boldsymbol{LKU} \qquad (B.42)$$

rearranging:

$$\boldsymbol{K} = k(\boldsymbol{I} - \boldsymbol{S_{D/L}})(\boldsymbol{I} - \boldsymbol{S_{U/R}}) \qquad (B.43)$$

and so

$$\boldsymbol{K^{-1}} = \frac{1}{k}\mathbf{UL} \qquad (B.44)$$

Then if the mass matrix defined in *equation B.35* is multiplied by, then:

$$\boldsymbol{K^{-1}M} = \frac{m}{2k}\mathbf{UL}(\boldsymbol{I} + \boldsymbol{S_{D/L}S_{U/R}}) \qquad (B.45)$$

Thus, in the constant case, the n^{th} iteration of the first eigenvector is:

$$\underline{v}_n = (\boldsymbol{K}^{-1}\boldsymbol{M})^n \underline{v} = \frac{m^n}{2^n k^n}[\,\mathbf{UL}(\boldsymbol{I} + \boldsymbol{S}_{D/L}\boldsymbol{S}_{U/R})]^n \underline{v} \qquad (B.46)$$

where again high n may simply be chosen to very closely approximate the true eigenvector, and neglect the constants. Thus the iterated Rayleigh quotient formula for k may be evaluated:

$$k = \frac{\omega_1^{\,2}\,\underline{v}^T M \underline{v}}{\left(\dfrac{\underline{v}^T K \underline{v}}{k_1}\right)} \qquad (B.47)$$

$$= \frac{\omega_1^{\,2}\,\dfrac{m}{2}\underline{v}^T (I + S_{D/L}S_{U/R})\underline{v}}{\underline{v}^T (I - S_{D/L})(I - S_{U/R})\underline{v}} \qquad (B.48)$$

which matches *equation B.40* where $d = 0$. $\underline{v}=\underline{v}_n$ may be substituted from *equation B.46*. The constants multiplying $\underline{v}_n$ and $\underline{v}_n^T$ are not required.

The performance of this formula is excellent as expected. It may be compared with the closed-form solution non-dimensionally:

$$\frac{k}{m\omega_1^{\,2}} = \frac{1}{4}\mathrm{cosec}^2\frac{\pi}{4N} \qquad (B.49)^{(2,p139)}$$

For $N = 10$, the closed-form solution yields *40.611909699 to 9 d.p.* E*quation B.48* yields:

Iterations	$\frac{m\omega_1^{\,2}}{k}$	Error (%)
0	33.5	17.51
1	40.556	1.4×10^{-1}
2	40.61124	1.6×10^{-3}
3	40.611901	2.1×10^{-5}
4	40.6119096	2.7×10^{-7}
5	40.611909698	3.4×10^{-9}

Table B1. The output of equation B.48 compared with the closed-form eigenvalue formula

As can be seen from table *B1,* with each iteration, the error is about two orders of magnitude better. It seems clear that using five iterations would ensure an entirely negligible difference between the estimated value and the true value. The software developed in this work uses 50 iterations, which is computationally trivial.

B.5.3. Parabolic Stiffness

Since seismic loading is parabolic in nature, a common strategy in building design is to have the stiffness form be parabolic.

It can be seen that if constant story drifts δ are required to ensure that damage is spread evenly, then:

$$\underline{k} = \frac{1}{\delta} \boldsymbol{F}_1 \boldsymbol{U} \underline{p} \qquad (B.50)$$

where $\underline{k}$ is the stiffness vector, and $\underline{p}$ is any load vector. The inspiration for this neat formula (*equation B.50*) is Jerome Connor's *Introduction to Structural Motion Control*, which gives a more general form for any desired drift arrangement[3,p58]. It so happens that for constant story drifts, the stiffness vector $\underline{k}$ may be expressed in terms of the standard matrices previously defined.

For equivalent seismic loading, that the loads p_j may be defined as:

$$p_j = \frac{V h_j^k m_j}{\sum_i h_i^k m_i} \qquad (B.51)^{(4,p130)}$$

in which $k = 2$ unless the period is less than $0.5s$, in which case $k = 1$, with the option for linear interpolation between 1 and 2 if the natural period is between $0.5s$ and $2.5s$. For the case $k = 2$, and for the standard top-light mass model, this can be expressed in vector form as:

$$\underline{p} = \frac{Vm}{\sum_i h_i^2 m_i} h_s^2 \begin{bmatrix} \frac{1}{2} & 0 & \cdots & 0 \\ 0 & 1 & & \vdots \\ \vdots & & \ddots & 0 \\ 0 & \cdots & 0 & 1 \end{bmatrix} \begin{bmatrix} N^2 \\ (N-1)^2 \\ \vdots \\ 1^2 \end{bmatrix} \tag{B.52}$$

where h_s is the single story height. Denote the constant:

$$\frac{Vm}{\sum_i h_i^2 m_i} h_s^2 = A \tag{B.53}$$

then:

$$\underline{p} = \frac{1}{2} A(\boldsymbol{I} + \boldsymbol{S}_{D/L}\boldsymbol{S}_{U/R}) \begin{bmatrix} N^2 \\ N^2 - 2N + 1^2 \\ N^2 - 4N + 2^2 \\ \vdots \\ \vdots \\ N^2 - 2(N-1)N + (N-1)^2 \end{bmatrix} \tag{B.54}$$

$$= \frac{1}{2} A(\boldsymbol{I} + \boldsymbol{S}_{D/L}\boldsymbol{S}_{U/R})[N^2 \underline{e} - \begin{bmatrix} 0 \\ 2 \\ 4 \\ \vdots \\ 2(N-1) \end{bmatrix} N + \begin{bmatrix} 0 \\ 1^2 \\ 2^2 \\ \vdots \\ (N-1)^2 \end{bmatrix}] \tag{B.55}$$

$$= \frac{1}{2} A(\boldsymbol{I} + \boldsymbol{S}_{D/L}\boldsymbol{S}_{U/R})[N^2 \underline{e} - 2N\boldsymbol{S}_{D/L}\boldsymbol{F}_l\boldsymbol{U}\underline{e} + \boldsymbol{F}_l(\boldsymbol{S}_{U/R}\boldsymbol{V}\boldsymbol{S}_{D/L})^2 \underline{e}] \tag{B.56}$$

$$= \frac{1}{2} A(\boldsymbol{I} + \boldsymbol{S}_{D/L}\boldsymbol{S}_{U/R})[N^2 \boldsymbol{I} - 2N\boldsymbol{S}_{D/L}\boldsymbol{F}_l\boldsymbol{U} + \boldsymbol{F}_l(\boldsymbol{S}_{U/R}\boldsymbol{V}\boldsymbol{S}_{D/L})^2]\underline{e} \tag{B.57}$$

where $V = diag(\underline{v})$:

$$V = \begin{bmatrix} N & 0 & \cdots & 0 \\ 0 & N-1 & & \vdots \\ \vdots & & \ddots & 0 \\ 0 & \cdots & 0 & 1 \end{bmatrix} \tag{B.58}$$

And thus substituting *equation B.57* into *equation B.50*:

$$\underline{k} = \frac{A}{2\delta} \boldsymbol{F_I U (I + S_{D/L} S_{U/R})[N^2 I - 2N S_{D/L} F_I U + F_I (S_{U/R} V S_{D/L})^2]} \underline{e} \tag{B.59}$$

And thus from *equation B.24*:

$$\boldsymbol{LKU} = diag(\underline{k}) \tag{B.60}$$

It is possible to determine $diag(\underline{k})$ in the parabolic case directly in terms of standard matrices, but the formula is very long, and there is no real benefit to it. Rearranging:

$$\boldsymbol{K} = \boldsymbol{(I - S_{D/L})} diag(\underline{k}) \boldsymbol{(I - S_{U/R})} \tag{B.61}$$

and thus:

$$\boldsymbol{K^{-1}} = \boldsymbol{U} [diag(\underline{k})]^{-1} \boldsymbol{L} \tag{B.62}$$

Then if the mass matrix defined in *equation B.35* is multiplied by, then

$$\boldsymbol{K^{-1} M} = \frac{m}{2} \boldsymbol{U} [diag(\underline{k})]^{-1} \boldsymbol{L\ (I + S_{D/L} S_{U/R})} \tag{B.63}$$

Thus, in the parabolic case, the n^{th} iteration of the first eigenvector is:

$$\underline{v}_n = \boldsymbol{(K^{-1} M)^n} \underline{v}$$

$$= \frac{m^n}{2^n} \boldsymbol{[U} [diag(\underline{k})]^{-1} \boldsymbol{L\ (I + S_{D/L} S_{U/R})]^n} \underline{v} \tag{B.64}$$

where high n may simply be chosen to very closely approximate the true eigenvector, with the constants neglected. Thus the iterated Rayleigh quotient formula may be evaluated, in this case solving for δ, the constant interstory drift:

$$\delta = \frac{\delta \underline{v}^T K \underline{v}}{\omega_1^2 \underline{v}^T M \underline{v}} =$$

$$\frac{\delta \underline{v}^T (\boldsymbol{I} - \boldsymbol{S}_{D/L}) diag(\underline{k}) (\boldsymbol{I} - \boldsymbol{S}_{U/R}) \underline{v}}{\omega_1^2 \frac{m}{2} \underline{v}^T (\boldsymbol{I} + \boldsymbol{S}_{D/L} \boldsymbol{S}_{U/R}) \underline{v}} \qquad (B.65)$$

$\underline{v}=\underline{v}_n$ may be substituted from *equation B.64*. The constants multiplying $\underline{v}_n$ and $\underline{v}_n^T$ are again not required. Taking $\frac{\delta}{A}$ *to the outside of diag(*$\underline{k}$*),* $\frac{\delta}{A}$ may now be substituted into *equation B.61* to obtain the stiffness matrix.

In summation, the stiffness vector, matrix and mode may be found in any of the three cases with inputs N, w_1, and m, with the addition of d in the linearly increasing case.

An alternative use for *equation B.65* is to specify the desired story drift δ for a parabolic stiffness arrangement, which will provide constant story drift under equivalent seismic loading, and solve for the resulting period and hence stiffnesses. The same is true for any of the previous stiffness arrangements.

B.6. Representative Model Building Data with Rocking Wall Design Data

56 representative model buildings are presented, with 116 rocking wall configurations, each with a graph of maximum storey drift vs. rocking wall size.

The storey drifts were determined using the static equivalent seismic loading method, and were based on a location of Los Angeles, California. The story stiffnesses were determined by extrapolation from the code-derived period and the mass of each structure. The constant data used to determine the period of the buildings and seismic loads from *ASCE 7-05* were:

Story Height	*3.3m*
Occupancy Category	*3 (e.g > 300 people)*
1-second Spectral Acceleration S_1	*0.75*
Short-period Spectral Acceleration S_s	*1.5*
Site Class	*D*
LLRS	*Concrete Moment Frame*
Response Modification Factor R	*4*
Long Period Transition Period T_L	*8*

Other constant data were:

Rocking Wall Depth	*0.61m*
Average Density	*400 kg/m^3*

The data modified for each model building were:

N	*Number of stories*
Height:width Ratio	*2 to 5 stories: 1* *6 to 10 stories: 2* *11 to 15 stories: 3* *(square plan)*
m	*The single story mass m based on the above.*
Stiffness Form (d)	*Four different linear stiffness forms were tested, with d (the increase in stiffness of lower stories as a fraction of the upper storey) as 0.0, 0.25, 0.5, and 1.0. Thus only the top story stiffness $\underline{k}_{top}$ is given in the tables. The other stiffnesses can be inferred from $\underline{k}_{top}$ and d.*
Number of Rocking Walls	*2-5 stories: one pair of rocking walls,* *6-10 stories: up to two pairs,* *15 stories: up to three pairs.*

Each graph has been cropped to show only the most relevant data. It may be noted that the small stiff buildings of 2-4 stories have very low story drifts, but from 5 to 15 stories, all of the data are in the 0.4-0.7% range, and produce some very interesting and sometimes unexpected graphs, which may be confirmed in any finite element software package.

N	Number Walls	d	m (kg)	T_1 (s)	k_{top} (N/m)	Maximum Story Drift Angle vs. Rocking Wall Width (m)
2	2	0	57499	0.2547	5.972E+07	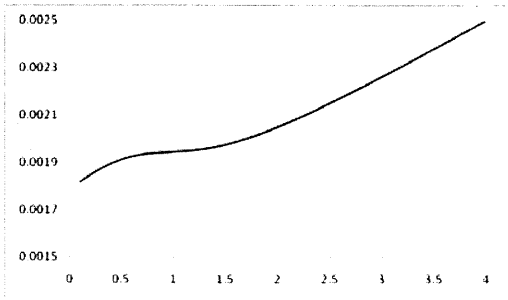
		0.25		0.2547	4.960E+07	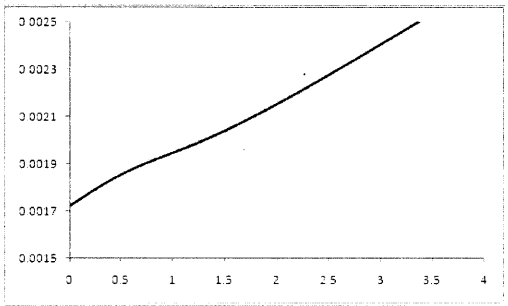
		0.5		0.2547	4.298E+07	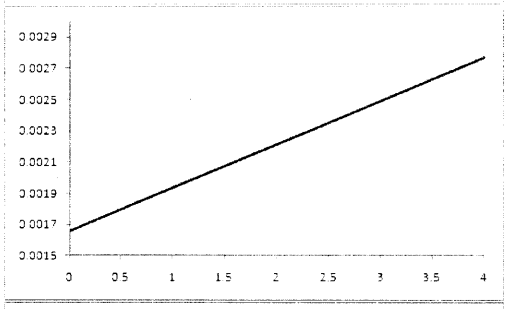
		1		0.2547	3.498E+07	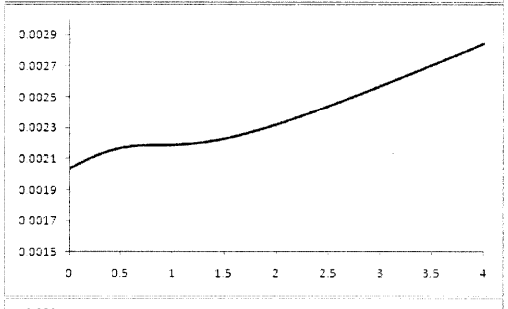
3	2	0	129373	0.3669	1.416E+08	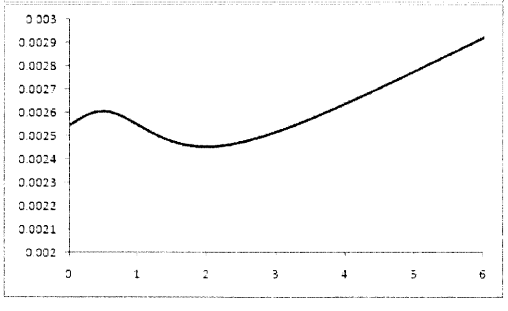

N	Number Walls	d	m (kg)	T_1 (s)	k_{top} (N/m)	Maximum Story Drift Angle vs. Rocking Wall Width (m)
		0.25		0.3669	1.030E+08	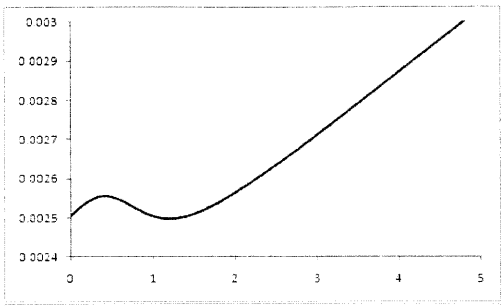
		0.5		0.3669	8.237E+07	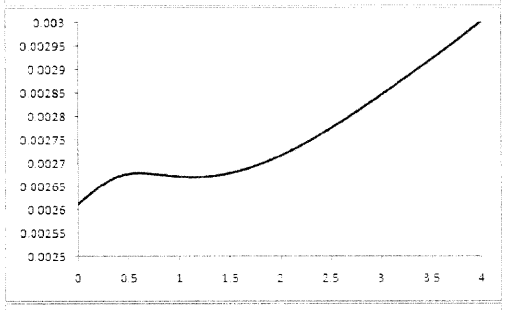
		1		0.3669	6.043E+07	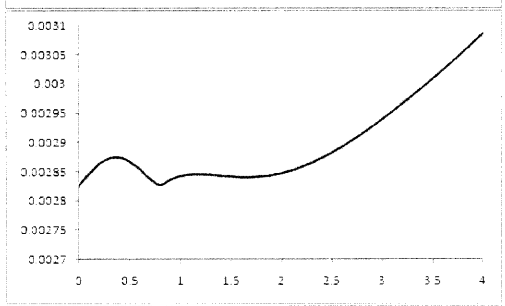
4	2	0	229997	0.4754	2.639E+08	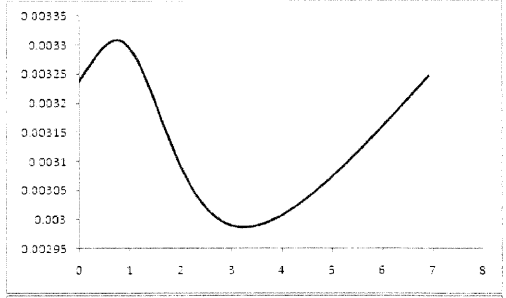
		0.25		0.4754	1.715E+08	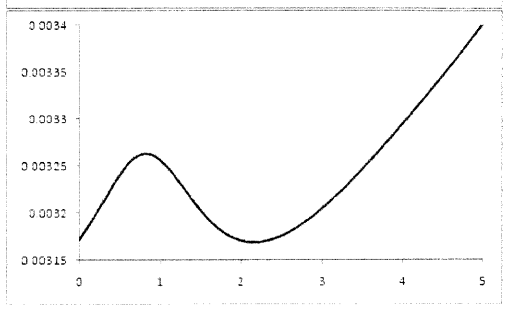

N	Number Walls	d	m (kg)	T_1 (s)	k_{top} (N/m)	Maximum Story Drift Angle vs. Rocking Wall Width (m)
		0.5		0.4754	1.296E+08	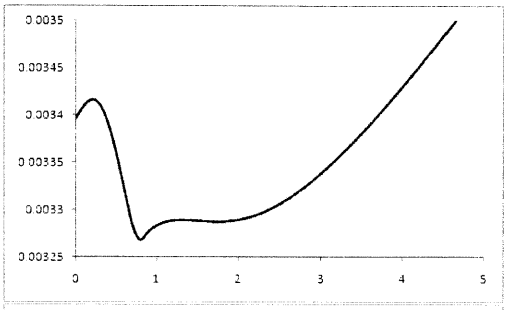
		1		0.4754	8.928E+07	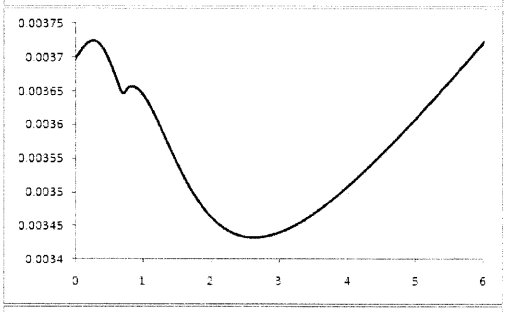
5	2	0	359370	0.5811	4.292E+08	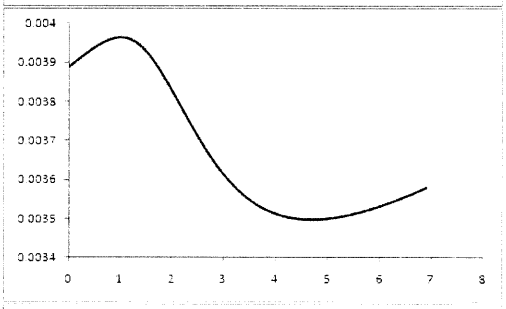
		0.25		0.5811	2.523E+08	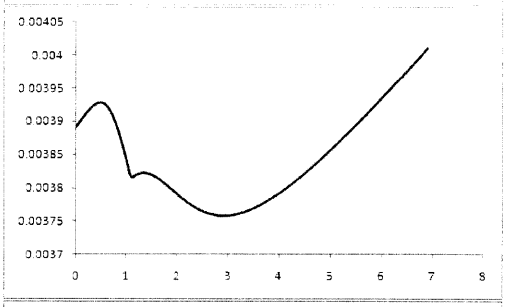
		0.5		0.5811	1.828E+08	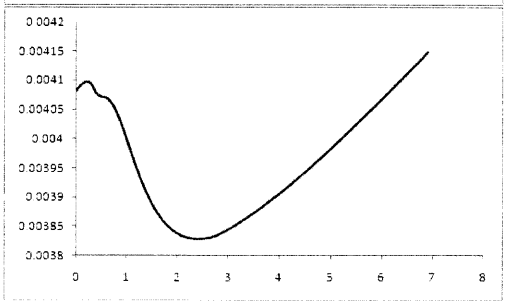

N	Number Walls	d	m (kg)	T_1 (s)	k_{top} (N/m)	Maximum Story Drift Angle vs. Rocking Wall Width (m)
		1		0.5811	1.205E+08	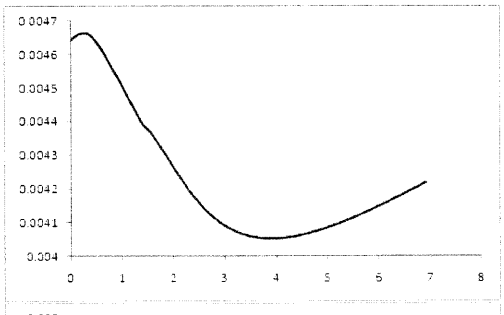
6	2	0	129373	0.6847	1.599E+08	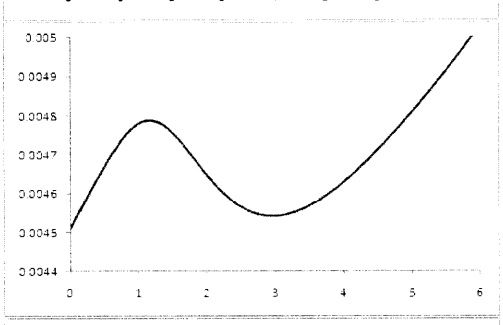
		0.25			8.590E+07	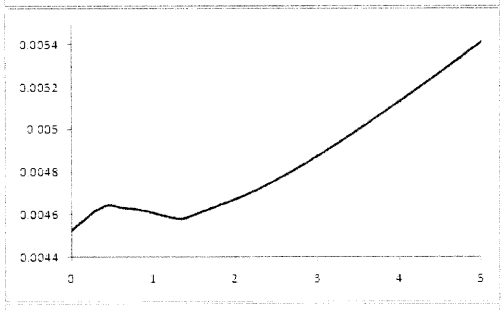
		0.5			6.017E+07	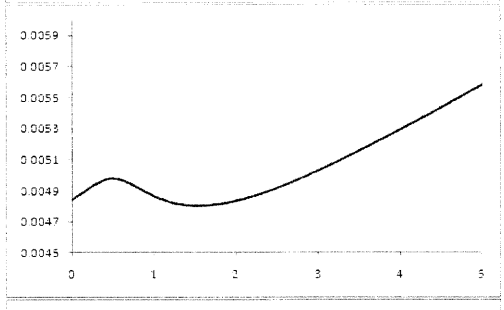
		1			3.842E+07	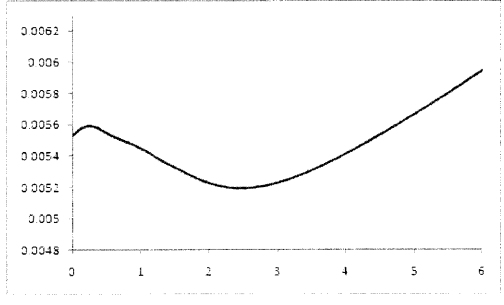

N	Number Walls	d	m (kg)	T_1 (s)	k_{top} (N/m)	Maximum Story Drift Angle vs. Rocking Wall Width (m)
	4	0	129373	0.6847	1.599E+08	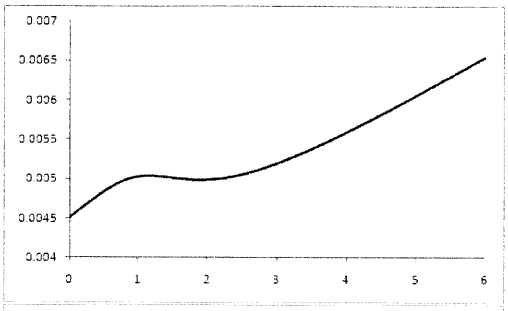
		0.25			8.590E+07	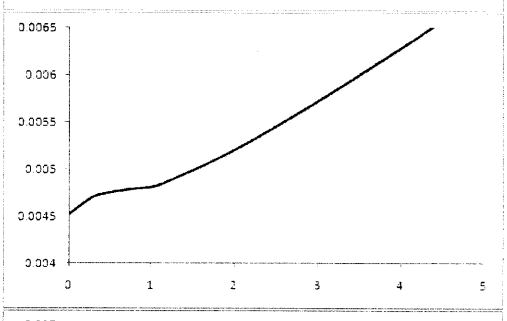
		0.5			6.017E+07	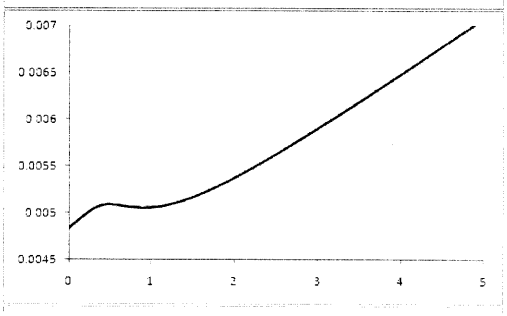
		1			3.842E+07	
7	2	0	176091	0.7866	2.241E+08	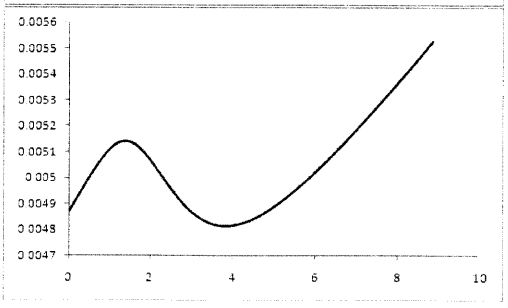

N	Number Walls	d	m (kg)	T_1 (s)	k_{top} (N/m)	Maximum Story Drift Angle vs. Rocking Wall Width (m)
		0.25			1.109E+08	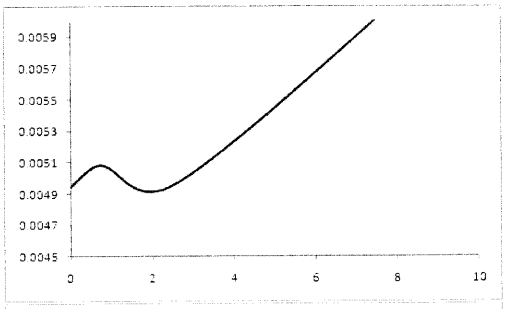
		0.5			7.561E+07	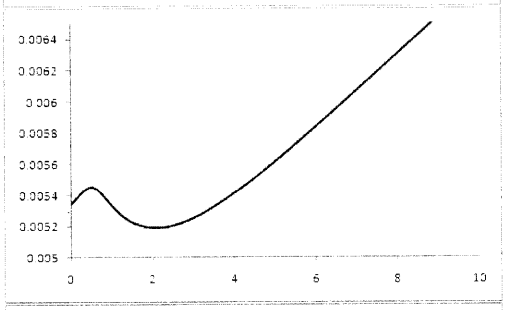
		1			4.709E+07	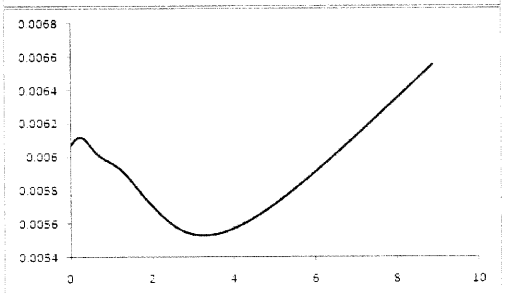
4		0	176091	0.7866	2.241E+08	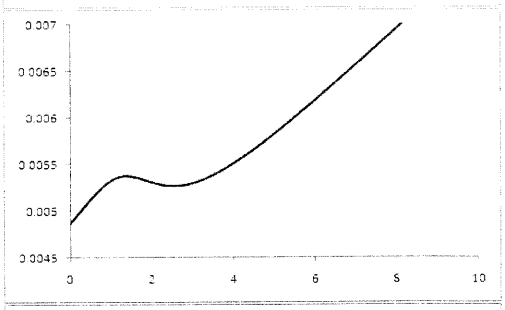
		0.25			1.109E+08	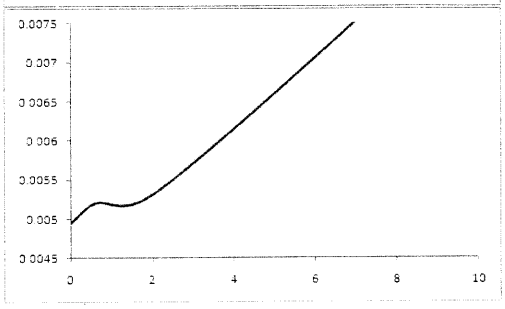

N	Number Walls	d	m (kg)	T_1 (s)	k_{top} (N/m)	Maximum Story Drift Angle vs. Rocking Wall Width (m)
		0.5			7.561E+07	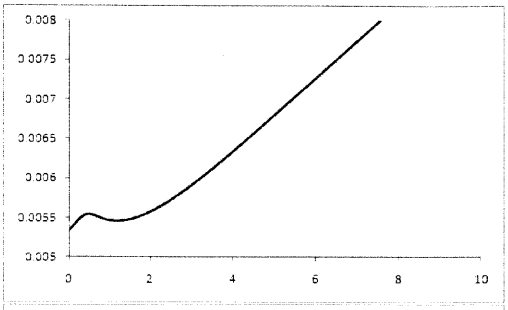
		1			4.709E+07	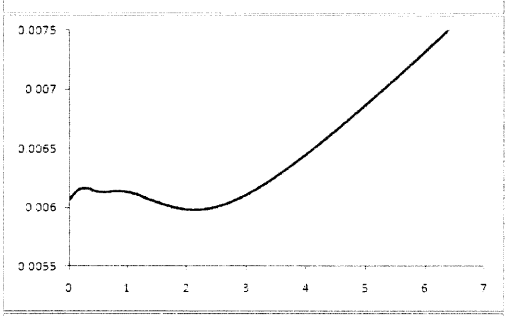
8	2	0	229997	0.8871	3.003E+08	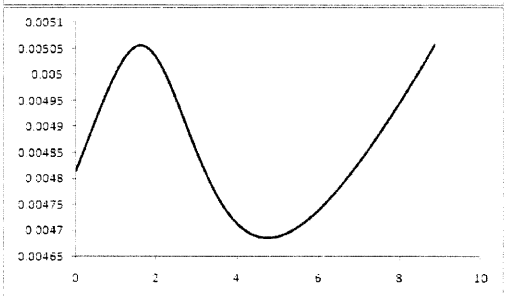
		0.25			1.379E+08	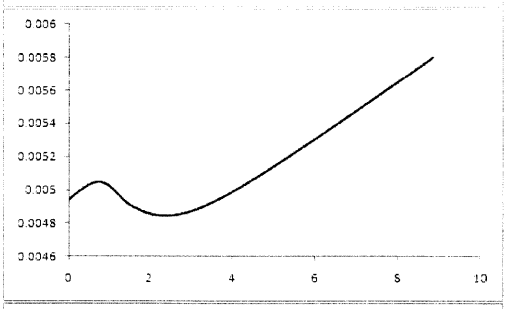
		0.5			9.189E+07	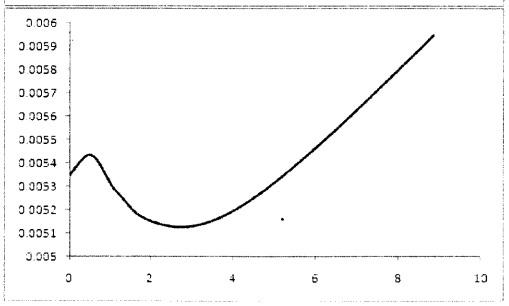

N	Number Walls	d	m (kg)	T_1 (s)	k_{top} (N/m)	Maximum Story Drift Angle vs. Rocking Wall Width (m)
		1			5.609E+07	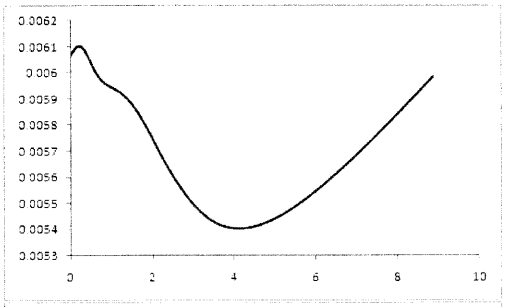
	4	0	229997	0.8871	3.003E+08	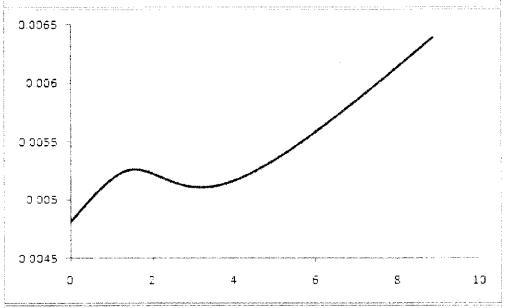
		0.25			1.379E+08	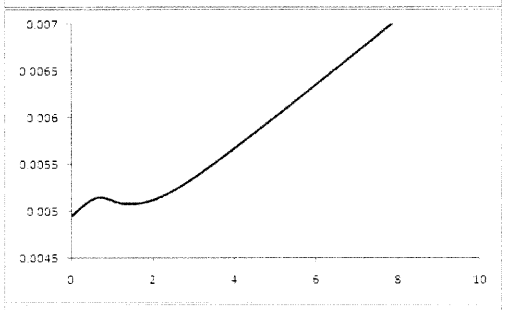
		0.5			9.189E+07	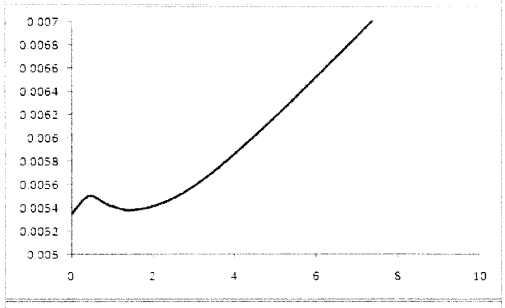
		1			5.609E+07	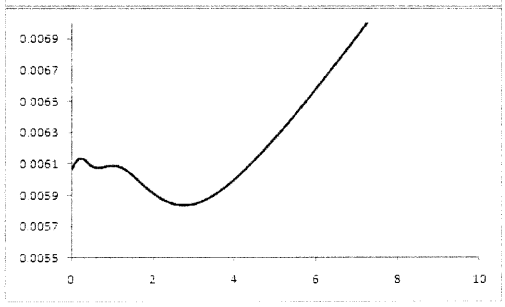

N	Number Walls	d	m (kg)	T_1 (s)	k_{top} (N/m)	Maximum Story Drift Angle vs. Rocking Wall Width (m)
9	2	0	291090	0.9863	3.888E+08	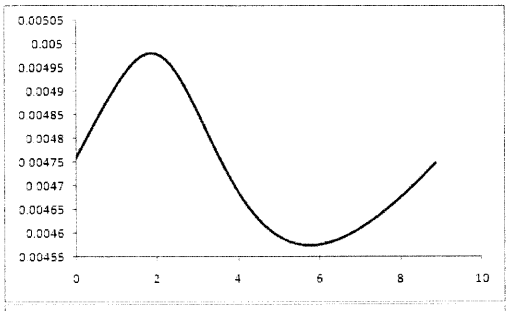
		0.25			1.666E+08	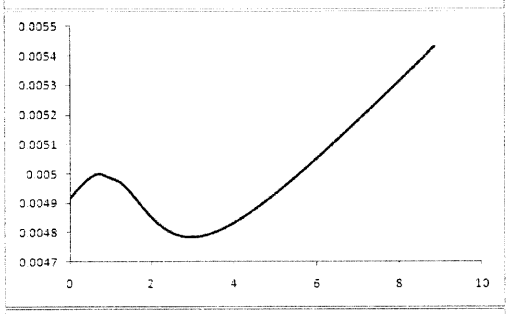
		0.5			1.089E+08	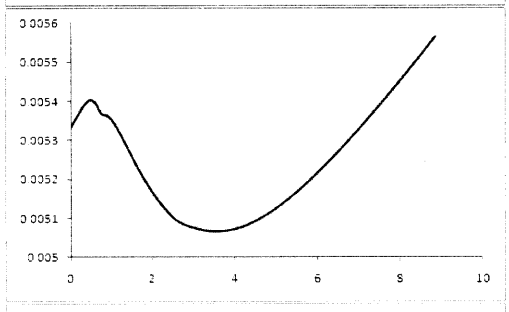
		1			6.538E+07	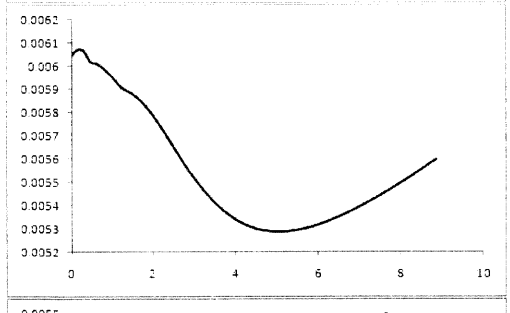
	4	0	291090	0.9863	3.888E+08	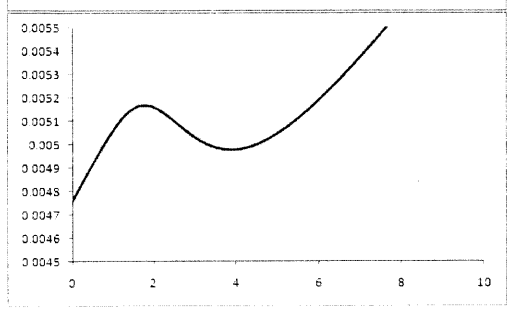

N	Number Walls	d	m (kg)	T_1 (s)	k_{top} (N/m)	Maximum Story Drift Angle vs. Rocking Wall Width (m)
		0.25			1.666E+08	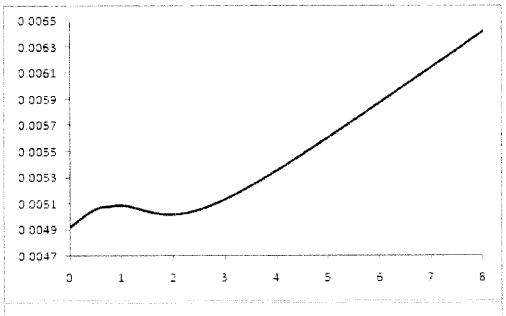
		0.5			1.089E+08	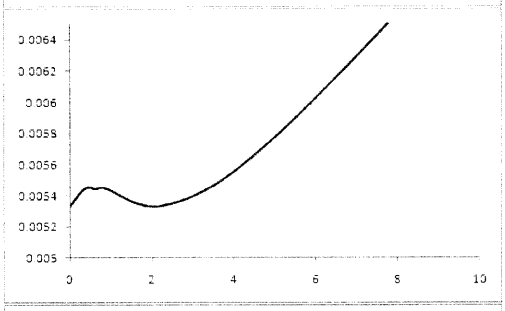
		1			6.538E+07	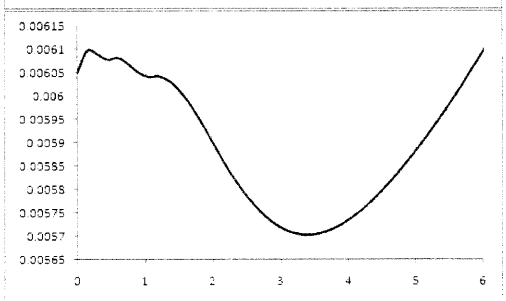
10	2	0	359370	1.0843	4.900E+08	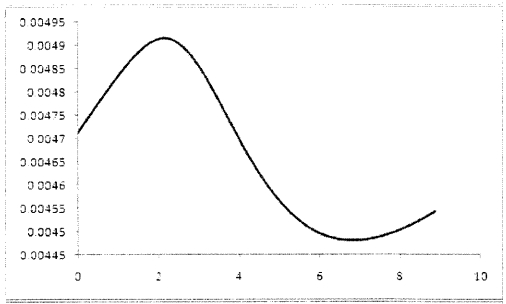
		0.25			1.969E+08	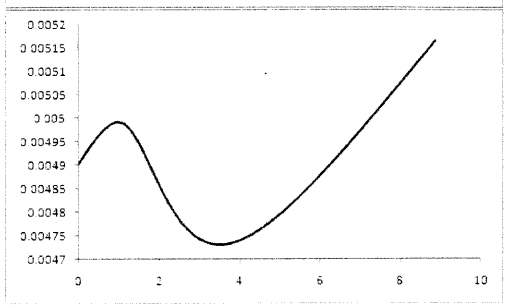

N	Number Walls	d	m (kg)	T_1 (s)	k_{top} (N/m)	Maximum Story Drift Angle vs. Rocking Wall Width (m)
		0.5			1.265E+08	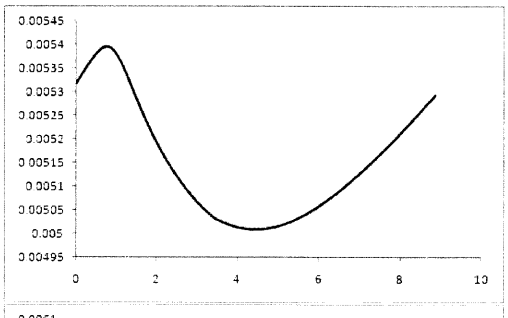
		1			7.493E+07	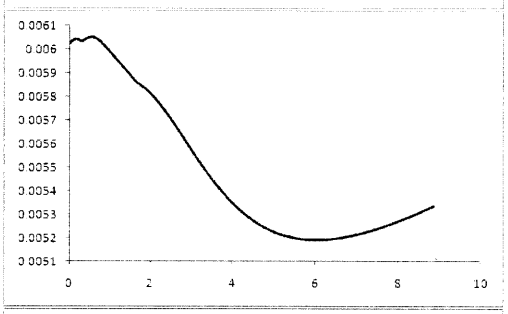
4	0	0	359370	1.0843	4.900E+08	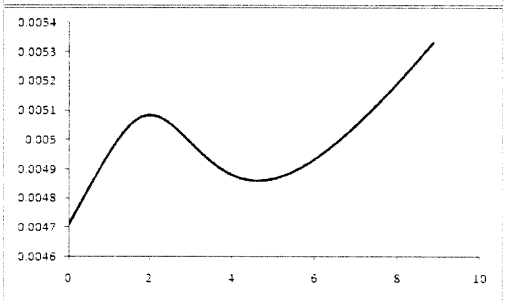
		0.25			1.969E+08	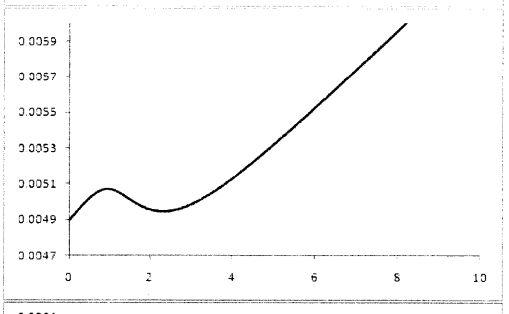
		0.5			1.265E+08	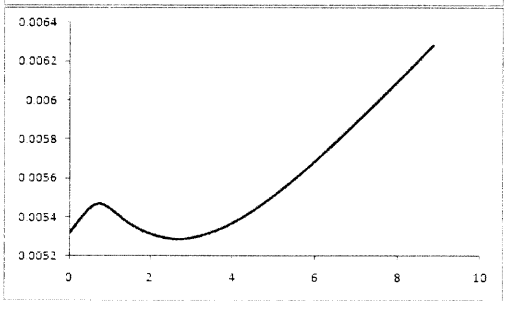

N	Number Walls	d	m (kg)	T_1 (s)	k_{top} (N/m)	Maximum Story Drift Angle vs. Rocking Wall Width (m)
		1			7.493E+07	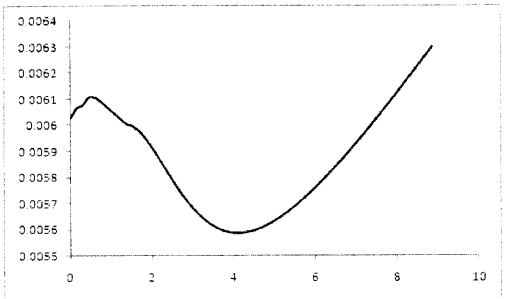
11	2	0	193261	1.1815	2.685E+08	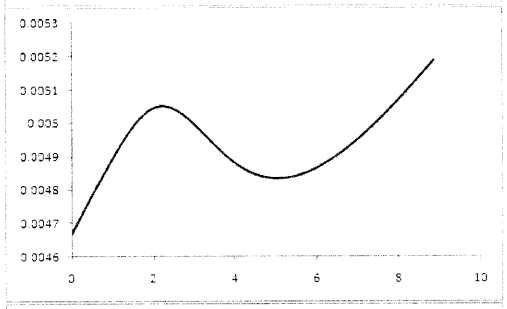
		0.25			1.016E+08	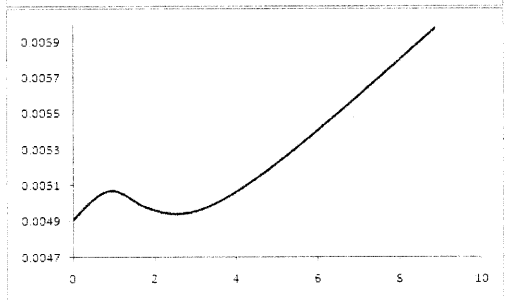
		0.5			6.432E+07	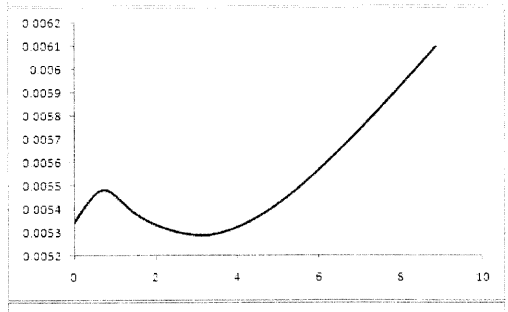
		1			3.765E+07	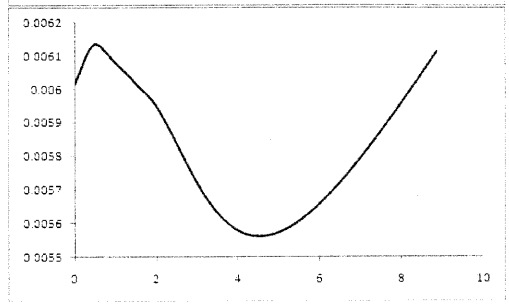

N	Number Walls	d	m (kg)	T_1 (s)	k_{top} (N/m)	Maximum Story Drift Angle vs. Rocking Wall Width (m)
	4	0	193261	1.1815	2.685E+08	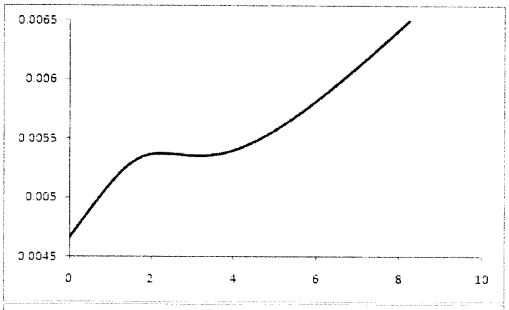
		0.25			1.016E+08	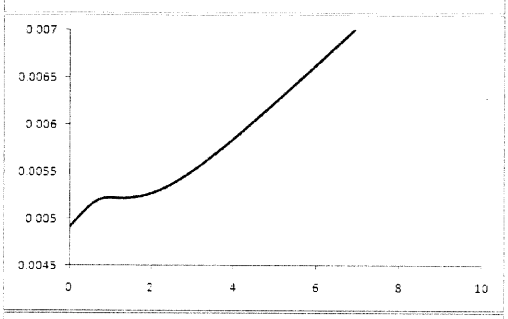
		0.5			6.432E+07	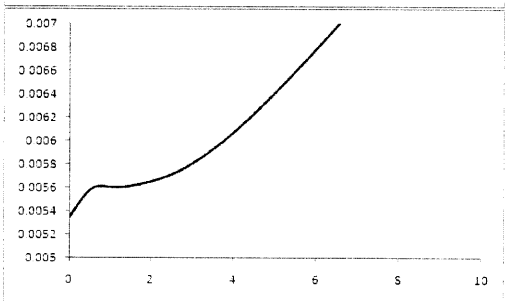
		1			3.765E+07	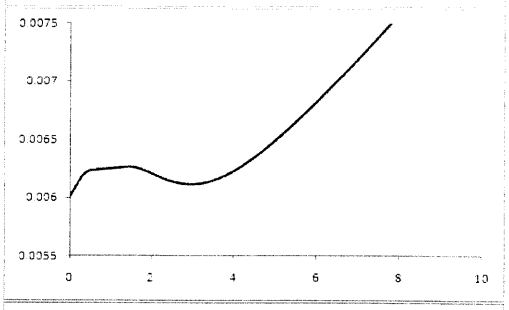
	6	0	193261	1.1815	2.685E+08	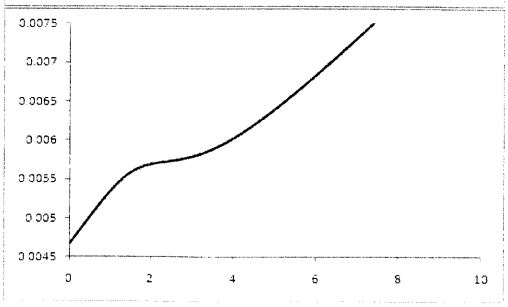

N	Number Walls	d	m (kg)	T_1 (s)	k_{top} (N/m)	Maximum Story Drift Angle vs. Rocking Wall Width (m)
		0.25			1.016E+08	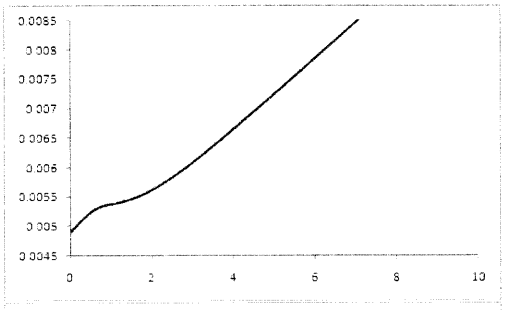
		0.5			6.432E+07	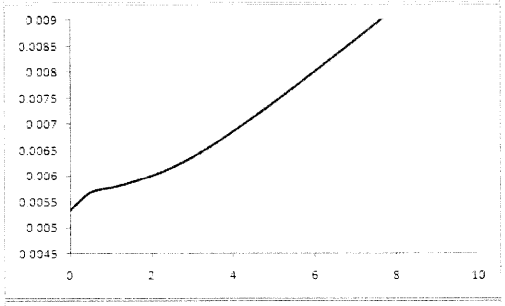
		1			3.765E+07	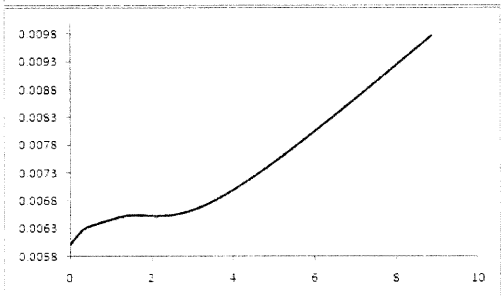
12	2	0	229997	1.2777	3.251E+08	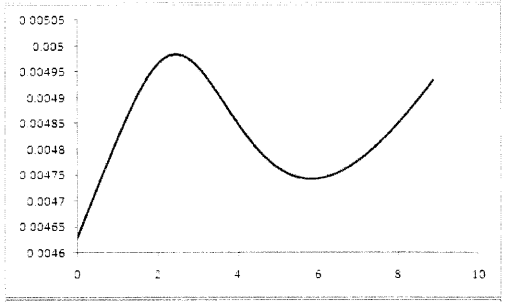
		0.25			1.162E+08	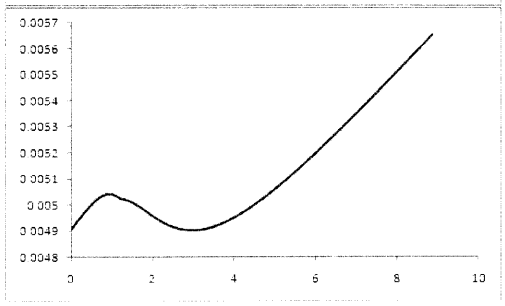

N	Number Walls	d	m (kg)	T_1 (s)	k_{top} (N/m)	Maximum Story Drift Angle vs. Rocking Wall Width (m)
		0.5			7.264E+07	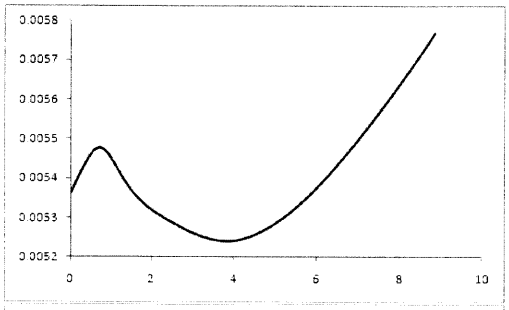
		1			4.210E+07	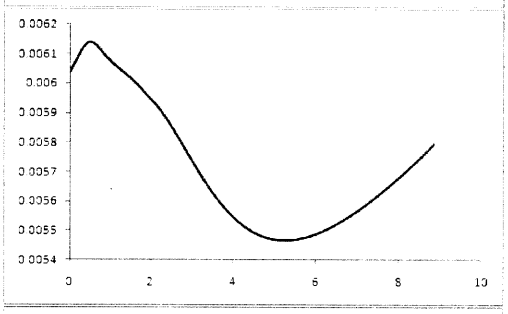
	4	0	229997	1.2777	3.251E+08	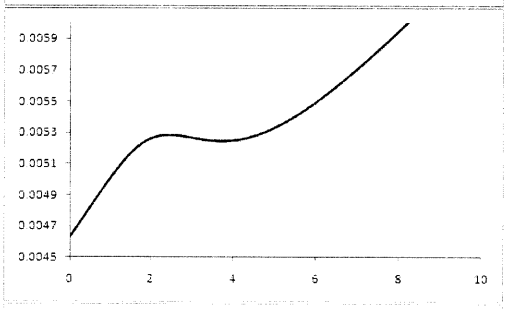
		0.25			1.162E+08	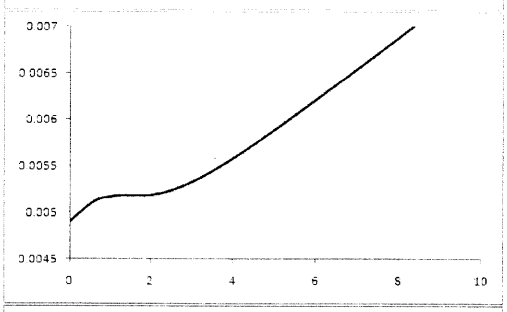
		0.5			7.264E+07	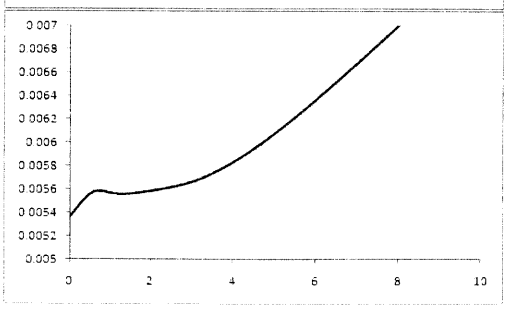

N	Number Walls	d	m (kg)	T_1 (s)	k_{top} (N/m)	Maximum Story Drift Angle vs. Rocking Wall Width (m)
		1			4.210E+07	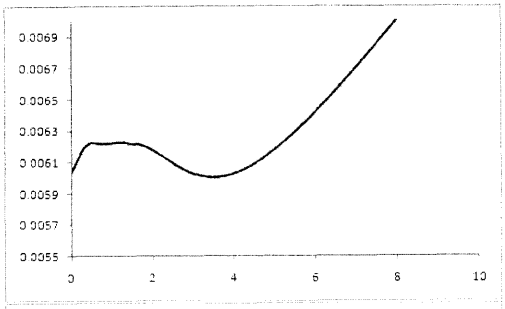
	6	0	229997	1.2777	3.251E+08	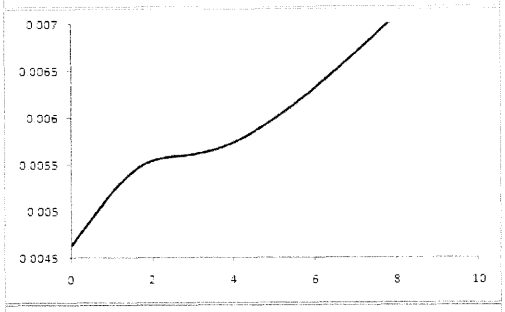
		0.25			1.162E+08	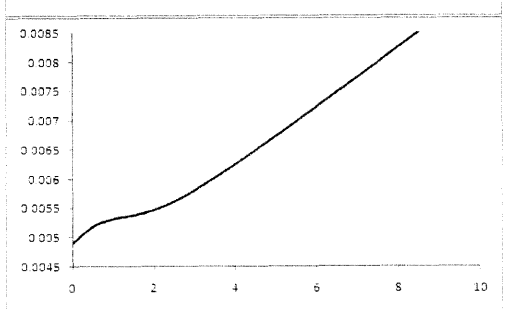
		0.5			7.264E+07	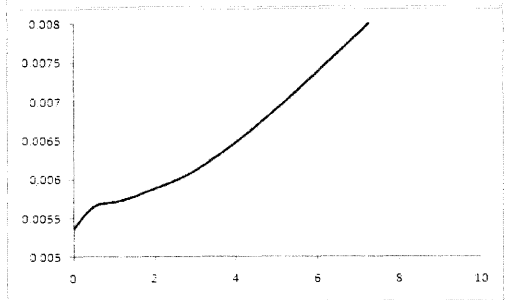
		1			4.210E+07	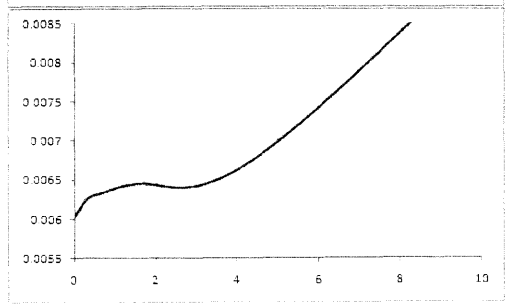

N	Number Walls	d	m (kg)	T_1 (s)	k_{top} (N/m)	Maximum Story Drift Angle vs. Rocking Wall Width (m)
13	2	0	269927	1.3732	3.876E+08	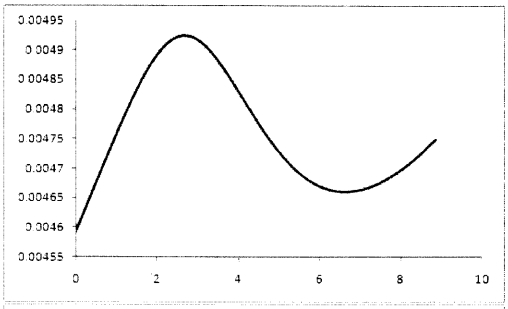
		0.25			1.313E+08	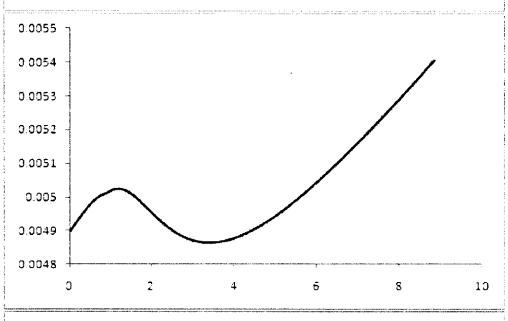
		0.5			8.116E+07	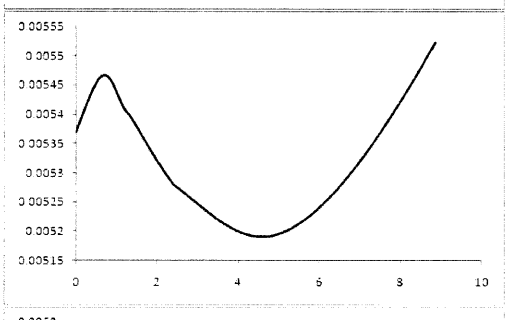
		1			4.663E+07	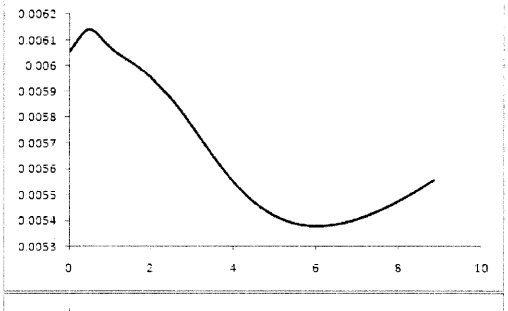
	4	0	269927	1.3732	3.876E+08	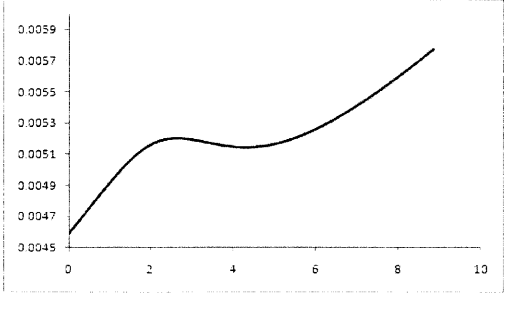

N	Number Walls	d	m (kg)	T_1 (s)	k_{top} (N/m)	Maximum Story Drift Angle vs. Rocking Wall Width (m)
		0.25			1.313E+08	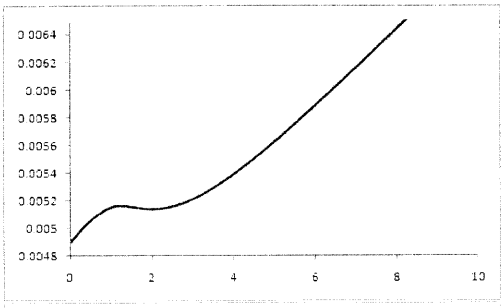
		0.5			8.116E+07	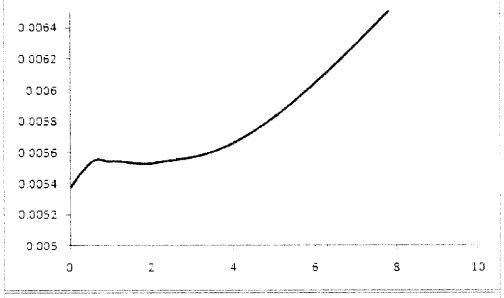
		1			4.663E+07	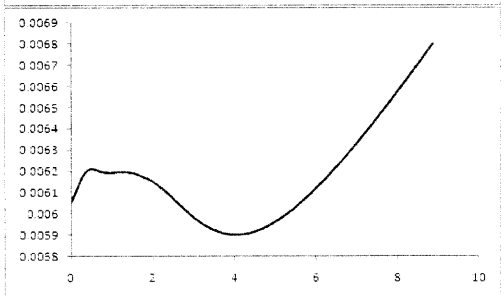
6		0	269927	1.3732	3.876E+08	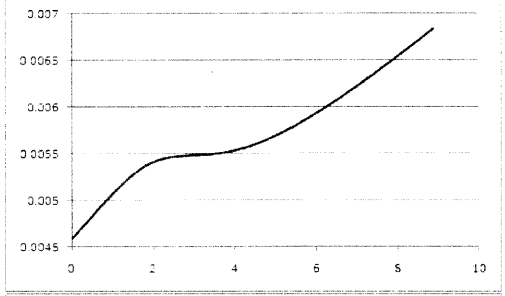
		0.25			1.313E+08	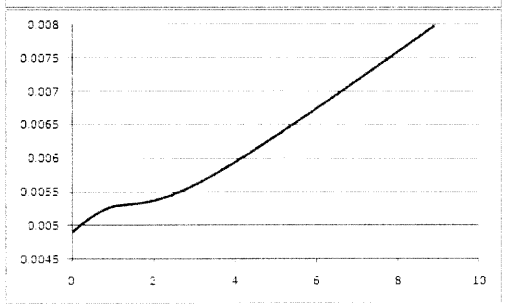

N	Number Walls	d	m (kg)	T_1 (s)	k_{top} (N/m)	Maximum Story Drift Angle vs. Rocking Wall Width (m)
		0.5			8.116E+07	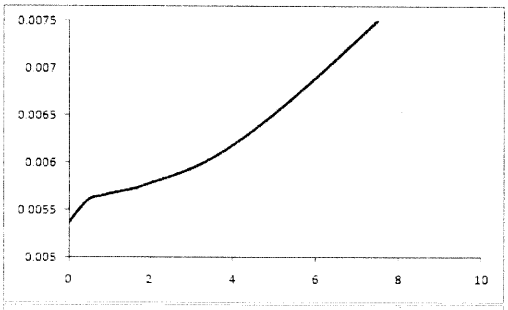
		1			4.663E+07	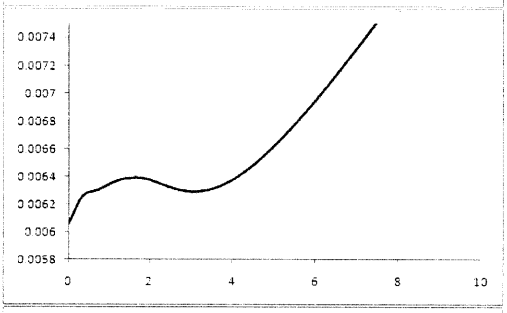
14	2	0	313051	1.4679	4.561E+08	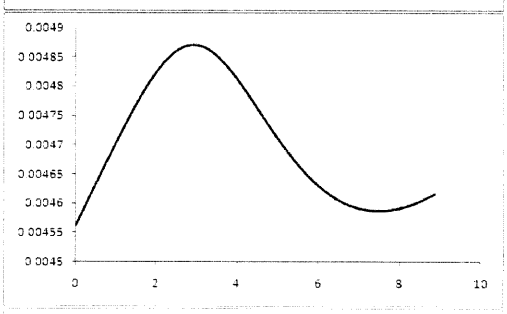
		0.25			1.469E+08	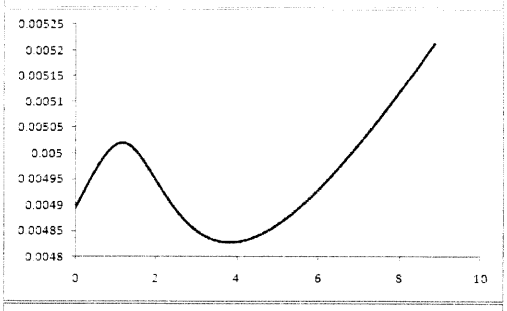
		0.5			8.989E+07	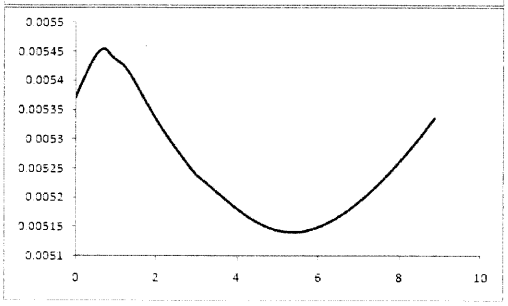

N	Number Walls	d	m (kg)	T_1 (s)	k_{top} (N/m)	Maximum Story Drift Angle vs. Rocking Wall Width (m)
		1			5.124E+07	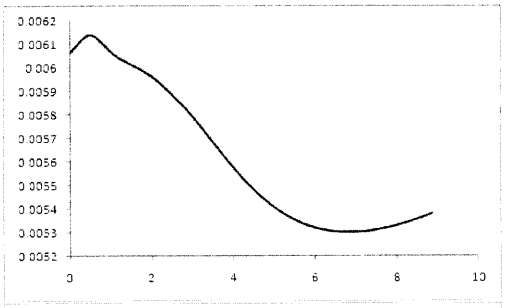
	4	0	313051	1.4679	4.561E+08	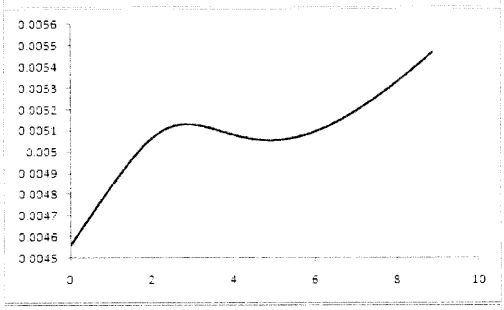
		0.25			1.469E+08	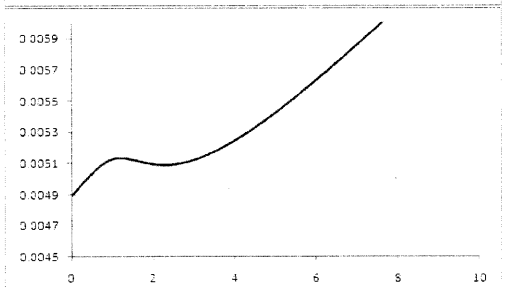
		0.5			8.989E+07	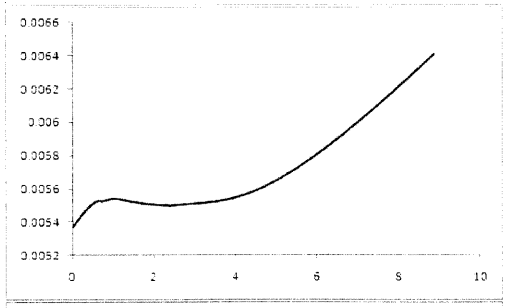
		1			5.124E+07	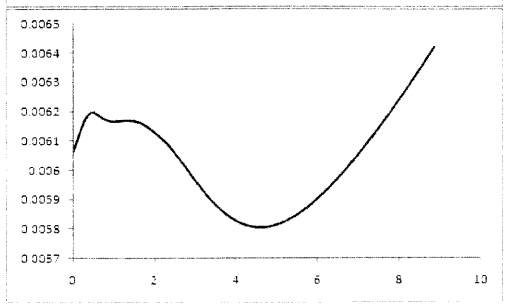

N	Number Walls	d	m (kg)	T_1 (s)	k_{top} (N/m)	Maximum Story Drift Angle vs. Rocking Wall Width (m)
	6	0	313051	1.4679	4.561E+08	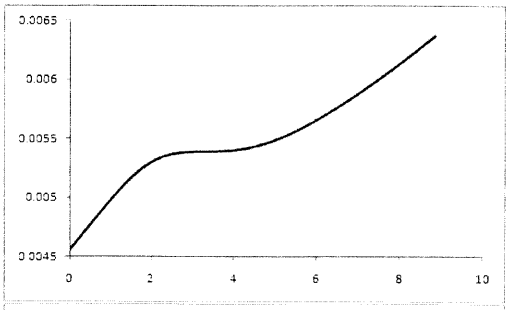
		0.25			1.469E+08	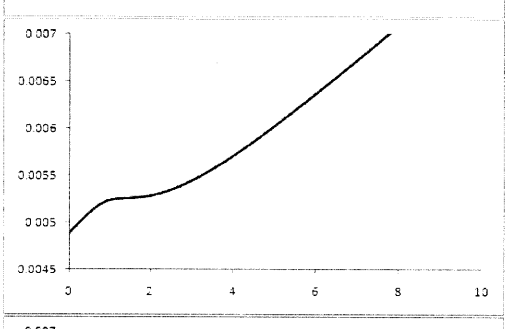
		0.5			8.989E+07	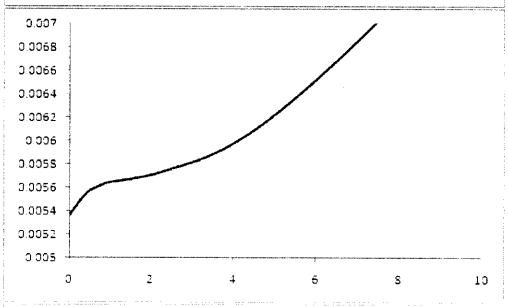
		1			5.124E+07	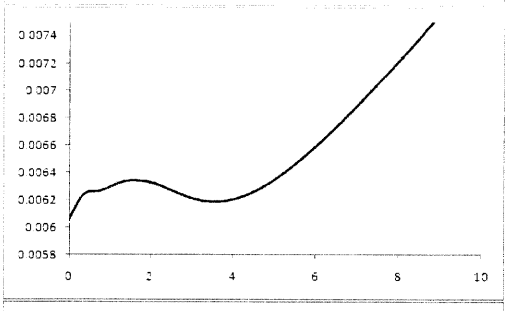
15	2	0	359370	1.5619	5.308E+08	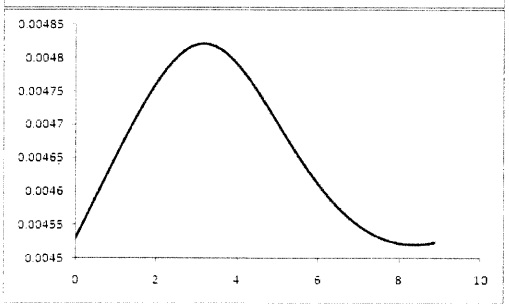

N	Number Walls	d	m (kg)	T_1 (s)	k_{top} (N/m)	Maximum Story Drift Angle vs. Rocking Wall Width (m)
		0.25			1.629E+08	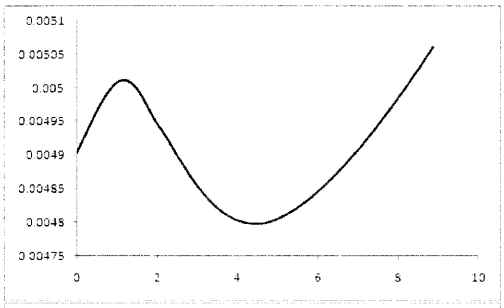
		0.5			9.879E+07	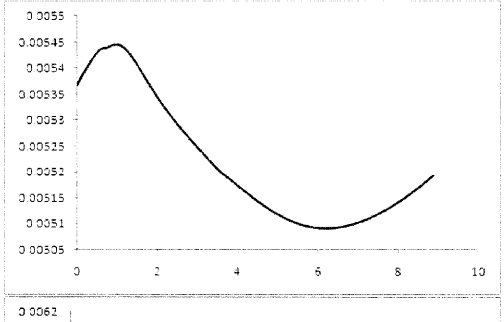
		1			5.592E+07	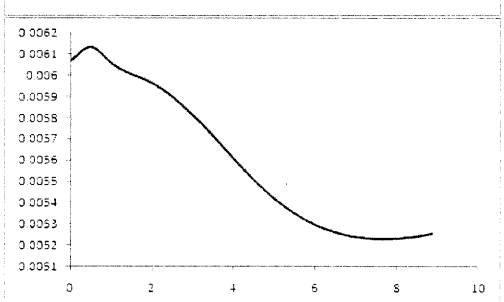
4		0	359370	1.5619	5.308E+08	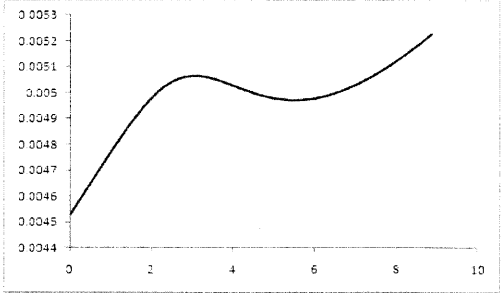
		0.25			1.629E+08	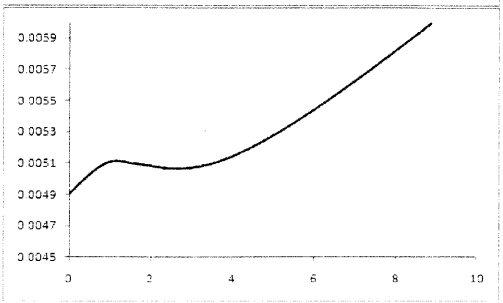

N	Number Walls	d	m (kg)	T_1 (s)	k_{top} (N/m)	Maximum Story Drift Angle vs. Rocking Wall Width (m)
		0.5			9.879E+07	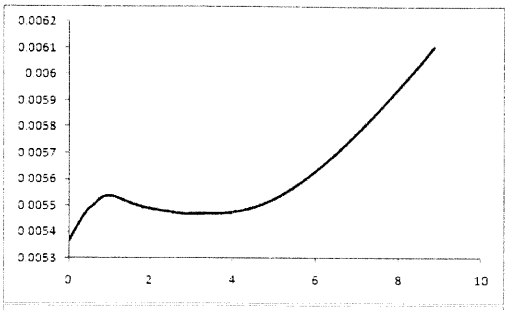
		1			5.592E+07	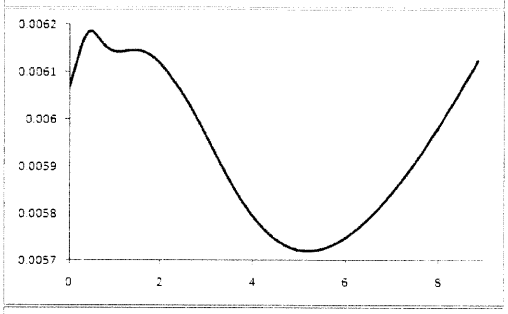
	6	0	359370	1.5619	5.308E+08	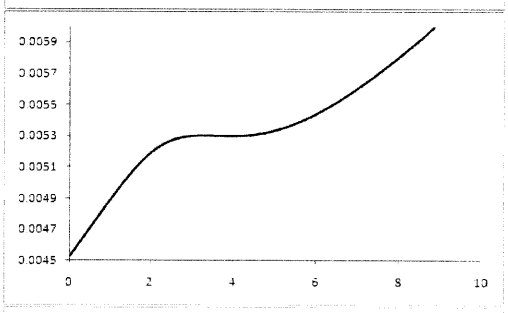
		0.25			1.629E+08	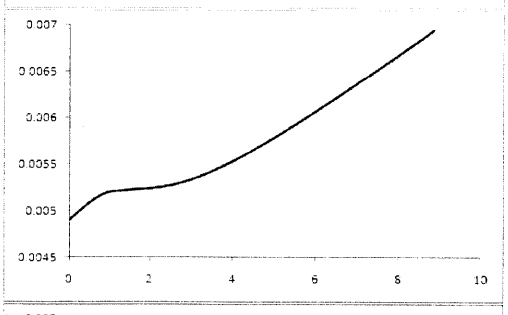
		0.5			9.879E+07	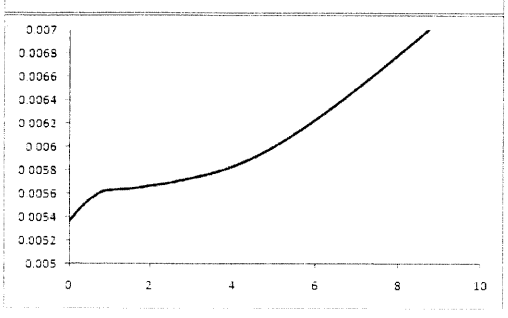

N	Number Walls	d	m (kg)	T_1 (s)	k_{top} (N/m)	Maximum Story Drift Angle vs. Rocking Wall Width (m)
		1			5.592E+07	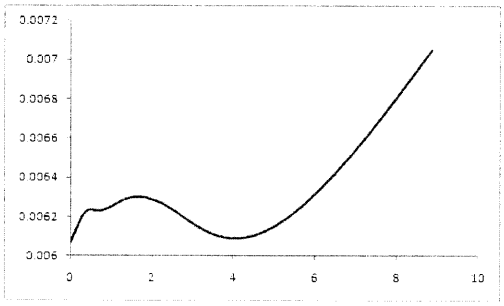

Appendix C: MATLAB Code for Solving the Rocking Wall as a Flexible Continuous System, using Lagrange, as in Section 3.6.

```
syms x L h k1 k2 rho A m EI q0 q1 q0dot q1dot q0dotdot q1dotdot;

% Building nodes are numbered from the top down. The top node is 1.
% This is unlike the work body, in which the top-node-N convention is used.
% This example demonstrates the method for a two-story model.
% The model expects the building shape to follow the wall shape (rigid links),
% so expects L to be about the same as h * number_storys or greater

% replace syms with values
number_storys = 2;
wall_width = 14.4 * 0.3048; % m
wall_depth = 2 * 0.3048; % m
m = 57000; % kg
concrete_modulus = 24.82*10^9; % Pa
rho = 2400; % kg/m^3, density of wall
h = 12 * 0.3048; % m, height of 1 story
k1 = 8*12*concrete_modulus*((0.3048)^4/12)/h^3;
k2 = k1; % 35.0237776 MN/m
L = number_storys * h;
wall_I = wall_depth*wall_width^3/12;
EI = concrete_modulus*wall_I;
A = wall_width*wall_depth;

% alpha factor for psi1
a = 5*pi/4/L;

% trial functions
psi0 = x/L;
psi1 = sin(a*x);

% position function u(x,t)
u = psi0*q0 + psi1*q1;

% find u at critical locations
u_1 = subs(u,x,2*h);
u_2 = subs(u,x,h);

% building stiffness matrix
K_building = [k1 -k1;-k1 k1 + k2];

% find loads on the wall from the building
P = K_building*[u_1;u_2];
% BUT! these forces are in the -ve direction on the wall
```

```
% when the movements by the wall are +ve. So we want the -ve of these forces.
% Check this by looking at the force vector P. For an all-positive mode
% such as rigid body rotation (q0), you want the force to be -ve WRT q0.
P = -P;
p1 = P(1);
p2 = P(2);

% 'differentiate' u wrt t by substituting the q functions with qdot
udot = subs(u,q0,q0dot);
udot = subs(udot,q1,q1dot);

% find udot at critical locations
udot_h = subs(udot,x,h);
udot_2h = subs(udot,x,2*h);

% differentiate u wrt x
dudx = diff(u,x);
d2udx2 = diff(dudx,x);

% energy functions for Lagrange
K_for_lumped_masses = 1/2*m*udot_h^2 + 1/2*1/2*m*udot_2h^2;
K = 1/2*rho*A*int(udot^2, x, 0, L) + K_for_lumped_masses;
V  = 1/2*EI*int(d2udx2^2, x, 0, L);
%(NB: there is no curvature associated with the rigid body mode
% so d2udx2 & thus V are not functions of q0)
W = 1/2*p1*u_1 + 1/2*p2*u_2; % is this definitely 1/2?

% differentiate energy functions
dKdq0dot = diff(K,q0dot);
ddtdKdq0dot = subs(dKdq0dot,q0dot,q0dotdot); % differentiation wrt t by substitution
ddtdKdq0dot = subs(ddtdKdq0dot,q1dot,q1dotdot); % differentiation wrt t by substitution
dKdq1dot = diff(K,q1dot);
ddtdKdq1dot = subs(dKdq1dot,q0dot,q0dotdot); % differentiation wrt t by substitution
ddtdKdq1dot = subs(ddtdKdq1dot,q1dot,q1dotdot); % differentiation wrt t by substitution
dKdq0 = diff(K,q0);
dKdq1 = diff(K,q1);
dVdq0 = diff(V,q0);
dVdq1 = diff(V,q1);
dWdq0 = diff(W,q0);
dWdq1 = diff(W,q1);

% get the matrix components
% (differentiation only works for this because there
% are no higher powers/functions of q0, q0dotdot, etc)
M11 = diff(ddtdKdq0dot,q0dotdot);
M12 = diff(ddtdKdq0dot,q1dotdot);
M21 = diff(ddtdKdq1dot,q0dotdot);
M22 = diff(ddtdKdq1dot,q1dotdot);
```

```
K11 = diff(dVdq0,q0) - diff(dWdq0,q0); % 1st term is 0 as explained above
K12 = diff(dVdq0,q1) - diff(dWdq0,q1); % 1st term is 0 as explained above
K21 = diff(dVdq1,q0) - diff(dWdq1,q0); % 1st term is 0 as explained above
K22 = diff(dVdq1,q1) - diff(dWdq1,q1);

% create the matrices
M_matrix = [M11 M12;M21 M22];
K_matrix = [K11 K12;K21 K22];

% display the matrices as approximate decimals
M_matrix_approx = double(M_matrix);
K_matrix_approx = double(K_matrix);

% solve the eigenvector problem
[Phi,Omega] = eig(K_matrix_approx,M_matrix_approx);

% now we can find q0,q1, etc.
% find the natural frequencies of the system
Wn0squared = Omega(1,1);
Wn1squared = Omega(2,2);
Wn0 = sqrt(Wn0squared);
Wn1 = sqrt(Wn1squared);
f0 = Wn0/2/pi;
f1 = Wn1/2/pi;
T0 = 1/f0;
T1 = 1/f1;

% q vectors give the relative strength of each mode
qAtWn0 = [Phi(1,1);Phi(2,1)];
qAtWn1 = [Phi(1,2);Phi(2,2)];

% sub the qs to get u
x = 0:0.1:2*h;
psi0_as_array = 1.*x/L;
psi1_as_array = sin(a.*x);
uAtWn0 = vpa(qAtWn0(1))*psi0_as_array + vpa(qAtWn0(2))*psi1_as_array;
uAtWn1 = vpa(qAtWn1(1))*psi0_as_array + vpa(qAtWn1(2))*psi1_as_array;
uAtWn0_normalized = psi0 + vpa(qAtWn0(2))/vpa(qAtWn0(1))*psi1 % for readability
uAtWn1_normalized = psi0 + vpa(qAtWn1(2))/vpa(qAtWn1(1))*psi1 % for readability
plot(x,uAtWn0)

% M_matrix output:
M11=(3*h^2*m)/L^2 + (A*L*rho)/3

M12 = (h*m*sin((5*pi*h)/(2*L)))/L + (h*m*sin((5*pi*h)/(4*L)))/L -
(A*rho*((16*2^(1/2)*L)/25 - (4*pi*2^(1/2)*L)/5))/(2*pi^2)
```

```
M21 = (h*m*sin((5*pi*h)/(2*L)))/L + (h*m*sin((5*pi*h)/(4*L)))/L -
(A*rho*((16*2^(1/2)*L)/25 - (4*pi*2^(1/2)*L)/5))/(2*pi^2)

M22 = (m*sin((5*pi*h)/(2*L))^2)/2 + m*sin((5*pi*h)/(4*L))^2 + (A*rho*(L -
(2*L)/(5*pi)))/2]
```

Appendix D: MATLAB Code to Find the Stiffness Matrix of Building-Rocking Wall System

```
% building nodes are numbers from the bottom up. the top node is N.
% This is like the work body, in which the top-node-N convention is also used.
% Get Input
N = input('Number Stories: ');
L = input('Total Height (m): ');
EI_wall = input('EI of Wall (Nm^2): ');
bldg_storey_stiffness = input('Building Storey Stiffness (N/m): ');
if (isempty(N))N=11;end; if (isempty(L))L=33;end; if (isempty(EI_wall))EI_wall=1000000;end; if
(isempty(bldg_storey_stiffness))bldg_storey_stiffness=1000000;end;

% wall stiffness matrix
F_wall_prime = zeros(N-1,N-1);
for i = 1:N-1; % i is point measured
    for j = 1:N-1; % j is point of application of load
        x = (i-2)/N*L;  % the distance to the point measured from the cantilever root
        a = (j-2)/N*L;  % distance to point of application of load from cantilever root

        % find the rotation term
        moment_arm = a;
        single_storey_height = L/N;
        distance_to_point_measured_from_cantilever_root = x;
        rotation_at_lowest_storey = moment_arm*single_storey_height/(3*EI_wall);
        rotation_term = rotation_at_lowest_storey*distance_to_point_measured_from_cantilever_root;

        % find the cantilever term
        if (i > j)
            % must use the x > a cantilever formula
            cantilever_term = a^2/(6*EI_wall)*(3*x - a);
        else
            % must use the x <= a cantilever formula
            cantilever_term = x^2/(6*EI_wall)*(-x + 3*a);
        end;
        F_wall_prime(i,j) = rotation_term + cantilever_term;
    end;
end;
K_wall_prime = inv(F_wall_prime);
K_wall = zeros(N,N);
for i = 1:N-1;
    for j = 1:N-1;
        K_wall(i+1,j+1) = K_wall_prime(i,j);
    end;
end;

% building stiffness matrix
Sum_bldg_stiffness = bldg_storey_stiffness;
K_bldg = zeros(N,N);
for j = 1:N;
    % diagonals
    K_bldg(j,j) = 2*Sum_bldg_stiffness;
end;
for j = 1:N-1;
    % off diagonals
    K_bldg(j,j+1)= -Sum_bldg_stiffness;
    K_bldg(j+1,j)= -Sum_bldg_stiffness;
end;
K_bldg(N,N)=K_bldg(N,N) - Sum_bldg_stiffness;

% moments matrix
M = zeros(N,N);
for j = 2:N;
    % top row
    M(1,j) = -j;
end;

% L_1 "linear-1"
L_1 = zeros(N,N);
for j = 1:N;
    % start of each row
    L_1(j,1) = j;
end;
```

```
% total stiffness matrix
K_total = K_bldg + (M + eye(N))*K_wall*(eye(N) - L_1);
```